M-AM-Sy1 DNA SEQUENCE DETERMINATION AND THE ASSIGNMENT OF GENETIC FUNCTIONS USING CONSTRUCTED MUTANTS. Michael Smith, Department of Biochemistry, Faculty of Medicine, University of British Columbia, 2075 Wesbrook Mall, Vancouver, B.C., Canada, V6T 1W5.

The new rapid (ladder) methods of DNA sequence determination provide the exact sequence extended regions of genomic DNA. Some genetic functions can be assigned by comparison with established RNA and protein sequences. However, this type of comparison is not possible for many regions of established DNA sequences. Consequently a number of strategies have been developed for the in vitro modification of DNA sequence. These include methods for constructing deletion mutants and mutants with short inserts of synthetic DNA. Such mutant DNAs, when incorporated into independently replicating plasmid vectors, can be used to transform appropriate host cells. The DNAs can also be used with specific in vitro transcription systems. Other methods of in vitro mutagenesis allow the construction of specific point mutations which can be used to precisely define genetic functions. A number of applications of these methodologies to problems of gene function will be described.

M-AM-Sy2 NUCLEIC ACID SEQUENCE DATA BASE: FOUR STAGES. M.O. Dayhoff. Georgetown University. Washington, D.C. 20007.

The elucidation of nucleic acid sequences can be conveniently discussed in four stages. The first stage started with the publication of the sequence and secondary structure of alanine tRNA in 1965 by Holley and his colleagues. The second started with the publication in 1970 of the first DNA work, 12 residues of phage lambda by Wu and his colleagues. By this time 25 distinct RNA sequences (mainly tRNA's) more than 5% different from others and sequences comprising 18% of the whole genome of bacteriophage R17 were known. The second stage culminated in 1977 in the elucidation of the genomes of ØX174, a DNA bacteriophage, by Sanger and his colleagues, and MS2, an RNA bacteriophage, by Fiers' group. By this time over 18,000 nucleotide residues had been elucidated. When the third stage ended Aug. 1, 1980, over 200,000 residues, including 21 prokaryote genes for proteins, 67 eukaryote genes for proteins, 4 complete genomes of bacteriophages, 7 complete virus genomes, and one viroid, had been elucidated. On September 15, we made this collection of over 255 sequences containing over 227,000 residues available in a retrieval system by telephone to all research workers. There are now (in February) approximately twice this many residues available in our computer system. This explosive growth in information will be analyzed and our computer system and manipulative programs, developed to make these data intellectually accessible, will be discussed and demonstrated. Supported by NIH grant GM-08710 and NASA contract NASW-3317.

M-AM-Sy3 COMPUTER ANALYSIS OF PATTERNS AND FEATURES IN NUCLEIC ACID SEQUENCES. Jacob V. Maizel, Jr., Head, Section of Molecular Structure, Laboratory of Molecular Genetics, National Institutes of Health, Bethesda, Maryland 20205

Since the advent of rapid nucleic acid sequencing techniques a body of remarkable data has begun to accumulate. Already the genomes of a number of simple viral organisms and numerous individual genes have been defined. Clearly the simple repetitive character of base and amino acid sequences is ideally suited to treatment by computer. Computers are a practical necessity for error-free copying of sequences, for transferring sequence data and for providing a number of useful analyses of composition, size, position of simple features, and translation by the genetic code. Computers can also detect subtle patterns in the organization of genes and proteins and have shown that many genes and proteins contain repeated structural elements. A simple method for the detection of regions of repeatedness, similarity or reverse complementarity has been developed using an enhanced graphic matrix (GM) analysis. A series of programs, collectively called REVEAL, have been prepared for use on a microcomputer utilizing graphics and printed outputs. GM analysis has the advantage over numerical matrix and plotted listings of simplicity, speed, low cost, esthetic quality, and facility of the investigator's interaction with all the data. Examples using monochrome and colored GM analyses will be presented of evolutionary comparisons, of globins and immunoglobulins, secondary structure analyses, and applications to sequence determination. In addition examples will be given of other uses of graphics in detection of complex features such as the splice sites for intervening sequences of higher organisms and promoter sites for prokaryotic RNA polymerase.

M-AM-A1 MASS BALANCE IN A SINGLE STAGE OF A MULTISTAGE MODEL OF THE RENAL MEDULLA. John L. Stephenson, NHLBI, NIH, Bethesda, Maryland 20205.

In earlier work (1,2) it has been shown that the mass balance equation for both single and multinephron models of the renal medulla can be cast into the normalized form

$$r = 1/[1 - f_T(1 - f_U)(1 - f_W)],$$

where r is the ratio of total osmolality at the papilla (assumed approximately the same in all structures) to plasma osmolality; f_T is fractional solute transport out of ascending Henle's limb; f_U is the fractional urine flow; and f_W, the fractional dissipation in the vascular exchanger, is a measure of the solute that is returned to the systemic circulation by ascending vasa recta unaccompanied by its isotonic equivalent of water. This form of the mass balance equation has proved very useful in understanding the qualitative behavior of medullary models and in checking detailed calculations.

We now show that with suitable interpretations of f_T, f_U, and f_W, one can derive a form of the equation that is applicable to a single stage of a multistage model. Applied recursively this form permits a much finer analysis of the behavior of multistage systems than was previously possible.

1. Stephenson, J. L. 1973. Biophys. J. 13:512-45.
2. Stephenson, J. L. 1976. Biophys. J. 16:1273-86.

M-AM-A2 Mg^{++}- ATPASE OF THE RED CELL MEMBRANE MAY FUNCTION AS AN ION PUMP

Rhoda Blostein and William Harvey. Division of Hematology, Royal Victoria Hospital and Departments of Medicine and Biochemistry, McGill University, Montreal, Canada.

Mg^{++}-ATPase activity of inside-out human red cell membrane vesicles is stimulated up to 3-fold by protonophores, namely dinitrophenol (DNP), carbonylcyanide m-chlorophenylhydrazone (CCCP) and carbonylcyanide p-trifluoromethoxyphenylhydrazone (FCCP). This stimulation is inhibited by oligomycin and is not observed following detergent (triton X-100)-disruption of the vesicular structure. From measurements of ATP-dependent changes in the ^{86}Rb content of vesicles pre-equilibrated with ^{86}Rb in the presence of valinomycin, it is suggested that this ATPase of inverted vesicles gives rise to a membrane potential, interior positive. We suggest that Mg^{++}-ATPase of the red cell membrane may function as an electrogenic (H^+?) pump. (Supported by the Medical Research Council of Canada).

M-AM-A3 CHLORIDE NET TRANSPORT OF THE HUMAN ERYTHROCYTE AT LOW EXTRACELLULAR CHLORIDE CONCENTRATIONS. O. Frӧhlich, University of Chicago, Dept. Pharmacol. Physiol. Sciences, Chicago IL 60637.

Net chloride efflux from intact red cells was measured in the presence of valinomycin as net tracer chloride efflux and as net potassium efflux into media of different extracellular chloride (Cl_o) and potassium (K_o) concentrations. Cl efflux (as determined by K efflux) into media of constant K_o and varying Cl_o was a nonlinear function of the chloride gradient. At K_o=2 mM and $Cl_o \leq 0.5$mM the flux was 40-50 meq/(kg cell solids·min) at 25°C and fell hyperbolically to about 10 meq/(kg cell solids·min), with half the decrease occurring at Cl_o= 2-3 mM. This nonlinear behavior is expected from the simple kinetic ping-pong scheme which we have used to model chloride exchange transport (Gunn and Frӧhlich, J.Gen.Physiol. 74:351, 1979) and which was modified to include net transport. According to this model, the concentration of Cl_o which half inhibits net efflux should be identical with the half-saturation constant of Cl_o-stimulated chloride exchange flux which we have determined independently to be about 3 mM. The agreement between these two experimental values strongly supports the model.

The effect of membrane potential (V_m) on net transport was determined in net tracer chloride efflux experiments at constant Cl_o and varying K_o. At high K_o (small inside negative V_m) net efflux was less than at small K_o (large negative V_m). This is to be compared with the observation that chloride exchange transport was not affected by the membrane potential. We conclude from these data that the empty transporter site which moves inward in the net efflux transport cycle bears a positive charge and that the loaded site bears no net charge.

Supported in part by NIH grants HL-20365 and GM-28893.

M-AM-A4 K^+ PUMP FLUXES AND PASSIVE K^+ PERMEABILITIES IN LARGE AND SMALL ERYTHROCYTE VOLUME POPULATIONS OF ANEMIC HIGH AND LOW K^+ SHEEP. P.K. Lauf and G. Valet*, Dept. Physiol. Duke Univ. Med. Ctr., Durham, N.C. 27710, & Max Planck Inst. Biochem. 8033 Martinsried,W-Germany.

Massively bled sheep produce large reticulocytes which appear 5-6 d later in the peripheral circulation. In low K^+ (LK) sheep these new cells experience major changes in steady state cationcomposition and K^+ transport (J.Gen.Physiol. 76:1980,109) while reticulocytes from high K^+ (HK) sheep have not yet been studied. To follow-up the changes in the newly released red cells, we have separated them from the older, smaller cells on consecutive days by elutriation centrifugation as verified by flow cytophotometry. Appearance of large cells coincided with the reticulocyte peak in whole blood and with 50% reticulocytes among the large cells. Disappearance of reticulum occurred within 2-3 d and was not accompanied by a likewise cell volume reduction. At early times, both HK and LK reticulocytes had very high K^+ contents which fell to respectively different steady state levels without major inverse changes in the Na^+ content. No such changes were seen in the older, smaller cell population. In both unseparated HK and LK red cells K^+ pump influx rose 3-6 fold after bleeding which was entirely due to the appearance of large cells with very high K^+ pump fluxes. The K^+ pump density (molecules ^{3}H-ouabain/mu^2 surface area) was only severalfold higher in the large reticulocytes than in the smaller cells. Hence the early high K^+ pump activity of both HK and LK reticulocytes is due to an increased number of K^+ pumps with a pump turnover several fold higher than that in adult cells. The drop of K^+ pump activity was more related to turnover changes than to a loss of sites. Concomittantly, the ouabain insensitive passive K^+ permeability was increased 6-10 fold in both HK and LK reticulocytes, only, and fell almost parallel with the K^+ pump activity. Hence quantitative and kinetic K^+ pump changes accompany the membrane maturation in HK and LK sheep reticulocytes. (Supp.by NIH grant 2 P01-12,157).

M-AM-A5 STEADY AND TRANSIENT STATE KINETICS OF ERYTHROCYTE ANION EXCHANGE. EVIDENCE FOR COOPERATIVITY IN SUBSTRATE AND INHIBITOR BINDING SUGGESTING SITE-SITE INTERACTIONS WITHIN THE BAND 3 PROTEIN DIMER, J.M. Salhany*, Elizabeth D. Gaines and Randy Sullivan, VA Medical Center & Depts. of Internal Medicine & Biomedicinal Chem. Univ. of Nebraska Medical Center, Omaha, Nebr. 68132.

We investigate the origin of the non-hyperbolic transport kinetics characteristic of the erythrocyte membrane anion exchange system. Steady state measurements of reversible single and multiple inhibition, as well as presteady state measurements, are presented. "Zero-trans" heteroexchange measurements which show negative cooperative transport, reveal that the degree of negative cooperativity is non-linearly dependent on stilbene disulfonate concentration, such that at low concentrations, the inhibitor enhances the degree of negative cooperativity. This is a classic result for a two site (i.e. two transport site) system, with site-site interactions and the inhibitor mimicking the substrate. A partially concerted dimeric model for band 3 protein function is presented and tested which explains how these cooperative effects can occur despite the presence of linear Dixon plots and a linear dependence of $K_{i-app.}$ on substrate concentration. Transient state measurements of divalent anion transport are also shown which confirm the presence of site-site interactions within a dimeric functional unit.

*J.M. Salhany is an Established Investigator of the American Heart Association.

M-AM-A6 CHARACTERISTICS OF VOLTAGES ASSOCIATED WITH Ca-INDUCED K CONDUCTANCE IN HUMAN RED BLOOD CELLS, AS STUDIED BY MEANS OF A FLUORESCENT OXONOL DYE, WW781. **Jeffrey C. Freedman and Terri S. Novak, Dept. of Physiology, SUNY-Upstate Med. Ctr., Syracuse, N.Y. 13210.**

The divalent anionic oxonol dye, WW781, is a rapidly responding fluorescent indicator of changes in the transmembrane potential of human red blood cells. In this study, WW781 was used to monitor and characterize the voltage changes associated with the selective increase of K conductance caused by elevated internal Ca, as induced by the Ca ionophore A23187 in the presence of Ca_o. The maximal hyperpolarization at low K_o occurs at 0.5 μM A23187 in 1.2% HCT buffered isotonic suspensions, and is slightly greater than that induced by valinomycin. With 500 μM EGTA, the voltage response to Ca is sigmoidal; half-maximal activation occurs at 200 μM Ca_o corresponding to an ionized Ca_o^{+2} of about 0.1 μM. The voltage changes are reversed by addition of excess EGTA, are partially inhibited by oligomycin (10 μg/ml) and by quinine (200 μM), and are not appreciably affected by up to 5 mM external $MgCl_2$. Between pH 6.5 and 7.5, the voltage change is maximal and insensitive to pH; outside of this pH region, K-activation of the voltage response is apparent. At pH 7, with 500 μM external Ca and EGTA, in either fresh or substrate-depleted cells, the hyperpolarization elicited by 1 μM A23187 monotonically decreases as K_o is increased from 0.1 to 150 mM by isotonic substitution with Na_o, until depolarization is evident when the normal K-gradient is reversed. However, at pH 6 in fresh cells, the voltage exhibits progressively greater hyperpolarization as K_o is increased from 0.1 to 1 mM, and then less hyperpolarization at higher K_o. This biphasic dependence on K_o, most evident at low pH, confirms the existence of a K-selective modifier site on the outward-facing side of the mechanism responsible for the Ca-induced K conductance. **Supported by USPHS grants 5S07RR05402-18 and 1R01GM28839-01.**

M-AM-A7 TEMPERATURE DEPENDENCE OF STEADY-STATE K AND Na LEVELS, ION FLUX, ATP, AND Na,K-ATPase IN HUMAN LYMPHOCYTES. W. Negendank & C. Shaller, Hematology-Oncology Section, Hosp. of the Univ. of Pennsylvania, Philadelphia, PA 19104.

The steady-state of ion levels between 0 and 37° C was defined rigorously by time courses over 24-48 hours; degree of reversibility was established; and cell viability, water content, total ions, Ca, Mg, and ATP were shown not to be confounding variables. Time-independent (steady-state) levels of cell Na and K are normal between 37 and 10°, and then change abruptly so that at 3° half of cell K is replaced (reversibly) by Na. The rate constant of steady-state isotopic Na exchange is unchanged between 37 and 10°, and then decreases below 10°. The rate constant of steady-state isotopic K exchange decreases markedly between 37 and 20°, and then levels off between 15 and 0°. The Na- and Na,K-ATPases in a plasma membrane-enriched preparation show a typical marked temperature dependence and a transition at 15-20°. There is no evident correlation between the critical temperature of the steady-state ion contents and the temperature-dependent behavior of steady-state ion exchange, no coupling between the steady-state Na exchange and the steady-state K exchange, and no correlation between either the ion levels or the ion fluxes and the activity of the Na,K-ATPase. At 0°, the steady-state Na level of cells in 145 mM external Na is near that of the medium; however, the Na level of cells in 19 mM external Na rises to become 6 times that of the medium at the same time that cell K is 9 times that of the medium. This simultaneous net accumulation of both Na and K at 0° is unexpected on the basis of known properties of the Na,K-ATPase pump. The results are discussed in terms of temperature effects upon membrane phospholipid, protein (enzyme) and water, and in terms of a cytoplasmic cooperative ion adsorption-desorption model. (Supported by the VA and ONR).

M-AM-A8 GLYCOLYSIS IN EHRLICH ASCITES TUMOR CELLS ACTIVATES ACTIVE ELECTROGENIC PROTON EFFLUX. Agnes Heinz, George Sachs and James A. Schafer, Nephrol. Res. & Training Ctr., and Lab. Membrane Biol., Univ. of Alabama in Birmingham, Birmingham, AL 35294

When 10 mM glucose is added to a suspension of Ehrlich ascites tumor cells in a 1.5 mM phosphate buffer solution (pH 7.4), the extracellular medium is acidified to a pH of 5.3-5.6 within 20 min. Addition of the protonophore tetrachlorosalicylanalide (TCS, 5μM) after the pH has dropped below 6.2 results in a transient alkalinization of 0.1-0.2 pH units followed by resumption of the acidification. We interpret this to show that at the point of TCS addition, the internal pH exceeded that of the medium. This was confirmed by measuring acridine orange absorption in the cell suspension with a dual beam spectrophotometer. Distribution of this pH-sensitive dye showed that immediately after glucose addition the intracellular pH decreased below that of the medium but then slowly became greater. The voltage-sensitive dye diethyloxydicarbocyanine (DOCC) showed that the cells dramatically hyperpolarized immediately after glucose addition, and that this hyperpolarization could be prevented or reversed by TCS or valinomycin but not by nigericin or ouabain. Valinomycin (also nigericin and TCS after a short delay) increased the rate of acidification caused by the addition of glucose. The hyperpolarization was also confirmed by using tetraphenylphosphonium (TPP^+): glucose increased the steady-state TPP^+ distribution ratio from 77±5 (SD) to 167±4, but TCS reduced it to 9±1. The observed increase in TPP^+ uptake was equivalent to a hyperpolarization of >100 mV more negative than the original membrane voltage of -30 to -40 mV. The hyperpolarization was not prevented by any of several combinations of mitochondrial inhibitors including: oligomycin, up to 100 μM of TPP^+, rotenone, CN^-, amytal and up to 20 nM TCS. We conclude that an active H^+ efflux pump is activated during glycolysis.

M-AM-A9 QUANTUM EFFICIENCY OF LIGHT DRIVEN METABOLITE TRANSPORT IN *RHODOSPIRILLUM RUBRUM*. Michael E. Zebrower and Paul A. Loach. Department of Biochemistry and Molecular Biology, Northwestern University, Evanston, IL 60201.

Light-driven uptake of L-alanine and L-malate have been examined with whole cells of *Rhodospirillum rubrum*. An all-glass apparatus was designed for anaerobic studies of metabolite transport under conditions of exactly known light intensities. In addition, the apparatus was designed so that it was possible to adjust the environmental potential to preselected values in order that this parameter could be controlled and evaluated. ^{14}C-Labeled L-alanine and L-malate were used to facilitate the assay for their uptake after an exposure to light. Cells were collected and counted by filtering on a Millipore filter. Dark or background levels of transport were found to be high in the presence of oxygen but were typically less than 0.1 Mμmoles taken up per min per mg of cells (dry wt) under anaerobic conditions. Maximal light-driven uptake was found to be 1.75 Mμmoles/min/mg cells for L-alanine and 1.70 Mμmoles/min/mg cells for L-malate. These are comparable to the highest values reported for such transport in photosynthetic bacteria. Under appropriate conditions these high rates of transport could be maintained to light intensities several orders of magnitude lower than those used in previously reported studies and thus higher efficiencies of metabolite transport were obtained. The effect of inhibitors, cations and small molecules which interact with the electron transport and membrane system are being examined. This research was supported by the U.S. Public Health Service (NIH Grant No. GM-11741) and the National Science Foundation (Grant No. PCM-7816669).

M-AM-A10 MEMBRANE REFLECTION COEFFICIENTS FOR VOLUME FLOW AND SOLUTE FLOW ARE NOT EQUAL IN NONIDEAL, NONDILUTE SOLUTIONS. M.H. Friedman and R.A. Meyer, Applied Physics Laboratory, The Johns Hopkins University, Laurel, MD 20810

The Kirkwood formulation of the Stefan-Maxwell equations is used to develop the transport equations for a membrane bounded by nonideal, nondilute solutions. The theory predicts that the reflection coefficients for volume flow and solute flow are not equal under these conditions, but are related by a simple expression which depends on the concentration of the bounding solutions. The ratio of the two coefficients is independent of heteroporous membrane structure and the thickness of adjacent boundary layers. Experimental measurements of these reflection coefficients for sucrose transport across Cuprophan verify this prediction. The two reflection coefficients may be made operationally identical by a simple redefinition of the osmotic driving force.

(Work supported in part by the Department of the Navy under Contract No. N00024-78-C-5384)

M-AM-A11 Na-Ca EXCHANGE: A THERMODYNAMICALLY-CONSTRAINED KINETIC MODEL AND ROLE IN E-C COUPLING. J.M. Kootsey, E.A. Johnson, Dept. Physiology, Duke University Medical Center, Durham, NC 27710.

A kinetic model of transmembrane Na-Ca exchange has been constructed using thermodynamic principles employed previously to formulate a kinetic model for Na-K active transport (J. Theor. Biol. 80:405, 1979). The stoichiometry in the model was

$$3[Na^+]_o + [Ca^{++}]_i \rightleftharpoons 3[Na^+]_i + [Ca^{++}]_o.$$

The expected deviation from simple mass-action kinetics was anticipated by assuming first order dependence of the forward and backward rates on sodium concentration and half-power dependence on calcium concentration. The thermodynamically-required dependence on membrane potential was satisfied either by symmetric exponential functions of Vm/2 for the forward and backward rates or by asymmetric functions. The current generated by such an exchange was added to the membrane current needed to generate a cardiac-like action potential and the differential equation for internal calcium concentration was solved simultaneously with that for the transmembrane potential. The behavior of the model was compared with published data for frog cardiac muscle where sarcolemmal transport of calcium appears to predominate. When the density of exchange sites (the only adjustable parameter in the exchange model) was such as to cause the exchange to approach equilibrium, the internal calcium concentration increased to a value similar to values reported during contracture. However, distortions of the action potential produced by such exchange are only acceptable if the number of intracellular binding sites is negligible. Supported in part by USPHS grant HL-12157.

M-AM-A12 REGULATION OF HYDROLYSIS OF PHOSPHORYLATED $(Na^+ + K^+)$ATPase BY Ca^{++}. Edward S. Hyman, Touro Research Institute, New Orleans, Louisiana 70115

The hypothesis that a phospholipid pore gates access to the phosphorylation site of $(Na^+ + K^+)$ATPase (E) (Hyman, Biophys. J., 16,28a, 1976; 17, 185a, 1977) calls for Ca^{++} to inhibit $E\cdot{}^{32}P \xrightarrow{k_4} {}^{32}P_i$; but prior work shows that the unimolecular decay constant, k_d, of $E\cdot{}^{32}P$ from rabbit kidney in the presence of 10 mM K^+ is almost unaffected by 10mM Ca^{++} and is inhibited by 30 mM Ca^{++}. These concentrations are too high to explain the effect of Ca^{++} on the overall kinetics of E. Epstein and Whittam (Biochem J., 99,232,1968) found $<$0.5 mM CaATP to be a competitive inhibitor of MgATP using E frim kidney and rbc, and Robinson (BBA, 341,232,1974) found $<$0.3 mM Ca^{++} to be a mixed inhibitor using brain E. Nor does 1 mM Ca^{++} significantly inhibit rapid phosphorylation of E. There most of the effect of CA^{++} can be explained by its competitive binding of ATP in free solution (Hyman, Biophys. J., 21, 12a, 1978). Using E from brain, Tobin et al. (Mol. Pharm., 9, 336,1973) found $E\cdot{}^{32}P$ formed with added Ca^{++} (instead of added Mg^{++}) to be more sensitive to ADP than to K^+. Fukushima and Post (J.B.C., 253,6853,1978) found that the k_d of $E\cdot{}^{32}P$ formed with Ca^{++} equals that formed with Mg^{++}, and that with E of kidney 30 mM Ca^{++} was necessary to form $E\cdot{}^{32}P$ which is more sensitive to ADP than to K^+. But k_d is an ambiguous measure of k_4. Assuming a single pathway through $E\cdot P$ to P_i, the true k_4 can be obtained from $v/E\cdot{}^{32}P$ in a steady state. Using kidney and 40 μM ATP at 37°C, k_4 is very sensitive to Ca^{++}, with inhibition detectable at μM levels of Ca^{++}. This suggests that even intracellular Ca^{++} could regulate k_4. The Mg^{++} phosphoenzyme treated with Ca^{++} for 1 second behaves like the Ca^{++} $E\cdot{}^{32}P$. This suggests that contaminant Mg^{++} may complicate the study of Ca^{++} $E\cdot P$, NIH AM 12718 and Glazer Medical Fund

M-AM-B1 LIPID-PROTEIN INTERACTIONS IN MEMBRANES CONTAINING THE ACETYLCHOLINE RECEPTOR. J. Ellena, A. Dalziel, E. Rollins and M. McNamee (Intr. by R. Baskin). Dept. of Biochem. and Biophys., Univ. of Calif., Davis, CA 95616.

Interactions between Torpedo californica acetylcholine receptor and its lipid environment have been studied in native acetylchlone receptor-rich membranes and in reconstituted vesicles containing purified receptor and defined lipid components. Mobile and immobile components were observed in the electron spin resonance spectra of native membranes containing 16-doxyl stearic acid. Removal of peripheral membrane proteins by alkaline extraction (Neubig, R.R. et al. Proc. Natl. Acad. Sci. USA 76, 690 (1979)) increased the mobility of the bulk lipid but did not signficantly affect the immobile component.

Solubilized acetylcholine receptor was incorporated into functional vesicles using a cholate dialysis technique. Activity was assayed by measuring agonist stimulated cation influx into the reconstituted vesicles. Specifically, the increased uptake of $^{86}Rb^{+}$ in response to 1 mM carbamylcholine was monitored using ion exchange columns or Millipore filtration to separate vesicles from free external ions. Agonist-induced influx into vesicles reconsituted with phsophatidylethanolamine and phosphatidylserine (molar ratio 3:1) required the presence of 25-50 mole % cholesterol. Cholesterol increased the order parameter of 5-doxyl stearic acid from 0.58 with no cholesterol to 0.63 with 50% cholesterol. Studies of the effects of lipid composition on lipid-protein interactions in the reconstituted vesicles are continuing.

M-AM-B2 LIPID TAIL GROUP DEPENDENCE OF THE fd COAT PROTEIN CONFORMATION. S. P. A. Fodor, and A. K. Dunker; Biochemistry/Biophysics Program and Chemistry Department, Washington State University, Pullman, WA 99164

Lipid/protein interactions form the foundation of biological membrane structure and function. It has been a strong implicit assumption that one hydrophobic environment would be pretty much like another, and thus (apparently) no one has inquired whether changes in the lipid tail group could lead to changes in the structure of the membrane associated protein. In our studies of model membrane systems containing the fd coat protein and various individual lipids, we have found that the lipid tail group dramatically affects the protein conformation.

Specifically we have found that the DPPC and DMPC promote the formation of a β-sheet conformation for the fd coat protein. We refer to this as the c-state conformation.

In contrast, unsaturated lipids such as egg PC and DOPC promote the formation of an α-helical conformation. We refer to this as the b-state conformation.

If the protein is first put into saturated lipids (DPPC), addition of excess unsaturated lipids followed by sonication to mix the lipids brings about conversion from the c-state to the b-state. Reversing the order of addition of lipids induces the b-state to c-state change.

The same structural changes can be observed without sonication if appropriate detergents are used. If deoxycholate is removed by dialysis from mixtures of the coat protein and DPPC, the coat protein is found to convert from the b-state to the c-state. Addition of SDS to DPPC/coat protein mixtures brings about the c-state to b-state conversion. We will present an hypothesis to account for the driving force for the structural change, but we welcome any and all suggestions.

M-AM-B3 STRUCTURAL STUDIES OF CYTOCHROME OXIDASE MEMBRANES IN A RECONSTITUTED SYSTEM BY X-RAY DIFFRACTION; A. Tavormina, M. Erecinska, and J.K. Blasie; University of Pennsylvania, Philadelphia, PA 19104

Cytochrome c oxidase was purified from beef heart mitochondria and reconstituted with an egg lecithin/cardiolipin/lauryl maltoside mixture by dialysis. The resulting preparation occurred as a single band of density 1.10 on a sucrose gradient. It was composed of unilamellar vesicles as shown by electron microscopy. The vectorial distribution of the cytochrome oxidase across the vesicle membrane was tested by several methods. Rates of oxygen consumption, measured before and after solubilization of the membranes by lauryl maltoside, indicate that 40% of the oxidase molecules are situated with their cytochrome c binding side facing out. Likewise, spectroscopic measurements of the reducibility of cytochrome a by cytochrome c when electron flow is blocked by azide also give a 40%/60% distribution in intact vesicles. Work is in progress to verify these sidedness estimates using other techniques.

The lamellar X-ray diffraction obtained from partially dehydrated multilayers of the unilamellar vesicles was phased to 20A resolution by the swelling method. The resulting electron density profile contains 2 asymmetric membrane profiles per unit cell. Efforts to separate the lipid and protein contributions to the membrane profile by variation of the lipid/protein ratio of the reconstituted membranes are in progress. (This work supported in part by NIH grant HL18708.)

M-AM-B4 EFFECT OF LIPID BILAYER STRUCTURE ON ATP HYDROLYZING ACTIVITY OF THE Ca-PUMP PROTEIN OF SARCOPLASMIC RETICULUM. B.M. Moore*, B.R. Lentz, M. Hoechli, and G. Meissner. Departments of Biochemistry and Anatomy, University of North Carolina, Chapel Hill, N.C. 27514.

The effects of structurally different lipid environments on Ca-ATPase activity of sarcoplasmic reticulum (SR) have been studied by transferring the enzyme into dilauroyl-, dimyristoyl-, dipentadecyl-, dipalmitoyl-, and palmitoyl,oleoyl-phosphatidylcholine bilayers using a procedure that replaced greater than 99% of the endogenous SR lipid. Freeze-fracture electron microscopy revealed vesicular structures and showed that the Ca-ATPase was incorporated into the bilayers. Enzymatic analysis indicated that the saturated acyl chains inhibited both overall ATPase activity and Ca-dependent phosphoenzyme formation below the lipid phase transition temperature (T_m), as measured in the lipid-protein recombinants by diphenylhexatriene fluorescence. At temperatures above T_m, ATPase activity but not phosphoenzyme formation was critically dependent on phospholipid acyl chain length and thus bilayer thickness. No activity was observed in dilauroyl-phosphatidylcholine bilayers. Use of the nonionic detergent dodecyloctaethylene glycol monoether demonstrated that the absence of activity was not due to irreversible inactivation of the enzyme. Increased bilayer thickness resulted in increased levels of activity. Incorporation of the enzyme into phospholipids containing one double bond produced vesicles that supported ATPase activity equivalent to that in SR. These results indicate that the Ca-ATPase requires for optimal function a "fluid" membrane, a minimal bilayer thickness, and perhaps the presence of unsaturated phospholipid acyl chains. Supported by NSF grant #PCM7922733 and USPHS grant #AM18687 and done during the tenure of an American Heart Association Established Investigator Award to BRL.

M-AM-B5 EPR AND SATURATION TRANSFER (ST-EPR) STUDIES OF THE MOTION OF SPIN-LABELLED D-β-HYDROXYBUTYRATE DEHYDROGENASE (BDH), A LECITHIN-REQUIRING ENZYME. J. Oliver McIntyre, Stephen Brenner, Norbert Latruffe, *Larry R. Dalton and Sidney Fleischer (Intr. by J. H. Venable), Dept. of Molecular Biology, Vanderbilt University, Nashville, TN 37235 and *Dept. of Chemistry, SUNY, Stony Brook, NY 11794.

BDH can be selectively labelled with NEM at either of two sulfhydryl moieties so that the enzyme is either inactivated or fully functional (Latruffe, Brenner and Fleischer, Biochemistry, in press). This methodology has been used to selectively label BDH with a sulfhydryl spin label, 3-maleimido-2,2,5,5-tetramethyl-1-pyrrolidinyloxyl (SL5) to obtain BDH-SL5. The EPR spectra of BDH-SL5 inserted into phospholipid vesicles indicates slow motion. The apparent rotational correlation time (τ_c) of BDH-SL5 was estimated from the ST-EPR spectra by comparison with a calibration curve of H"/H versus τ_c for the isotropic rotation of hemoglobin-SL5. The enzyme labelled at either the essential or non-essential sulfhydryl gave similar motional characteristics when inserted into mitochondrial phospholipid vesicles. A linear Arrhenius plot of BDH activity is obtained in phospholipid which does not undergo a phase transition (2-25°C) and no significant change in τ_c (4×10^{-5} sec) for BDH-SL5 is observed in this temperature range. However, BDH inserted into a phospholipid codispersion which undergoes a liquid crystalline to gel transition at 19±1°C, exhibits a biphasic Arrhenius plot for BDH activity with a break at the transition temperature. τ_c of BDH versus temperature in this same phospholipid codispersion exhibits a significant decrease from about 4×10^{-5} (25°C) to 1×10^{-4} sec at 2°C. Thus, a change in the phospholipid, from liquid crystalline to gel, state can modulate both functional and motional characteristics of BDH in the membrane. [Supported by NIH AM 21987]

M-AM-B6 A NEW PEPTIDE-PHOSPHOLIPID MODEL FOR A SITE OF ANESTHETIC ACTION. J.R. Trudell, H.J. Galla, B. Bosterling. Department of Anesthesia, Stanford University School of Medicine, Stanford, CA 94305.

Recent evidence suggests that the site of action of inhalation anesthetics may be a phospholipid-protein interaction in nerve cell membrane. We have prepared a model for peptide-phospholipid interaction by adding the positively-charged antibiotic polymyxin to vesicles of phosphatidic acid. Polymyxin interacts strongly with phosphatidic acid membranes, causing lateral phase separations. The phase transition of the polymyxin-phosphatidic acid domain, measured by electron paramagnetic resonance using the spin-probe 2,2,6,6-tetramethylpiperidine-1-oxyl (TEMPO), is decreased by about 20° compared to a pure phosphatidic acid bilayer. The phosphatidic acid matrix surrounding these domains exhibits a broadened and lowered phase transition due to the presence of some monomeric polymyxin. Addition of the inhalation anesthetic methoxyflurane progressively disrupts the polymyxin-induced lateral phase separation leading to a homogenously dispersed phase at concentrations above 100 mmol anesthetic/mol lipid. A concentration of 30 mmol methoxyflurane/mol lipid corresponds to clinical anesthesia. At this concentration, the phase transition temperatures of the free phosphatidic acid and of the polymyxin/phosphatidic acid domains are lowered and the phase transition widths are broadened. This model system provides a clear example of the disruption of a peptide-induced lateral phase separation by an inhalation anesthetic. Supported by ONR Contract N00014-75-C-1021 and by NIH Grant 0H00622.

M-AM-B7 EFFECT OF PHOSPHOLIPID FLUIDITY ON INTERMEMBRANE TRANSFER OF INTRINSIC PROTEINS. Wray H. Huestis, S.L. Cook, and S.R. Bouma. Chemistry Department, Stanford University, Stanford, CA.

Transfer of intrinsic membrane proteins between intact cells and model membranes has been studied. Using intact erythrocytes as donor membranes and sonicated phosphatidylcholine vesicles as recipient membranes, the effects of membrane fluidity on protein distribution were examined. Two types of experiments were conducted to explore separately the effects of the donor and recipient membrane fluidity on the rate and extent of protein transfer. Binary mixtures of saturated phosphatidylcholines were used to generate phospholipid vesicles in gel, liquid-crystalline, and intermediate phase states at a single temperature. This permitted continuous variation of the fluidity of the recipient membrane while the properties of the donor membrane were held constant. In the reciprocal experiment, the phase state of the recipient membrane was held constant by selection of its phospholipid composition while the fluidity of the donor membrane was varied by changes in temperature. The rate and equilibrium extent of protein transfer were found to be sensitive functions of the relative fluidities of donor and recipient membranes, both being increased greatly where the recipient membrane is more fluid than the donor.

M-AM-B8 RETINAL ROD OUTER SEGMENT LIPIDS ARE ABLE TO FORM BILAYERS IN THE PRESENCE AND ABSENCE OF RHODOPSIN: A ^{31}P NMR STUDY. A.J. Deese*, E.A. Dratz, and M.F. Brown, Division of Natural Sciences, University of California, Santa Cruz, CA 95064 and Department of Chemistry, University of Virginia, Charlottesville, VA 22901.

We have examined the phase behavior of the lipids of the retinal rod outer segment (ROS) disc membrane using ^{31}P NMR. Our studies show that both ROS lipids and ROS membranes yield ^{31}P NMR spectra indicative of the lamellar phase under preparative conditions similar to those employed in our previous NMR studies (1,2). ^{31}P NMR spectra were obtained for the total chloroform: methanol extracted ROS lipids, as well as for column purified (either silicic acid or Sephadex LH-20) ROS phospholipids. In each case, the spectra were predominantly characteristic of the lamellar phase over the temperature range 5-45°C. These results disagree with a similar study of De Grip et al. (3), who reported that ROS lipids exist largely in the hexagonal phase in the absence of rhodopsin. The chemical shielding anisotropy of the ROS membranes and ROS lipid dispersions was found to be quite similar in our study. Thus we are able to draw the following conclusions: (i) both ROS membranes and ROS lipids exist largely in the lamellar phase under the conditions previously employed for NMR studies (1,2), (ii) rhodopsin does not greatly influence the degree of ordering of the ROS phospholipid head groups, (iii) no immobilized or ordered "boundary" lipid is detected, consistent with previous NMR studies of ROS membranes (1,2). However, under different conditions we have observed ^{31}P NMR spectra of total ROS lipids similar to the hexagonal phase of model systems. Further study is needed to fully understand the phase behavior of these interesting lipids. (Work supported by NIH grants 9F32 EY 05314 and R01 EY 00175 and by the Cystic Fibrosis Foundation.)

1) M.F. Brown et al., Meth. Enzymol. (L. Packer, Ed.) in press. 2) M.F. Brown et al., Biochemistry 16 2640 (1977). 3). W.J. De Grip et al., Biochim. Biophys. Acta 558, 330 (1979).

M-AM-B9 IMMUNOSPECIFIC TARGETING OF LIPOSOMES TO CELLS: A NOVEL AND EFFICIENT METHOD FOR COVALENT ATTACHMENT OF FAB' FRAGMENTS VIA DISULFIDE BONDS. F. Martin, Cancer Research Institute, UCSF, San Francisco, CA 94143

An efficient method for covalently crosslinking 50,000 dalton Fab' antibody fragments to the surface of lipid vesicles is reported. Coupling up to 600 μg Fab'/μmole phospholipid (about 6000 Fab' molecules per each 0.2 μ diameter vesicle) is achieved via a disulfide interchange reaction between the thiol group exposed on each Fab' fragment and a pyridyl-dithio derivative of phosphatidylethanolamine present in low concentrations (< 5m%) in the membranes of preformed large unilamellar vesicles. The coupling reaction is efficient, proceeds rapidly under mild conditions and yields well-defined products. Each vesicle-linked Fab' fragment retains its original antigenic specificity and full capacity to bind antigen. We have used Fab' fragments, coupled to vesicles by this method, to achieve immunospecific targeting of liposomes to cells in vitro. Vesicles bearing anti-human erythrocyte fragments bind quantitatively to human erythrocytes (at multiplicities up to 5000 0.2 μ vesicles per cell) while essentially no binding is observed to sheep or bovine red blood cells. Vesicle-cell binding is stable over a pH range 6-8 and is virtually unaffected by the presence of fresh human serum (50%). Cell-bound vesicles retain their aqueous contents and can be eluted intact from cells by treatment with reducing agents (DTT or mercaptoethanol) at alkaline pH. (Supported by NCI grant CA-25526-01).

M-AM-10 PROPERTIES OF A MG^{2+}-ATPASE OF TRANSVERSE-TUBULE MEMBRANES FROM RABBIT WHITE SKELETAL MUSCLE. Cecilia Hidalgo, Department of Muscle Research, Boston Biomedical Research Institute, 20 Staniford Street, Boston, MA 02114.

Transverse-tubule membranes isolated from rabbit fast skeletal muscle are highly enriched in cholesterol and display high Mg^{2+}-ATPase activity that is irreversibly inactivated by Triton X-100 but not affected by inhibitors of mitochondrial ATPase.

Arrhenius plots of the Mg^{2+}-ATPase activity revealed a break at 26°C, with activation energies above and below the break of 4.2 and 12.7 Kcal/mol, respectively. The optimum pH is 6.5, with 20% or 50% of the maximum activity remaining at pH 4.0 or 5.0, respectively.

Of several ionic and non-ionic detergents tested, only lysolecithin and sodium dodecyl sulfate solubilize the membrane and at the same time preserve enzymatic activity. Furthermore, extraction of transverse-tubule membranes with sodium dodecyl sulfate at low concentration results in partial purification of the Mg^{2+}-ATPase, which remains in the cholesterol-enriched insoluble fraction. These combined observations reveal that the Mg^{2+}-ATPase of transverse tubule membranes has properties that distinguish it from the Ca^{2+}-ATPase of sarcoplasmic reticulum.

(This work was supported by NIH grant HL-23007 and by a grant from the American Heart Association.)

M-AM-C1 ISOPROTERENOL HYPERPOLARIZATION OF CANINE CARDIAC PURKINJE FIBERS IS NOT MEDIATED BY ENHANCED NA^+/K^+ PUMP ACTIVITY. David C. Gadsby and Paul F. Cranefield, Laboratory of Cardiac Physiology, The Rockefeller University, 1230 York Ave., New York, N.Y. 10021.

β-catecholamine hyperpolarization of cardiac cells is often attributed to enhanced Na^+/K^+ pump activity. We used a two-microelectrode voltage clamp and fast-flow system to study the rapid, isoproterenol-induced hyperpolarization of small canine Purkinje fibers. In 4 mM K^+ solution, at holding potentials, V_H, near -40 mV, brief applications (e.g., 5-60 sec) of isoproterenol (1 nM - 1 μM) cause a temporary outward shift of net membrane current (the Figure shows the net outward current transients induced by 10 sec exposures to 50 nM isoproterenol). This effect is abolished by 10 μM propranolol but is unaffected by 1 μM phentolamine and it is unlikely to result from a temporary increase in the rate of electrogenic Na^+/K^+ exchange since the net outward current is recorded even in the presence of 2 μM acetylstrophanthidin or in K^+-free solution (Figure). On the other hand, the amplitude of the outward current shift is reduced either when V_H is moved towards the K^+ equilibrium potential, E_K, or when E_K is moved towards V_H (by raising external K^+ concentration; see Figure) suggesting that the outward current results from an isoproterenol-induced increase in steady-state membrane K^+ conductance. Supported by USPHS grant #HL-14899.

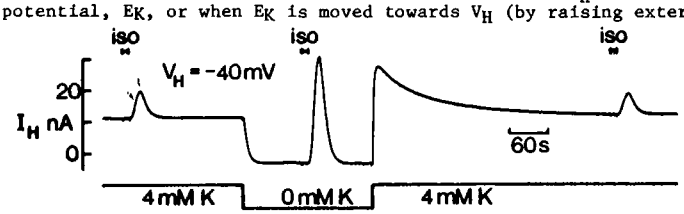

M-AM-C2 THE EFFECTS OF EPINEPHRINE ON THE RESTING MEMBRANE POTENTIAL, EXTRACELLULAR K ACTIVITY, AND THE ELECTROGENIC NA-K PUMP IN HEART MUSCLE. F.G. Martin, S.R. Houser, and A.R. Freeman, Dept. of Physiol., Temple Univ. Sch. of Med., Phila., Pa. 19140

Two components, the potassium equilibrium potential (E_K) and an electrogenic potential (Ep) generated by the Na-K pump, are thought to be the major contributors to the membrane potential (MDP) of cardiac muscle cells during diastole. Changes in these parameters resulting from epinephrine treatment of cat papillary muscle were studied. K^+-selective microelectrodes were used to measure changes in extracellular K^+ activity (aK_o^+) and voltage recording microelectrodes or sucrose gap techniques to determine changes in MDP. In normal Tyrode solution, muscles stimulated after a period of quiescence showed an initial depolarization of the MDP and an increase in aK_o^+. After reaching a plateau both parameters returned toward base line levels. When epinephrine was added to the bathing medium (10^{-7} M) MDP and aK_o^+ behaved differently during the period of stimulation. After reaching the plateau, MDP repolarized more rapidly and even hyperpolarized the membrane while aK_o^+ decreased more slowly and remained significantly higher than the predrive level. Upon returning to normal Tyrode solution, changes in both MDP and aK_o^+ during stimulation again followed the patterns observed before epinephrine treatment. These results suggest that epinephrine causes a shift in the relative contribution of the K gradient and the Na-K pump to the MDP with the result that the depolarizing tendency of increased aK_o^+ is compensated for by an increase in Ep. (Supported in part by NIH #HL22673 and a special investigatorship from AHA).

M-AM-C3 EVIDENCE FOR A ROLE OF SODIUM-CALCIUM EXCHANGE IN THE REGULATION OF CONTRACTILITY IN CHICK EMBRYONIC MYOCARDIAL CELL AGGREGATES. W.T. Clusin Stanford University School of Medicine, Stanford, Ca. 94305.

Na^+-dependent Ca^{2+}-efflux is thought to mediate relaxation and regulate contractility in certain types of cardiac muscle. Optical recordings from spontaneously-beating chick embryonic myocardial cell aggregates have revealed slow, exponential edge movement between action potentials, which does not behave in a manner consistent with viscoelasticity, and which can be shown to represent slowly decaying contractile force (Clusin, PNAS 77: 679). In the present study, sudden, partial replacement of extracellular Na^+ by Li^+ produced a prompt, progressive increase in the amplitude of contraction, along with selective slowing of the edge movement between beats. The time constant of the diastolic movement, which normally averaged 69±34 msec, increased 2-3 fold within a few sec. after 50% Na^+ replacement. Selective slowing of diastolic edge movement also occurred when aggregates were rapidly cooled from 37 to 34° C., or when staircase was produced by 2-3 sec. of pacing at 200-300 beats/min. Diastolic edge movement was selectively accelerated when spontaneous beating was slowed by hyperpolarizing current. These alterations of diastolic relaxation were not a direct consequence of changes in amplitude because movement between action potentials was unaffected by variations in amplitude that resulted from prematurity, spontaneous mechanical alternans, or prolongation of the action potential by depolarizing current pulses. These findings suggest: (1) That reduction of intracellular free Ca^{2+} between action potentials is largely mediated by Na^+-dependent Ca^{2+}-efflux; (2) That temperature- and rate-related changes in contractility may reflect alterations of Na-dependent Ca^{2+}-efflux; and (3) That recordings of contractile deformation in enzymatically-dispersed cardiac cells may be useful in monitoring small changes in intracellular free calcium. Similar phenomena may occur in intact adult cardiac muscle, but be concealed by the stiffness of connective tissue elements.

M-AM-C4 THE STOICHIOMETRY OF Na/Ca EXCHANGE IN THE MAMMALIAN MYOCARDIUM. S-S. Sheu and H.A. Fozzard, Department of Medicine, The University of Chicago, Chicago, Il. 60637.

Neutral ligands ETH 227 and ETH 1001, obtained from Professor Simon, were used to construct Na^+ and Ca^{2+} selective microelectrodes. The intracellular Na^+ and Ca^{2+} activities (a^i_{Na} and a^i_{Ca}) of sheep trabecular muscles from the right ventricle were measured. At resting state, the membrane potential V_m = -89.6 ± 3.0mV (S.D.), a^i_{Na} = 7.5 ± 3.7mM (8 exp.), and a^i_{Ca} = 99 ± 39nM (6 exp.) (this is equal to free Ca^{2+} concentration $[Ca^{2+}]_i$ = 310 ± 122nM by using Ca^{2+} activity coefficient of 0.32). If the Na/Ca exchange mechanism is in equilibrium, then the exchange number of n Na^+ to 1 Ca^{2+} can be calculated from equation $n = 2(V_{Ca}-V_m)/V_{Na}-V_m$, where V_{Na} is Na^+ equilibrium potential and V_{Ca} is Ca^{2+} equilibrium potential. This gave a result of n=2.5. When the Na^+ activity of external solution was decreased to 40%, V_m hyperpolarized approximate 3mV, a^i_{Na} decreased to 5.6mM and a^i_{Ca} increased to 288nM. The coupling ratio under these conditions was 2.6. In conclusion, the Na/Ca exchange mechanism in mammalian cardiac muscle has an exchange ratio for Na^+ and Ca^{2+} larger than 2. Therefore, it may be potential dependent. (Supported by HL-20592).

M-AM-C5 IONIC CHARACTERIZATION OF PACEMAKER CURRENT IN VOLTAGE CLAMPED RABBIT SA NODE. J. Maylie and M. Morad, Dept. of Physiol., Univ. of Penn., Philadelphia, PA, 19104

Measurement of paracellular K^+ activity under voltage clamp conditions in the SA node (Maylie et al., 1981, J. Physiol., 311) has shown that the pacemaker potential results from activation of an inward current with a reversal potential positive to the maximum diastolic potential (MDP). Cs^+ (2-5 mM) which is known to suppress the resting K^+ conductance reduced the rate of diastolic depolarization but hyperpolarized the MDP by 3 to 8 mV. Though the pacemaker current (I_p) was slightly reduced fro clamps between -55 and -75 mV, I_p was blocked (80-90%) with clamps between -80 and -120 mV. Other inhibitors of K^+ conductance (ba and TEA) had no affect on I_p and the pacemaker potential. These findings suggest that Cs^+ blocks I_p in potential dependent manner. The contribution of the slow Ca^{2+} and Na^+ current to I_p was tested by examining the effects of D600, Cd^{2+}, Mn^{2+} and reduced $[Ca]_o$. Ca-antagonists and reduced $[Ca]_o$ blocked the action potential, the slow inward current, developed tension and depolarized the muscle to -45 mV. However, following depolarizing clamp steps the preparation was still able to generate post-clamp hyperpolarization. Furthermore, I_p was suppressed in the pacemaker potential range, but was reactivated during larger hyperpolarizations. These results show that the slow inward current is not responsible for initiation of diastolic depolarization but may contribute to the diastolic depolarization as a result of its activation. Complete replacement of Na^+ with Tris blocked pacemaking activity and the preparation hyperpolarized to about -95 mV. I_p was completely blocked and hyperpolarizing clamps generated only K^+ depletion-type currents. These results show that SA nodal cells have a large resting TTX-insensitive Na^+ conductance which maintains the pacemaker potential positive to E_K. This Na^+ conductance is separate form the slow inward current and may contribute to generation of I_p and the initiation of diastolic depolarization.

M-AM-C6 MEMBRANE CONDUCTANCE CHANGES DURING THE TIME COURSE OF THE SLOW INWARD CURRENT IN FROG VENTRICLE. Leslie Tung* and Martin Morad, Dept. of Physiology, Univ. of Pennsylvania, Philadelphia, PA 19104

The single sucrose gap chopped-current clamp technique was used to study the slow inward current in frog ventricle. TTX was used to block the fast inward sodium current. The magnitude of the remaining transient inward current is maximal at 0 mV, reverses between +20 and +40 mV, increases with increasing Ca^{2+} and decreases with decreasing Na^+. The transient inward current is always followed by a slowly increasing outward current, which could not be dissociated from the inward current either by ionic or pharmacological blockers. To determine the relative contributions of inward and outward current components to the slow inward current, the time course of membrane conductance was measured during clamps to 0 mV. Total conductance was measured using small pulse perturbations. For large voltage excursions, the clamp steps were preceded by a 3-5 ms "overshoot" pulse in order to rapidly charge the membrane capacitance. The total conductance measured by clamps to rest increased with time, and the amplitude of the resulting "tail" currents reached a constant value. The instantaneous I-V relations measured at 50-100 ms into the clamp were found to have a marked non-linearity for potentials negative to -20 mV. Ba^{2+} (20-50 μM) was found to reduce the degree of non-linearity, implicating the activation of the inwardly rectifying K^+ current. In the presence of Ba^{2+} the magnitude of the transient inward current relative to late outward current increased. During the time course of the clamp, the total membrane conductance still increased, while the amplitude of tail currents now decreased. Ba^{2+} also reversed the ratio of plateau to rest conductance (normally higher at rest). Our results suggest that the slow transient current results from the activation and inactivation of a Ca^{2+}-dependent inward current accompanied by the activation of an outward current.

M-AM-C7 KCl vs VOLTAGE CLAMP CONTRACTURES IN FROG VENTRICULAR MUSCLE. M. Morad, S. Reech and M. Rao, Univ. of Penn., Dept., of Physiol., Philadelphia, PA, 19104.

High $[K]_o$ are used to generate contracture tension in skeletal and heart muscle. Conractures are thought to result directly from depolarizing effects of K^+, ignoring possible effects of K^+ on the Ca-transport system. We examined the effect of $[K]_o$ on the development of tension in ventricular strips (0.5 mm dia.) under voltage clamp conditions. Depolarization with 100 mM KCl produced 2-3 times less tension than generated by clamps to the same potential. Contractures generated by lower $[K]_o$ were also smaller than those produced by appropriate clamp steps. Contracture tensions were also higher when clamp-induced depolarzations were achieved slowly, to mimic the time course of KCl depolarizations. The discrepancy between KCl and clamp depolarization was largest at lower $[Ca]_o$ (0.2 mM). These results are consistent with the finding that increasing the $[K]_o$ from 3-6mM suppresses while decreasing $[K]_o$ from 3-1mM enhances the tension generated at each clamp step. When $[K]_o$ was increased during the time course of a clamp step, tension decreased rapidly. These results suggest that increases of $[K]_o$ have direct negative ionotropic effect on the Ca^{2+} transport mechanism. K^+ selective μ-electrodes were used to measure how rapidly extracellular K^+ activity changes within the depth of the muscle when the bath K^+ concentration is changed. Measurements of K^+ activity at the surface and at the depth of the muscle simultaneous with development of contracture showed that K^+ diffuses much slower ($t_{\frac{1}{2}}$ 30-90 sec) than the spread of depolarization across the cross-section of the muscle. Thus the transient nature of KCl-contractures and their lower amplitude in heart muscle compared to the clamp-induced contractures may be due to the dual effect of K^+: its rapid depolarization of surface fibers, "clamping" the centrally located fibers, and the slow diffusion of K^+ into the tortuous extracellular space leading to suppression of tension.

M-AM-C8 CELLULAR CONNECTIONS AND PROPAGATION IN CARDIAC PURKINJE FIBERS. F.A.Dodge, IBM Research, T.J.Watson Research Center, Yorktown Heights, NY 10598.

Schoenberg, Dominguez, and Fozzard (SDF, 1975, J.G.P. 65: 441) have recently demonstrated that the cable constants of sheep Purkinje fibers depend on diameter as predicted from the number of similar cells in a cross section of the fiber. But they found that the membrane capacitance calculated from the foot of the action potential was independent of diameter, and concluded that the greater part of the total fiber capacitance is decoupled by a series resistance, presumably arising in the narrow clefts between cells. They also found, unexpectedly, that conduction velocity was independent of diameter. Taking advantage of the axial symmetry of the SDF model, I have computed impulse propagation using only a few parallel cables, one represented cells on the fiber surface, others, interior cells whose local circuit current flows through the clefts. I found that conduction velocity increased with diameter slightly less than the square root relation expected of a simple cable if the cells are connected radially with negligible resistance; but, velocity became independent of diameter when about half the series resistance is ascribed to the radial coupling resistance. The computations further showed that this coupling resistance would not affect measurements of passive cable constants, but that in large fibers the foot of the action potential of a surface cell would be distorted from a single exponential and the intracellular potential of an interior cell would have a much slower rate of rise.

M-AM-C9 ANALYSIS OF PACEMAKER OSCILLATIONS IN CHICK EMBRYONIC HEART CELL AGGREGATES. John R. Clay and Alvin Shrier, Lab. of Biophysics, NINCDS, MBL, Woods Hole, MA 02543; Dept. of Physiology, McGill University, Montreal, PQ, Canada H3G 1Y6; and Dept. of Anatomy, Emory University, Atlanta, GA 30322.

Reaggregates of 7 day old chick embryonic heart cells beat spontaneously at irregular intervals with a mean rate of 1 beat/10 sec in tissue culture medium containing 2.5mM K_o. Intracellular recordings revealed subthreshold pacemaker oscillations in membrane potential during the interbeat interval (IBI). These oscillations could also be induced by injection of current into aggregates made quiescent by application of TTX (3 μM). Voltage clamp analysis revealed an underlying time dependent pacemaker current (I_{K_2}) which we have characterized elsewhere (Shrier and Clay, 1980, Nature, 283, 670-71; Clay and Shrier, 1981, J. Physiol., In press). The voltage clamp results were expressed in a mathematical model which was used to simulate the oscillations, both in control and in TTX conditions. The TTX sensitive sodium current I_{Na} was incorporated into the model using the Hodgkin-Huxley equations with slight modifications which appear to be appropriate to describe measurements of I_{Na} in aggregates (Ebihara et al., 1980, J.G.P. 75, 437-456). Small amplitude (noise level) current perturbations of the model produced a pattern of oscillations which grew in amplitude until AP threshold was reached. This result compared favorably with experimental records of spontaneous activity. The model failed to explain the relatively long duration IBI. The latter effect appears to be attributable to currents activated during the plateau phase of the AP.

Supported by grants from the NIH.

M-AM-C10 ELECTROPHYSIOLOGY OF HUMAN MUSCLE IN CULTURE. Michael B. Merickel, Richard A. Gray*, Priscilla Chauvin* and Stanley H. Appel*. Baylor College of Medicine, Houston, Texas 77030.

Human muscle obtained from biopsy specimens was grown in a primary tissue culture system and studied electrophysiologically. Myotubes with well-developed striations were formed three to five weeks in culture. The myotubes obtained stable resting potentials (-50 mV) and generated all-or-none action potentials (92 mV amplitude) when stimulated by anode break excitation. The resting permeability of the myotubes was found to be primarily dependent upon K^+ and to a lesser extend Na^+ ($P_{Na}/P_K = 0.14 \pm 0.06$). Changes in external Cl^- did not affect the resting potential or resting conductance of myotubes indicating that the Cl^- permeability is low compared to the permeabilities of K^+ and Na^+. A small but significant electrogenic Na-K pump component to the resting potential was identified at low K^+ concentrations (<10 mM) and with the pump inhibitor ouabain which caused a rapid 2 to 4 mV depolarization. The passive membrane parameters of myotubes were determined by analyzing the voltage decay transients of uniform fibers in response to the injection of a short hyperpolarizing pulse of current. The resting membrane resistance was 7780 ohm-cm^2; membrane time constant, 22.9 ms; membrane capacitance, 3.8 μF; and electrotonic length, 1.1. The identification of the electrical characteristics of normal human muscle grown in primary tissue culture will serve as the basis for detailed comparative studies on diseased human muscle. Support for this work was obtained from the Muscular Dystrophy Association and the Kleberg Foundation.

M-AM-C11 RELEASE OF MEMBRANE SIALIC ACID INDUCES VOLTAGE FLUCTUATIONS IN CULTURED HEART CELLS. M.L. Bhattacharyya and R.D. Nathan. Department of Physiology, Texas Tech University Health Sciences Center, Lubbock, TX 79430.

Spontaneously beating aggregates of 7-day embryonic chick heart cells were treated with neuraminidase (0.5-1.0 U/ml), an enzyme which catalyzes specifically the hydrolysis of sialic acids bound to glycoproteins, glycolipids, and oligosaccharides. Release of these anionic residues, as verified by a fluorometric assay for free sialic acid, resulted in shortening of the action potential, arrhythmic beating, and 2- to 10-mV depolarizing fluctuations in the membrane potential. Such voltage fluctuations were more frequent in high calcium (5.0 mM) or in caffeine (0.5-3.0 mM), but were less pronounced at lower temperatures (23-27°C). Neither tetrodotoxin (TTX; 10^{-5} g/ml) nor D600 (2×10^{-6} g/ml), which blocks the slow inward current, were able to prevent the perturbations. When neuraminidase was added in the presence of low calcium (0.9 mM), the aggregates beat 3- to 4-fold faster and eventually depolarized. In beating aggregates, voltage fluctuations occurred during diastole; however, whenever spontaneous activity had been inhibited by TTX (10^{-5} g/ml) or elevated potassium, the removal of sialic acid produced fluctuations in the resting potential which often initiated trains of slowly rising action potentials. These effects were diminished after about an hour but were not reversed by removing the enzyme. The addition of heat-inactivated neuraminidase, exogenous sialic acid, or phospholipase C (at concentrations up to ten times impurity levels) failed to reproduce the actions of neuraminidase. We suggest that elevation of intracellular calcium may be one cause for these observations. Supported by NIH grants HL 20708 and HL 07289.

M-AM-C12 DIPHENYLHYDANTOIN: ACTIONS ON PLATEAU CURRENTS AND TENSION IN CARDIAC PURKINJE FIBERS. Todd Scheuer, Robert S. Kass, T. Begenisich, Dept. of Physiology, Univ. of Rochester, Rochester, N.Y. 14642 (Intr. by R. J. Connett).

The anti-arrhythmic compound, Diphenylhydantoin (DPH, Dilantin, Phenytoin) has been shown to block sodium currents in squid axon (K_d=60uM). At low to moderate concentrations DPH reduces action potential plateau height and twitch tension in various cardiac tissues, suggesting that the compound may have additional effects on membrane current in these preparations. We have used a conventional two microelectrode voltage clamp technique in combination with simultaneous tension measurements to investigate the effects of DPH on membrane currents and tension in isolated dog and calf Purkinje fibers. The voltage dependence of the DPH effect was tested using 500 msec. voltage clamp steps to plateau potentials. 10-250 uM DPH shifted net membrane currents in the outward direction for potentials positive to -40 mV. Peak tension was reduced over the same potential range. Similar results in fibers pretreated with 10 uM TTX suggest that the majority of this effect is not due to a reduction in maintained sodium current. Effects of DPH on the 1 sec. isochronal I_x activation curves show that it reduces I_x at these concentrations. Thus, I_x does not contribute to the outward shift. We conclude that DPH has important effects on the currents of the action potential in addition to any effects it may have on I_{Na}. These are consistent with a reduction in I_{si}, but changes in I_{qr} or the background currents cannot be ruled out at this point. Supported by AHA 78-993 and NIH HL21922.

M-AM-D1 POSTSYNAPTIC CURRENTS OF THE MAUTHNER FIBER-GIANT FIBER SYNAPSE IN THE HATCHETFISH. W.D. Huse* and M.V.L. Bennett. Albert Einstein College of Medicine, Bronx, N.Y. 10461.

Postsynaptic membrane of the hatchetfish giant fiber was voltage clamped during intracellular stimulation of a single Mauthner fiber. At the holding potential (-90 mV) postsynaptic current (PSC) had a rise time of 90μs and decayed in two phases an initial fast component and a later slow component (τ's of about 250μs and 750μs respectively). The fast component showed little voltage dependence. The slow component became faster at depolarizing potentials and merged with the fast component near the reversal potential (-15 mV). Miniature PSC's had amplitudes and rise times of 1.5 nA and 60μs, respectively, at -90 mV. The decays were comparable to those of the PSC's, but noise prevented determination of deviation from simple exponential decay. The relation of the peak PSC to voltage was curvilinear, the slope being greater for more negative potentials. To exclude the possibility that the curvature was due to inadequate clamping, the giant fiber was impaled with an additional voltage electrode in the synaptic region. No deviation from isopotentiality occured during voltage steps in the relevant range, although the evoked currents were much larger than the PSC's. Also, peak PSC during inward Na current at the onset of a clamping pulse was the same as during the late current. The non-linear relation between peak PSC and voltage may arise from voltage dependence of opening and closing rates that shifts channels to the closed state or from rectification in the channels themselves.

M-AM-D2 SINGLE CHANNEL CURRENTS ACTIVATED BY GABA, MUSCIMOL, AND (-) PENTOBARBITAL IN CULTURED MOUSE SPINAL NEURONS. D.A. Mathers, M.B. Jackson, H. Lecar, J.L. Barker, NINCDS, NIH, Bethesda, Maryland 20202

The patch clamp technique was applied to mouse spinal neurons grown in cell culture in an attempt to observe the elementary events underlying membrane responses to agonists known to activate Cl^- conductance in these cells. Prior impalement of the cells with a 3M KCl recording pipette allowed manipulation of membrane potential and changed the Cl^- equilibrium potential from about - 60mV to about -15mV. When 0.5μM γ-aminobutyric acid (GABA) was included in the patch electrode and the membrane potential held at -80mV, discrete, all-or-none jumps in inward current were recorded from the membrane patch. Similar all-or-none jumps were observed when 0.5μM muscimol or 50μM (-) pentobarbital were included in the patch electrode. Quantitative analysis of the current events revealed that each agonist induced channels of approximately similar amplitude (1.5-2.0pA), but different mean duration. The amplitudes of the channel events deceased as membrane potential was depolarized to -60mV. The inter-jump intervals associated with muscimol-induced events showed a number of short durations which exceeded the number expected from the mean jump frequency for a single Poisson process. Thus some channels can close and open by additional very rapid processes. The present results show that naturally occurring and synthetic substances activate conducting channels in cultured central neuronal membranes. These results confirm and extend observations made from previous studies of electrical noise induced by these three agonists.

M-AM-D3 FUNCTIONAL STOICHIOMETRY OF THE NICOTINIC RECEPTOR. Robert E. Sheridan and Henry A. Lester. Division of Biology, California Institute of Technology, Pasadena, CA 91125

An important parameter of drug-receptor interaction is the number of occupied binding sites necessary for activation of a receptor. This stoichiometry is usually determined from the Hill plot of dose-response data at equilibrium. However, such data can be inaccurate due to limitations inherent in the process of adding drug to receptor. We have eliminated such errors for the nicotinic receptor by measuring the response to instantaneous removal of agonist molecules already present at their binding site.

The photoisomerizable nicotinic agonist trans-Bis-Q was applied to isolated, voltage-clamped eel electroplaques. When this preparation was exposed to a 1 μs flash of light, some of the trans-Bis-Q molecules already bound to receptor were isomerized to the inactive cis configuration. The receptors thus affected promptly closed their channel with a time constant on the order of 100 μs, more than 50 times faster than the normal channel lifetime in Bis-Q. The fraction of open channels which closed in response to the light flash was a function of the light intensity during a flash, increasing as twice the probability of trans to cis isomerization for low intensity flashes and saturating at a value of 0.2 for high intensity flashes. The initial slope of this function suggests that the isomerization of either of two bound agonist molecules is sufficient to close a receptor channel. This is consistent with the initial slope of the Hill plot for trans-Bis-Q (1.9 ± 0.1, $n = 6$). However, this interpretation predicts a saturation level of 0.57 which is more than twice the observed value. We are as yet unable to explain these apparently irreconcilable results.

Supported by USPHS grants NS-11756 and NS-272, MDA, and PCM 74-2140.

M-AM-D4 FLUORESCENCE SPECTROSCOPY AS A TOOL FOR QUANTITATION OF CATION TRANSLOCATION IN ACETYLCHOLINE RECEPTOR-RICH MEMBRANE VESICLES. M. Martinez-Carrion, J.M. Gonzalez-Ros, and J. Mattingly. Department of Biochemistry, Medical College of Virginia, Virginia Commonwealth University, Richmond, Virginia 23298

Measurement of neurotransmitter mediated Na^+ and K^+ ion translocation through postsynaptic membranes has been largely hampered by slow and cumbersome methodologies. Trapping or efflux of radioactive ^{22}Na, or other monovalent cations, from vesicles are the prevailing tools. We have devised methods which use our original observations that fluorescent probes trapped in membranes are sensitive to quenching effects by Tl^+ ion and this can be a measure of the collisions between the cation and the fluorescent probe (Martinez-Carrion, et al, J. Supramol. Struct. 4, 373 (1976) and Sator, et al. Arch. Biochem. Biophys. 192, 250, 1979). Fluorescent probes by themselves, or covalently bound to dextran molecules, are trapped inside membrane vesicles rich in acetylcholine receptor prepared from Torpedo californica electroplax. The entrapped probe's fluorescence sensitivity to the entry of Tl^+ can be monitored as a quantitative tool for external monovalent cation permeation. The effect of local anesthetics, neurotransmitters, detergents and other known mediators of cation transport through synaptic cholinergic endings is explored. Quantitation of molecular events is possible and the potentials for detailed kinetics and membrane function modulation measurements are illustrated. (Supported by a grant from the National Science Foundation).

M-AM-D5 A FINITE DIFFUSION RATE SLOWS NUMERICALLY SIMULATED VOLTAGE JUMP RELAXATIONS. M. E. Krouse, H. A. Lester, Div. of Biol., Caltech, Pasadena, CA 91125; and J. Wathey*, Dept. of Neurosci., UCSD, La Jolla, CA 92093.

Several models have been proposed to describe the molecular events involved in acetylcholine receptor channel gating at nicotinic synapses. These models are used to extract molecular rate constants from voltage jump relaxations and spontaneous fluctuations. However, these models assume that the agonist concentration near receptors remains constant during a voltage jump. Although this assumption is necessary to provide a simple analytical solution to the proposed models, it may not be true within the synaptic cleft.

We have developed a computer program to simulate voltage jumps numerically (Biophys. J. 1979. 27:145-154). We assumed a sequential binding model, that is, two agonist molecules must bind to the receptor before the channel can undergo a conformational change from closed to open. Our simulation constrains the agonist diffusion constant to a finite value which we varied around its value in free solution. The effect of a finite diffusion rate is to slow the voltage jump relaxation by altering the free agonist concentration in the cleft during the voltage jump. Other parameters such as cleft geometry, receptor density, and microscopic rate constants modify the free agonist concentration by changing the buffering capacity of the cleft. Thus diffusional effects can alter the molecular interpretation of the experimental data. Furthermore, these effects have different consequences depending on whether binding or conformational change is rate limiting.

Supported by NIH grants NRSA GM 07737 and NS-272, MDA, and the Pew Foundation.

M-AM-D6 LIGHT-FLASH RELAXATION STUDIES ON THE MUSCARINIC RECEPTOR OF BULLFROG ATRIUM. J. Nargeot*, M.-C. Nargeot*, and H. A. Lester, Div. of Biol., Caltech, Pasadena, CA 91125; N. Birdsall*, and J. Stockton*, NIMR, London, NW7 1AA, U.K.; N. H. Wassermann* and B. F. Erlanger*, Dept. of Microbiol., Columbia Univ., New York, NY 10032.

Both dose-response data (frog atria) on the agonist-induced K^+ conductance and binding studies (rat atria) with (^3H)-N-methylscopolamine show that trans-3,3'-bis-(α - (trimethylammonium)methyl) azobenzene (trans-Bis-Q) is a competitive antagonist in this preparation, with a K_D of 4 μm. The cis configuration is severalfold less potent. Voltage-clamped bullfrog trabeculae were exposed to both carbachol and Bis-Q and were subjected to appropriately filtered flashes (<1 msec duration) from a xenon flashlamp. Trans → cis and cis → trans photoisomerizations cause small (<20%) increases and decreases, respectively, in the agonist-induced current. The relaxation follows an S-shaped time course, including an initial delay or period of zero slope. The entire waveform is described by $(1 - \exp(-kt))^n$. At 23°C, k is about 3 s^{-1} and n is two. Neither k nor n are affected when: (a) [Bis-Q] is varied between 5 and 100 μM; (b) [carbachol] is varied between 1 and 50 μM; (c) carbachol is replaced by other agonists (muscarine, acetylcholine, or acetyl-β-methacholine); or (d) the voltage is varied between the normal resting potential and a depolarization of 80 mV. However, in the range of 13-30°C, k increases with temperature; the Q_{10} is between 2 and 2.5. In the same range, n does not change significantly. Like others, we conclude that the activation kinetics of the muscarinic K^+ conductance are not determined by ligand-receptor binding, but rather by a subsequent sequence of two (or more) steps with a high activation energy.

Supported by USPHS grants NS-11756 and NS-272, MDA, NSF grant PCM-74-02140, DGRST (78.7.2582), the Pew Foundation, and a NATO Fellowship to J.N.

M-AM-D7 RAPID FLOW MEASUREMENTS OF DESENSITIZATION AT FROG ENDPLATES. R.B. Clark and P. R. Adams, Dept. of Physiology and Biophysics, Univ. of Texas Med. Br., Galveston, TX 77550

Desensitization by carbamylcholine (Carb) was studied at voltage-clamped endplates of cutaneous pectoris muscle fibers. A rapid-flow superfusion system applied a known, uniform concentration of agonist to the entire endplate within 1-2 seconds. Ringer was injected at 1 ml s^{-1} into the space between the water immersion objective used to visualize endplates and the muscle through two 1.5 mm glass tubes attached to the edge of the objective. Electrically operated valves switched flow between 'control' and 'test' solutions. Changes in clamp current produced by low (10-30 μM) concentrations of Carb rose to 90% of their final amplitude within 0.5-1.5 sec. The decline in agonist-induced current in the continued presence of Carb was taken as a measure of desensitization of endplate receptor population. At many endplates, the decline in current had a double exponential time course. For example, at endplates on 7 different fibers clamped at -60 mV, onset of desensitization produced by 20 μM Carb had a 'slow' time constant of 178 ± 32 sec (mean ± S.E.) and a 'fast' time constant of 14 ± 3 sec. The ratio of the amplitude of the 'slow' phase of desensitization onset (A_s) to the 'fast' phase of onset (A_f) varied from 0.8 to 5 (mean A_s/A_f = 2.4 ± 0.6, same 7 fibers). Recovery from desensitization was measured by applying brief (0.5-2 sec) 'test' doses of Carb (same concentration as desensitizing dose) at various times after removal of the prolonged desensitizing dose. For 7 different endplates clamped at -60 or -80 mV, recovery from desensitization caused by 100-260 sec exposure to 20 or 30 μM Carb showed at least 2 phases, with a 'slow' time constant of 517 ± 94 sec and a 'fast' time constant of 54 ± 7 sec. Recovery from short (10-20 sec) exposures to 100-200 μM Carb had an initial 'fast' phase with a time constant of less than 10 sec. Supported by NIH grant NS-14920 and the M.D.A. R.B.C. is an M.D.A. Postdoctoral Fellow.

M-AM-D8 STRUCTURAL MODEL OF ACETYLCHOLINE RECEPTOR (AChR) NEUROTOXIN- AND AGONIST-BINDING SITES BASED ON N TERMINAL SEQUENCES OF AChR SUBUNITS. H. Robert Guy, Physiology Department, Armed Forces Radiobiology Research Institute, Bethesda, Md. 20014

N terminal sequences of the four AChR subunits from Torpedo californica were used to design a model of the outermost surface of the AChR. The model was developed in three stages. Secondary structures of the α subunit were predicted by the Chou and Fasmen (1974, Biochem. 13:211) and Lim (1974, J. Mol. Biol. 88:873) methods of analysis. Using these predictions, a tertiary structure of the α subunit was designed that should strongly bind α cobra toxin and erabutoxin b. Eighty-one percent of the proposed tertiary structure is predicted by the Chou and Fasmen analysis, and the rest of the structure is consistent with the Chou and Fasmen parameters. Using the Raftery et al. (1980, Science, 209:1454) numbering scheme, residues 1-16 form an α helix, residues 16-19 form a β turn, and residues 20-56 form β sheets that are broken in positions 22-23, 32, 39, 42, and 49 by residues that have an α helical type conformation. Erabutoxin b and α cobra toxin bind to the α subunit segment from residue 15-48 by forming, respectively, 6 and 5 salt bridges, 29 and 26 hydrogen bonds, and 9 and 11 hydrophobic bonds. The homologous β, γ, and δ subunits were assumed to have tertiary backbone structures similar to that of the α subunit. A quaternary structure was developed from $\alpha_2\beta_1\gamma_1\delta_1$ stoichiometry of the subunits, electron microscopy images of AChR's, interactions between adjacent subunits, and stereochemical analysis of agonist and competitive antagonist binding. The positively charged groups of the agonists and antagonists bind to the α subunit Glu-15 carboxyl group. The channel is formed between the five subunits. When the channel is closed, the two α subunits' α helices bind together to block the entrance to the channel. These helices swing from a horizontal to a vertical position when the channel opens.

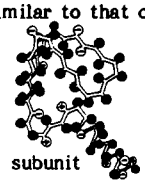

α subunit

M-AM-D9 LIGAND-RECEPTOR BINDING ANALYSIS WHERE ONE-WAY RATE CONSTANTS VARY WITH OCCUPANCY: APPLICATION TO ADIPOCYTE AND ERYTHROCYTE INSULIN RECEPTORS. H.J. Goren and J.S. Beck, Faculty of Medicine, The University of Calgary, Calgary, Alberta, Canada T2N 1N4.

Many hormone-receptor interactions are non-linear on Scatchard analysis. Possible reasons for this include coöperativity in binding, receptor loss during binding, and receptor heterogeneity. We have derived a mathematical model in which the association (k_a) and dissociation (k_d) rate constants may vary with receptor occupancy (λ):

$$\kappa = (1-\lambda)\left(\frac{1}{\mu} - 1\right),$$

where κ is a dimensionless parameter ($k_d/\eta k_a$; η is receptor concentration) and μ is the fraction of total radioligand bound. Insulin receptors give concave-up Scatchard plots, currently explained as resulting from negative coöperativity (dissociation equilibrium constant increasing as occupancy increases). We applied our analysis to insulin receptors in rat epididymal adipocytes and in human erythrocytes. ^{125}I-insulin bound to cells at steady state in the presence of increasing amounts of insulin was measured. Our results show κ to vary with λ in a manner consistent with earlier reports. In addition, using the differential equations of the model, we found with both cells that both k_a and k_d decrease with increasing occupancy; the fall in affinity is due to greater sensitivity of k_d to λ

Supported by the Medical Research Council of Canada and the Canadian Diabetes Association.

M-AM-D10 QUANTITATIVE DESCRIPTION OF THE BINDING OF G_{M1} AND ITS OLIGOSACCHARIDE BY CHOLERA ENTEROTOXIN. David E. Schafer and Ajit K. Thakur, VA Medical Center, West Haven, CT 06516, Department of Physiology, Yale University School of Medicine, New Haven, CT 06510, and Hazleton Laboratories America, Inc., Vienna, VA 22180.

We present a quantitative interpretation of binding between ganglioside G_{M1} or its oligosaccharide (G_{M1}-OS) and the five B subunits of cholera enterotoxin, based on the probable quaternary structure of the toxin and the principles of multiple equilibria. Using this model we have reexamined G_{M1}-OS binding data from equilibrium dialysis experiments at low concentrations with intact toxin, reduced toxin, and isolated B subunits. Previous analysis by the Hill equation indicated that such binding is positively cooperative, and appeared to suggest that there might be only four binding sites per toxin molecule; values of .2-20 x 10^{-9} M were obtained for the parameter K, and 4-8 x 10^{-6} M for the concentration of G_{M1}-OS at half maximal binding, but affinity constants for individual steps of the multivalent binding process could not be estimated from the Hill equation because of its empirical nature. Our present analysis shows that the available data are fully consistent with the five-site sequential binding model, its behavior diverging substantially from the Hill equation curve only at concentrations somewhat greater than those so far investigated. Moreover, it confirms that, within experimental error, binding probably is positively cooperative for two of the three preparations. Finally, it yields values of the physical affinity constant for the first binding step of about 2.0-2.1 x 10^6 M^{-1} for isolated B subunits and 2.5-2.7 x 10^6 M^{-1} for the two toxin preparations, and indicates that the constants for the other binding steps are probably within the range of 2-6 x 10^6 M^{-1}. Implications of these results for recent binding studies by differential scanning calorimetry and ^{13}C NMR are considered. (Supported by VA and by GM 24704)

M-AM-D11 EFFECTS OF ANTHRACENE 9 CARBOXILIC ACID (A9C) ON ACTION POTENTIALS OF PURKINJE FIBERS AND VENTRICULAR MUSCLE OF THE DOG. Antonio Morales-Aguilera and Enrique Castillo-Henkel. Centro de Investigación y Estudios Avanzados del IPN. México 14, D.F.

The increase of the contractile force of the mammalian skeletal muscle produced by some aromatic monocarboxilic acids described by Bryant and Morales-Aguilera has been explained by the tetanic contractions produced by the repetitive discharges of the membrane, in turn due to a blockade of chloride conductance. However, Kranbuhl described an increase in the contractile force of the dog heart-lung preparation produced by A9C and such increase could not be explained by repetitive discharges. Honerjägger, Morales-Aguilera and Reiter found that A9C produced a positive inotropic effect in the guinea pig isolated papillary muscle which depends on the frequency of the stimulation. This effect reaches a maximum at 0.5 Hz and it is accompanied by an increase in the repolarization time of the ventricular muscle at all levels.

The effect of the A9C on the action potentials of Purkinje fibers and ventricular muscle was tested by us on a preparation of isolated papillary muscle of the dog. In the dog, as well as in the guinea pig, A9C produces an increase in the repolarization time and that increase is greater with low frequencies (maximum, 0.2 Hz). The effect on the Purkinje tissue is greater than on the ventricular muscle. These observations suggest that A9C blocks chloride current conductance also in the dog heart. With the diminution of the repolarizing current, the contractile force increases, due to a longer repolarization time or, due to an increase, absolute or relative, in the calcium influx.

M-AM-D12 TWO SYSTEMS OF DOPAMINE TRANSPORT IN BLOOD PLATELETS.
Nihei, T. and Stewart, M.W., University of Alberta, Edmonton, Alberta
Platelets have been known to accumulate serotonin and dopamine. Although the mechanism of serotonin transport through the platelets membranes has been studied extensively, information of dopamine transport system in platelets is relatively sketchy. Since the dopamine uptake by platelets has been shown to reflect certain pathological states of some dopaminergic brain cells, it is thought of value to explore the mechanism of dopamine uptake by platelets. As in the case of serotonin transport, blood platelets appear to accumulate dopamine through two types of transport systems. This was observed by incubating intact platelets with dopamine in the presence and absence of NH_4Cl, the concentration of which was sufficient to collapse pH gradient across the membrane. The results indicated that the NH_4-insensitive uptake level is not saturable, whereas the NH_4-sensitive uptake reaches maximum level at 0.1-0.2 µM dopamine. The dopamine uptake by platelets, however, was almost completely inhibited by 10 µM haloperidol, suggesting that both types of transport are mediated by a receptor. Using a double isotope method (^3H_2O and ^{14}C-sucrose), the intracellular volume and dopamine concentration were calculated. The results indicated that the NH_4-insensitive uptake allows dopamine to enter the platelets until its concentration reaches that of extracellular dopamine.

M-AM-E1 CONSIDERATIONS OF PHOTOSYNTHETIC GLOW PEAKS. D. DeVault, Govindjee, Univ. of IL, Urbana, IL 61801, and W. Arnold, Oak Ridge Natl. Laboratory, Oak Ridge, TN 38730

We have recalculated the data of Tatake, Desai, Govindjee and Sane (Photochem. Photobiol. in press, 1980) on the thermoluminescence from green plants by methods which fit curves, calculated by Randall-Wilkins theory, to all the data points. The method enabled separation of overlapping peaks and yielded parameter values that are qualitatively similar to those calculated by Tatake et al. They enclude values of S, the Arrhenius pre-exponential frequency factor as high as 10^{26} s^{-1} associated with values for E, the activation energy ranging up to 1.5 eV. We agree that the values of S much larger than 10^{13} s^{-1} are difficult to conceive and present a problem for simple application of R-W theory. We may note that a single glow peak is normally emitted in about 100 seconds at a heating rate of 0.2 deg s^{-1}. A rate constant for the glow process should therefore, be of the order of 10^{-2} s^{-1} or faster. Absolute reaction rate theory then gives $\Delta G^{\ddagger}$, the free energy of activation, to be 0.9 eV or smaller. Activation energies (enthalpies) much larger than 0.9 eV imply impossibly large positive entropies of activation. We suggest that the error may lie in the assumption that the rate of rise of the glow peak is due simply to Arrhenius activation of the detrapping process and may, instead, be governed by a membrane phase transition or an equilibrium shift between trapped states which change the parameters from inhibiting values below the transition temperature to permissive values above it. A further observation is that at least peak V follows the empirical formula: $I = nK\epsilon^{\lambda T}$ over its rising and much of its falling portion. (I is the glow intensity, n the number of trapped electrons, T the temperature and K and λ are constants). The value of λ was close to 0.2 deg^{-1}. We do not have any theory that give this dependence on temperature. (Supported by NIH BMR grant RR-7030 and NSF grant PCM 78-23194.)

M-AM-E2 DIVALENT CATION EFFECTS ON SIGNAL IIf KINETICS AND Mn^{2+} RELEASE ON THE OXIDIZING SIDE OF PHOTOSYSTEM II. Christine T. Yerkes, Gerald T. Babcock, Charles F. Yocum, Department of Chemistry, Michigan State University, East Lansing, MI 48824

Inactivation of oxygen evolution by 0.8 M Tris at pH 8.6 (4°C) results in a change in the binding of functional Mn (as evidenced by the appearance of a weak EPR detectable six-line hyperfine signal) as well as the induction of a flash-induced EPR transient, signal IIf. Previous studies have shown that Ca^{2+} serves to accelerate the decay of IIf following a flash when an exogenous electron donor is present. This acceleration is independent of the charge on the donor species, suggesting that non-electrostatic effects produced by the presence of Ca^{2+} are responsible for the rapid decay of IIf. We have extended these investigations using Ca^{2+} and Zn^{2+} in Tris inhibited thylakoid membranes with and without exogenous donors. Addition of Ca^{2+} (1-10 mM) accelerates IIf decay by introducing a rapid component to the predominantly slow phase. At similar concentrations, Ca^{2+} also releases functional Mn^{2+} from binding sites affected by Tris incubation, as evidenced by an increase in the magnitude of the six-line hyperfine spectrum due to hexaquomanganese. Taken together, these results suggest that Ca^{2+} (and Zn^{2+}) may act to alter the interaction between Signal IIf and Mn^{2+} whose function in water oxidation has been altered by exposure to Tris. (Supported by USDA 79 00 764 (CTY, GTB) and NSF PCM 78-7909 (CFY)).

M-AM-E3 LOCALIZATION OF REACTION CENTER PROTEIN IN SPHEROPLASTS FROM RHODOPSEUDOMONAS SPHAEROIDES BY FERRITIN LABELING.† G. Valkirs and G. Feher, U.C.S.D., La Jolla, CA 92093.

Reaction centers (RCs) of R. sphaeroides R-26 are composed of three proteins: L, M, and H. RCs can be dissociated to yield LM, L, M, or H of high purity. Previous results with ferritin labeled antibodies indicated that RCs and LM span the photosynthetic membrane and that H was exposed on the cytoplasmic side [Valkirs, et al., Biophys. J. 16 (1976) 223, and in review by Feher and Okamura, Brookhaven Symposia in Biology No. 28 (1976) 183]. We report here on the extension of this work. Anti-L and anti-M IgG fractions were obtained from antiserum against LM and anti-H IgG from anti-RC antiserum by affinity chromatography. The degree of contamination present in a particular affinity purified antibody fraction was determined by radioimmunoassay techniques and was found to be < 0.1%. Spheroplasts of R. sphaeroides R-26 were incubated with the different affinity purified antibodies and with normal rabbit IgG as a control. After washing by sucrose gradient centrifugation, ferritin labeled goat antibodies against rabbit IgG were added. Electron micrographs revealed labeling of both sides of the photosynthetic membrane for both the anti-M (see Fig.) and anti-H treated (partially ruptured) spheroplasts while only the periplasmic side was labeled with anti-L. Thus, both the M and the H subunits span the photosynthetic membrane. Since a definitive conclusion from labeling experiments can only be drawn from a positive result, additional antisera against L are being prepared to determine whether this subunit also spans the membrane. It should be noted that out of six different antisera only one affinity purified anti-H labeled the periplasmic side of the membrane.

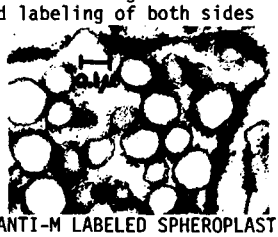

ANTI-M LABELED SPHEROPLAST

†Work supported by grants from the NSF and the NIH.

M-AM-E4 DISSOCIATION AND RECONSTITUTION OF THE H SUBUNIT FROM RCs OF R. SPHAEROIDES R-26.† R. J. Debus, M. Y. Okamura, and G. Feher, U.C.S.D., La Jolla, CA 92093.

The H subunit of bacterial RCs can be dissociated to yield a complex of LM which has full primary photochemical activity (reversible bleaching of P_{865} at cryogenic temperatures).[1] The LM complex contains ∿ 1 Fe/RC, exhibits a broad g=1.8 light-induced EPR signal at low temperature and upon illumination rapidly oxidizes cytochrome-c, indicating that the primary quinone, iron, and cytochrome-c binding sites are located on LM. However, as judged by room temperature donor-acceptor recombination kinetics, and cytochrome photooxidation measurements, the LM complex shows a lack of normal electron transfer from the primary to the secondary quinone. When H subunits, isolated by sucrose density gradient centrifugation,[1] were added to LM, reconstituted RCs (i.e., LMH units) were obtained. The extent of reconstitution was determined by LDAO-PAGE (the electrophoretic mobility of RCs is ∿ 20% higher than that of LM). Reconstitution restored the 25 msec low temperature (P^+_{865}-Q_I^-) recombination kinetics characteristic of RCs (for LM it is 40 msec). The reconstituted sample exhibited electron transfer from the primary to the secondary quinone, suggesting that the H subunit is required to provide a proper active site for the secondary quinone. Our procedure for dissociating H from RCs is very similar to that used by Blankenship and Parson to remove iron from RCs.[2] The loss of electron transfer from primary to secondary quinone that they observed may therefore have been caused by removal of H rather than of iron. Experiments are in progress to reassess the role of iron by reconstituting iron-free LM with H.

† Work supported by grants from the NIH and the NSF.

1 G. Feher and M. Y. Okamura (1978) in The Photosynthetic Bacteria, eds. R. K. Clayton and W. R. Sistrom (Plenum Press, N.Y.).

2 R. E. Blankenship and W. W. Parson, B.B.A. 545 (1979) 429-444.

M-AM-E5 N-TERMINAL SEQUENCE OF THE H SUBUNIT OF THE PHOTOSYNTHETIC REACTION CENTER PROTEIN OF RHODOPSEUDOMONAS SPHEROIDES R-26. M. R. Sutton* and L. A. Steiner, Dept. of Biology, Massachusetts Institute of Technology, Cambridge, MA 02139; E. C. Abresch* and G. Feher, Dept. of Physics, University of California, La Jolla, CA 92093.

The photosynthetic reaction center of *R. spheroides* contains equimolar amounts of 3 polypeptides, L, M, and H (Okamura *et al.*, Biochemistry *13:*1394, 1974). The subunits are hydrophobic in composition, consistent with their origin in the chromatophore membrane (Steiner *et al.*, Biochemistry *13:*1403, 1974). The sequence of the first 24 residues of the L subunit has been reported (Rosen *et al.*, Biophysical J. *17*, 67a, 1977). We have now determined, by automated Edman degradation, the amino-terminal sequence of the H subunit:

$$H_2N\text{-(Met)-Val-Gly-Val-}\overset{5}{\text{Thr}}\text{-Ala-Phe-Gly-Asn-}\overset{10}{\text{Phe}}\text{-Asp-Leu-Ala-Ser-}\overset{15}{\text{Leu}}\text{-}$$
$$\text{-Ala-Ile- X -Ser-}\overset{20}{\text{Phe}}\text{-Trp-Ile-Phe-Leu-}\overset{25}{\text{Ala}}\text{- X -Leu-Ile-}$$

The yields of phenylthiohydantoin-amino acids, extrapolated to the beginning of the sequence, were low and variable (15-50%), possibly due to the poor solubility of this subunit and/or to partial blocking of the amino-terminus. Methionine was detected in low yield at position 1 and is tentatively assigned to the amino-terminal position. Only 5 hydrophilic residues (at positions 5, 9, 11, 14, and 19) have been identified in the first 28 positions, a polarity of 18%. This suggests that the amino-terminal segment of H is buried in the membrane. The H subunit as a whole is more hydrophilic, having a polarity of 38% (Steiner *et al.*, Biochemistry *13:*1403, 1974).

(Supported by grants from the National Science Foundation, National Institutes of Health, Dept. of Agriculture and Petroleum Research Fund, American Chemical Society.)

M-AM-E6 PHOTO-INDUCED CURRENTS AND POTENTIALS FROM REACTION CENTER MONOLAYERS SANDWICHED BETWEEN TRANSPARENT ELECTRODES. P. Mueller, J. Antanavage, L. Dutton, N. Packham, D. Tiede. Dept. of Biochem. & Biophys., U. of Pennsylvania.

Reaction centers (RC) from Rhodopseudomonas sphaeroides were spread as monolayers from detergent solutions at an air-water interface, and compressed to 30dynes/cm. The monolayer was transferred to a glass slide covered with a transparent conductive layer of tin oxide by dipping the slide through the monolayer from the air phase. A transparent layer of aluminum was subsequently vacuum deposited onto the monolayer. The dark conductance of the device is 10^{-8}S/cm^2 and the capacitance is 1μF/cm^2. Light-induced currents and potentials were measured by voltage and current clamp connected to the metal conductors. The current response consists of an initial peak, a zero steady state current and a reverse current at the cessation of illumination. The current sign corresponds to electron transfer toward the hydrophobic part of the RC. The peak amplitude is proportional to the light intensity. At 100photons/sec/RC, the peak current is 5×10^{-7}A/cm^2;i.e., less than 1% of the theoretical value for a densely-packed monolayer. The reverse current has a time constant of ~80msec, commensurate with the spectroscopically-determined time constant of the Q_1^- to $(BChl)_2^+$ back reaction. Current integrals for peak and reverse response are equal, and the device can be driven as an alternating current generator by repetitive light pulses. The response action spectrum matches the RC absorption spectrum. 'Single turnover' potentials are 5-10 mV and agree with the currents and capacity. Steady state currents are observed when the hydrophilic side of the RC is in contact with an electron donor of appropriate redox potential. This is accomplished either by adding ferrous ions to the aqueous phase or by inverting the RC orientation on the tin oxide. Thus the rate limiting step for the electron transfer to the electrodes lies at the entrance to the $(BChl)_2$. (Supported by NIH GM12202 and NSF PCM 79-09042)

M-AM-E7 MONOMERIC CHLOROPHYLL A ENOL. EVIDENCE FOR ITS POSSIBLE ROLE AS THE PRIMARY ELECTRON DONOR OF PHOTOSYSTEM I. M.R. Wasielewski,J.R. Norris,L.L Shipman,C.P.Lin,W.A. Svec
Chemistry Division, Argonne National Laboratory, Argonne, IL 60439
While ESR and ENDOR spectroscopy have provided evidence that a special pair of BChl a molecules act as the primary donor (P865) in several strains of photosynthetic bacteria, similar studies of Photosystem I (P700) reactions centers cannot be adequately described by the special pair model. P700 is about 400 mV easier to oxidize than Chl a in vitro whereas the difference between the oxidation potentials of P680 and P865 donors and their respective chlorophylls in vitro is substantially smaller,about 100-200 mV. Chlorophyll dimer formation accounts for less than 75 mV of this change. Enolization of the ring V beta keto ester of Chl a yields a very different pi electronic structure. The Chl a enol can be trapped as a silyl enol ether. In addition, 9-desoxo-9,10-dehydro-Chl a may be prepared. Both the trapped enol and its 9-H analog are about 350 mV easier to oxidize than Chl a. The ESR spectrum of their respective cation radicals consist of a single gaussian line of 6.1 G linewidth. This compares with 7.0 G for $P700^+$ and 9.3 G for Chl a^+. The ENDOR spectrum of the cation at 77 K shows hyperfine splittings which are tentatively assigned to the 1 and 3 methyl groups. The ENDOR spectra of $P700^+$ and these compounds is consistent. The second moment of the ESR line of fully ^{13}C enriched 9,10-dehydro-Chl a cations agrees with that of similarly enriched $P700^+$ to within 10%. Similar application of the special pair model yields 100% disagreement. Ab initio SCF calculations on the Chl a enol cation bear out the ESR and ENDOR data. Thus we conclude that the Chl a enol model offers a serious alternative to the Chl a special pair model of P700. (This work was supported by the Office of Chemical Sciences, Division of Basic Energy Sciences of the Department of Energy)

M-AM-Po1 AN ALTERNATIVE STRUCTURAL MODEL OF VERTEBRATE MUSCLE. G.H. Pollack and M.J. Delay. Dept. of Anesthesiology & Div. of Bioengineering, RN-10, University of Washington, Seattle, WA 98195

The molecular structure of the thick filament lattice remains unsettled. Several models have been proposed, but no single model is consistent with all features of the X-ray diffraction pattern. A model is presented which accounts for the principal features of the meridional X-ray diffraction pattern. In the model it is assumed that cross-bridges interconnect adjacent thick filaments. While this is contrary to accepted views, it is consistent with a large number of published electron micrographs, and does not necessarily preclude actomyosin interaction. The model is sketched in the figure. A more extensive physical model was built. The physical model reveals a secondary helix whose pitch is 1/6 of 43 nm, explaining the observed, relatively strong 7.1 nm reflection. The model also accounts for the observed but "forbidden" 21.5 nm reflection; this is the longitudinal repeat of bridges along the muscle axis. The model offers distinct predictions about bridge disposition that can be tested using serial sections of electron micrographs.

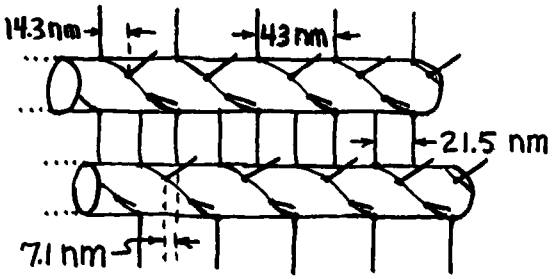

M-AM-Po2 MYOFIBRILLAR CONNECTIONS: THE ROLE OF TITIN, N_2-LINE PROTEIN AND INTERMEDIATE FILAMENTS, Kuan Wang and Ruben Ramirez-Mitchell*, University of Texas At Austin, TX 78712.

The possible existence in striated myofibrils new type of filaments distinct from thin and thick filaments has been much debated. The detection of fine filaments (25-80A) in highly stretched or extracted myofibrils led to various proposals in which these fine filaments connect thin filaments, thick filaments or Z lines. However, its biochemical identity has not been demonstrated.

We have recently discovered a group of three extremely large major myofibrillar proteins which are present in a wide range of vertebrate and invertebrate striated muscles. Titin (a doublet of $M_r \simeq 1 \times 10^6$) differs in solubility and location from thin and thick filament proteins. The unexpected presence of titin on A-I junctions suggests that titin containing structure might regulate the insertion of thin filaments into the distal ends of A band. The possibility of titin being a component of the putative connecting filament is being explored. A third protein ($M_r \simeq 5 \times 10^5$) is an N_2-line associated protein which appears to participate in the regulation or maintenance of the changing spatial arrangement of thin filaments from a square lattice at the Z line to a hexagonal array near the A-I junction.

These proteins are resistent to KI-extraction which removes the majority of thin and thick filament proteins and causes extensive translocation of titin and N_2-line protein. We observed two types of residual filaments in such extracted myofibrils. One type, tentatively identified as intermediate filaments (80-180A), forms inter- and intrafibrillar bridges connecting residual Z structures as well as M lines. The second type consists of randomly oriented, ill-defined ultrathin filaments (20-60A) which are probably composed of titin because purified titin aggregates into similar size filaments in solution.

M-AM-Po3 ORIENTATION AND ROTATIONAL DYNAMICS OF SPIN-LABELED MYOSIN HEADS: A COMPARISON OF VERTEBRATE STRIATED AND INSECT FLIGHT MUSCLES. David D. Thomas, †Roger Cooke, Vincent A. Barnett, and Les Sommerville, Intr. by Rufus Lumry, Dept. of Biochemistry, University of Minnesota Medical School, Minneapolis, MN 55455; †Dept. of Biochemistry/Biophysics and CVRI, University of California, San Francisco, CA 94143.

We have used electron paramagnetic resonance (EPR) to monitor the orientation and rotational motion of myosin heads in glycerinated muscle fibers. In our previous studies on vertebrate striated (rabbit psoas) muscle, we found that myosin heads attached to actin are strongly immobilized (on the microsecond time scale) and are sharply and uniformly oriented (with respect to the fiber axis); but when detached from actin, the heads become mobile and disordered. Thus, EPR is a sensitive indicator of the fraction of heads that are attached, and we concluded that all myosin heads are attached to actin in rigor. Since the best X-ray diffraction data on fibers is from insect flight muscle, where models have been proposed in which not all of the myosin heads can be attached to actin at once, we have carried out EPR experiments on insect flight muscle. We have obtained preliminary results similar to those of vertebrate striated muscle: a high degree of immobilization and orientation is observed, suggesting that a high percentage (more than half) of the heads are attached to actin at an orientation similar to that observed in vertebrate striated muscle. However, significant spectral components are observed corresponding to disordered and mobile probes, suggesting that a significant fraction of the heads (up to one half) are detached. Further studies should allow precise quantitation of this fraction, thus providing a test for proposed models of muscle fiber structure. Supported by grants from NSF, NIH, and MDA.

M-AM-Po4 THE EFFECT OF ACTIVATION ON THE HIGHER ORDER EQUATORIAL X-RAY REFLECTIONS FROM FROG SKELETAL MUSCLE. Leepo C. Yu, Geoffrey R.S. Naylor, and Richard J. Podolsky, Laboratory of Physical Biology, NIAMDD, National Institutes of Health, Bethesda, MD 20205, and Ronald C. Gamble, Div. of Chemistry and Chemical Engineering, California Institute of Technology, Pasadena, CA 91125.

Diffraction experiments with muscle cells were made with the intense radiation source at the Stanford Synchrotron Radiation Laboratory during a run dedicated to the production of X-rays. The experiments were designed to examine the effect of physiological activation on the equatorial reflections that lie beyond the generally studied strong [1,0] and [1,1] reflections. These higher order reflections ([2,0], [2,1], [3,0], [2,2], and [3,1]) are well defined in relaxed frog muscle fibers. It was found that $I_{2,1}$, and $I_{3,0}$ become much weaker and broader when the muscle was electrically stimulated, which contrasts sharply with the several fold increase in $I_{1,1}$. The [2,2] and [3,1] reflections, which form a doublet, are much smaller than the other reflections and were occasionally seen in the activated state. It was also observed that the equatorial patterns of muscle in contraction and in rigor were similar in that the higher orders beyond [1,1] were considerably weaker than in the rest pattern. These observations indicate that crossbridge attachment is similar in both the active and rigor states. In addition, they suggest that the structure is more disordered in these two states than in the relaxed state. This disorder may arise from a less crystalline arrangement of cross-bridges in attached states than in the relaxed state.

M-AM-Po5 CROSSBRIDGE STRUCTURE IN RIGOR AND AMPPNP STATES OF INSECT FLIGHT MUSCLE. Mary Reedy, M. K. Reedy and R. S. Goody. Anatomy, Duke Univ., Durham, NC, Max Planck Inst. f. Medforsch., Heidelberg, and EMBL, Heidelberg.

Tannic acid in fixatives helps preserve more order and detail in glycerinated Lethocerus flight muscle, including actin substructure (5.9 nm and 5.1 nm layer lines), evident by optical diffraction (OD) and filtration (OF) of thin-section images. Goniometer electron-microscopy (GEMy) along with OD and OF have been used to analyze crossbridge patterns in 15-25 nm sections showing actin or myac single filament layers (longit. sections) or single crossbridge levels (cross sections showing flared X images).

RIGOR: Differences between rear (R) and leading (L) members within each double chevron (1) are now clear. GEMy shows R and L bridges are helically related, not just axially repeating. R and L chevrons respond differently to GEMy tilt; the basis is evident in the asymmetric flared X structure, which shows that individual crossbridges are tangentially applied to actin, resembling single myosin heads (2) on decorated actin (3). An apparent difference in average axial tilt between R chevron (@ 90° off-axis) and L chevron bridges (@ 45° off-axis) remains difficult to evaluate. 3-D reconstruction to 5 nm resolution is now possible and appropriate to decide such questions.

AMPPNP: The distinctive diffraction pattern in 1mM at 2° C. has been preserved through sectioning, GEMy, OD and OF. Myac layer OF images show coexistence of 14.5 nm striping (relaxed structure) with 38.7 nm chevron repeat (rigor structure) uniformly along each thick filament. Two different conformational populations are suggested here, but our evidence alone cannot yet decide between two bridge groups, or a rigor-like and a relaxed-like component of every crossbridge. (1) Reedy, J. Mol. Biol. 31, 155. (2) Offer and Elliott, Nature, 271, 325. (3) Moore et al., J. Mol. Biol. 50, 279. (Supported by NIH, DFG and EMBL).

M-AM-Po6 EFFECTS OF Z-PLATE MIS-REGISTRY ON OPTICAL DIFFRACTION BY STRIATED MUSCLE. M.M. Judy, V. Summerour*, T.L. LeConey* and G.H. Templeton. University of Texas Health Science Center at Dallas, Department of Physiology, Dallas, Texas 75235.

Equations from fundamental diffraction theory show that lack of lateral registry of the z-plates of sarcomeres in a three-dimensional array of parallel myofibrils can cause important modulation of meridional peak intensity not only in a direction parallel to the incident light (Yeh, Y. et al., Bioph J 29: 509-522, 1980) but also in the equatorial direction within a plane perpendicular to the direction of incident light. Both computer generated and optical diffraction patterns of stained thin sections show that z-plate mis-registry extending in a direction perpendicular to both the optical and myofibrillar axes causes the intensity of meridional diffraction peaks to be modulated in the perpendicular equatorial direction. Results show that if the mis-registry is asymmetric about the central myofibril of the array then the positive and negative order meridional diffraction peaks are shifted asymmetrically away from an axis parallel to the myofibrillar axis, and if mis-registry is symmetrical about this axis, all the meridional diffraction peaks are split into peaks of equal intensities shifted in the equatorial direction both above and below the meridional axis. If the mis-registry is wavey or multi-valued, the meridional peaks also become widened or multi-peaked in the equatorial direction with degree of widening and number of multiple peaks increasing with the amplitude of the z-plate mis-registry and the number of periods characterizing the wavey trajectory of the z-plates. Application to published diffraction patterns (Cleworth, D.R. and K.A.P. Edman, J Physiol 227: 1-17, 1972) suggests the presence in these preparations of wavey multi-valued z-plate mis-registry. (Supported by Ischemic SCOR HL-17669).

M-AM-Po7 ANALYSIS OF VARIATION IN Z BAND WIDTH IN NORMAL, CONTROL AND ANOXIC MYOCARDIUM. M.A. Goldstein, Department of Medicine, Cardiovascular Sciences, Baylor College of Medicine, Houston, Texas 77030.

Our studies of striated muscle have revealed a similar Z lattice unit in Z bands of different widths. We observed Z bands 2 to 3 times the "normal Z width" in papillary muscle cells exposed to acute hypoxia (J. Molec. Cell. Cardiol., 9:285, 1977) but did not quantitate the variation in Z width. Chase and co-workers (J. Molec. Cell. Cardiol., 10:1077, 1978) using the same experimental model determined from a random sample that the mean Z band width in hypoxia was no greater than that in control muscle. We have now gone back to these hypoxic and control mucles and to normal in situ muscle to determine if variation at the level of individual Z bands can be obscured by statistical pooling and to compare random vs. non-random sampling. Each Z band measurement (the largest consistent distance between lines parallel to edges of dense Z material) was recorded in successive sarcomeres for single myofibrils near and away from intercalated discs for several cells from a given block for each experimental group. Thus, a three level analysis was set up (group to group, cell to cell, myofibril to myofibril). Although sarcomere length was remarkably uniform in all three groups, the Z band width varied considerably within a myofibril and from myofibril to myofibril. Yet when normal Z width values were pooled according to animal, a histogram showed a distribution pattern observed by Salmons et al. (J. Anat., 127:17, 1978) for a control slow skeletal muscle. The mean values for each group (control n=591, exp. n=366) were similar. Distribution for each group was assessed for normality, normal shape and kurtosis. The considerable variation in Z band width in normal cardiac muscle has prompted us to examine the number of subunits within individual Z bands.

M-AM-Po8 CHEMICAL CROSS-LINKING PREVENTS CALCIUM-INDUCED STRUCTURAL CHANGES IN THICK FILAMENTS OF SKINNED MUSCLE CELLS. P. Paolini, R. Sabbadini, and G. Rieser. Biology Dept. and Molecular Biology Institute, San Diego State University, San Diego, CA 92182

In earlier studies (Sabbadini et al., BBA 578:526, 1979; Rieser et al., BBRC 90:179, 1979), we provided evidence suggesting that low [calcium] (pCa 6.95-5.49) and high pH (7.3-8.6) produced structural changes in thick filaments which were detectable as decreases in the intensities of first-order diffraction lines from chemically skinned skeletal muscle cells stretched beyond myofilament overlap. The precise structural changes responsible for the intensity decreases were, however, enigmatic.

We now have evidence that the Ca-induced intensity decrease results from structural changes within, rather than between, thick filaments. Skinned fibers were incubated for 16 hr. in 5 mg/ml 3-3'-dithiobispropionimidate (DTBP), a cross-linking agent known to restrict movement of S-1 heads and limit changes in the association of rod segments within the core of the thick filament without affecting interfilament lattice structure (Chiao and Harrington, Biochem. 18:959, 1979). Diffraction patterns from DTBP-treated cells were identical to those from untreated cells. Calcium (pCa 5.49), however, totally failed to produce the typical attenuation of the first-order line. Although reductions in first-order line intensity can result from decreases in the myofilament lattice (relative intensity decreased linearly from 100% to 5% as the osmolarity of the relaxing medium increased from 240 to 280 mOsm using PVP-10 or 40), the prevention of the calcium effect by DTBP indicates that the Ca-induced decrease in diffraction line intensity is due to intrafilament rather than interfilament changes in structure.

(Supported by NIH #PO1-HL16607)

M-AM-Po9 POWER SPECTRAL DENSITY ANALYSIS OF FIRST ORDER DIFFRACTION LINE POSITION FLUCTUATIONS FROM INTACT SINGLE FIBERS OF THE FROG. W.Halpern and J.Koniarek(Intr. by B.Hamrell), Dept. of Physiology and Biophysics, Univ. of Vermont, Burlington, VT 05405.

Although the mean local sarcomere length of skeletal muscle fibers remains essentially invariant during a fused tetanus, high resoltuion of the position of the first order (1^{o}) diffraction line undergoes microfluctuations. We have explored the nature of these fluctuations and the possibility that they arise from myofibrillar sarcomere motion and synchronized crossbridge activity made manifest in sarcomeres contained within a 0.75 mm axial length of the fiber. A modified laser diffraction pattern analyzer system (W. Halpern, Proc. San Diego Biomed. Symp., 1977, Academic Press 16:429-458, 1977) was used to obtain 1^{o} diffraction line position every 0.7 ms at a spatial resolution of about 0.5 mm referred to the half-sarcomere. Power spectra from 0.2 - 51.2 Hz were obtained using a spectrum analyzer (HP 3582A). Single fibers of the frog anterior tibialis muscle were examined under isometric conditions at 2.5 μm sarcomere length, at 4 and 14^{o}C at rest, and during 6.5 s tetani. The total rms power of 1^{o} fluctuations was approximately 2.5 times larger during tetani than in the resting fiber. A major fraction of this resting and tetanic power was contained in frequencies below 7 Hz, and no differences were found in muscles examined at the two temperatures. Specific frequency peaks were noted in some fibers but were not consistent from fiber to fiber. Logarithmically expressed spectral power was distributed as a f^{-n} function between 0.2 - 20 Hz where $n \geq 2$. These results suggest that any crossbridge movements detected at the sarcomere level represent broad band, low frequency, behavior and that they may be determined more by load than by temperature. This method provides a sensitive means to explore dynamic microstructural alterations in intact fibers.

M-AM-Po10 SUBSTRUCTURE IN THE OPTICAL DIFFRACTION PATTERN FROM FROG SINGLE SKELETAL MUSCLE FIBERS. N. Ishide*, T.Tameyasu and G.H. Pollack, Dept. of Anesthesiology and Div. of Bioengineering (RN-10), University of Washington, Seattle, WA 98195.

Individual orders of the optical diffraction pattern of muscle fibers consist of closely spaced parallel lines. This could imply closely spaced discrete values of sarcomere length. The present study tests this hypothesis. Single fibers from tibialis anterior or toe muscle of Rana pipiens were illuminated by a He-Ne laser. The diffraction pattern obtained without lens or aperture, was projected onto a screen and photographed with a 35mm cine camera (5 frames/sec) during rest and tetanus. The spacing between the substructural lines was measured, using a microdensitometer, by scanning the film with 5-10 lines normal to the zeroth order line. In the resting muscle, the distribution of spacings had a prominent peak at intervals corresponding to sarcomere length difference of 0.04 μm. During contraction, the distribution of the spacings became wider. This substructure could be due to some repetitive feature in the fiber. If so, this structure must have a length of over 100 μm, which is difficult to imagine. If Bragg reflections are responsible for the substructure, either discrete sarcomere lengths or discrete skewness of the striations is required. The latter seems unlikely. Thus, the most likely interpretation is that the sarcomere lengths take on discrete values at rest and during contraction. Measurements with increased resolution are in progress to determine whether or not the separation of discrete sarcomere lengths is, in fact, 43 nm.

M-AM-Po11 CHARACTERIZATION OF STEPWISE SHORTENING AT THE MYOFIBRIL LEVEL. M.J. Delay, R.C. Jacobson , R. Tirosh and G.H. Pollack. Dept. of Anesthesiology and Division of Bioengineering (RN-10), University of Washington, Seattle WA 98195.

It has been reported that records of sarcomere shortening in striated muscle show periods of rapid shortening alternating with periods of virtually no motion. In order to verify this phenomenon and to determine the size of local regions showing synchronized behavior, studies were performed on two kinds of optical image made from contracting muscle fibers. In the first, coherent light incident on the muscle resulted in a banded pattern, whose spacing derived from effectively all emergent diffraction orders. In the second, incoherent light microscopy was used to generate an image with a limited depth of field. The images were recorded on film taken at 4000 frames/sec., and analyzed by projecting sections taken across the striation pattern upon a photodiode array. The striation spacing was determined using an autocorrelation procedure and occasionally using a phase-locked loop. For the method using incoherent light, the image size on the photodiode array corresponded to about 30 striations with lateral and depthwise dimensions of about 1 μm each. The system noise was less than 0.1%. Preliminary results for the coherent method show (1) the presence of smooth shortening, suggesting that stepwise shortening may not be obligatory, but also (2) the presence of stepwise shortening with lateral synchronization of up to about 8 μm.

M-AM-Po12 SARCOMERE FLUCTUATION SPECTROSCOPY IN CARDIAC MUSCLE. Andrés Manring, Dept. of Physiol., Duke Univ. Med. Ctr., Durham, NC 27710.

When exposed to a solution of low Na or high K concentration, cardiac muscle develops a sustained contracture. Although the force is constant, microscopic examination reveals large rapid fluctuations in sarcomere lengths. Throughout the muscle, small groups of sarcomeres twitch rapidly and repeatedly while other groups do not twitch at all. The distribution of the twitch groups appears to be random and there does not appear to be any synchrony among the different twitching groups. Thus contracture lends itself for study using fluctuation analysis, in particular, photon correlation spectroscopy. The macroscopic behavior of the muscle is modeled by a string of N sarcomeres which have an average spacing of σ. The length of the jth sarcomere fluctuates in time by an amount $c_j(t)$. It is shown that the field autocorrelation function $G^{(1)}(\tau)$ of light scattered by such a model is approximately

$$\frac{G^{(1)}(\tau)}{L(N,q,\sigma)} = [1 - q^2 \sum_{j=1}^{N} [\langle c_j^2 \rangle - \sum_{k=1}^{N} \langle c_j(t) c_k(t+\tau) \rangle]],$$

where $L(N,q,\sigma) = (\sin Nq\sigma/2)/(\sin q\sigma/2)$ and $q = (4\pi n/\lambda)\sin\theta/2$ is the wave-vector of the scattered light; λ is the wavelength of the light, n is the refractive index; θ is the scattering angle; and $\langle\ \rangle$ denotes a time average. Two further self-consistency tests are discussed. One is the fluctuation of overall muscle tension, the other is the fluctuation of the mean sarcomere length. (Supported by NIH grant HL11307-16).

M-AM-Po13 DIFFERENTIAL HOLOGRAPHIC RECORDING OF PRECONTRACTILE AND EARLY CONTRACTILE EVENTS IN ELECTRICALLY STIMULATED SINGLE FIBERS OF VERTEBRATE SKELETAL MUSCLE. M. Sharnoff, L. J. Lingg*, and N. J. Rumer*, Department of Physics, University of Delaware, Newark, DE 19711.

We have followed the optical concomitants of the events which ensue during the first few msec. after stimulation of single fibers dissected from semi-tendinosi of Rana pipiens. The fibers were suspended either barely slack or lightly stretched in isotonic Ringer solution at room temperature and were focally stimulated by electrical pulses ca. ½ msec. in duration. The onset of tension was recorded isometrically. The fibers were trans-illuminated on the stage of a microscope by 5147 Å light from an argon ion laser which, after passing through the microscope, was directed to a holographic plate illuminated also with a plane reference wave. The field of view usually included the stimulating electrodes. The responses of the fibers were monitored by doubly exposing the holographic plate, one exposure flash (ca. 1 msec. long) occurring a few msec. before, and the other following, each stimulus pulse. Between these exposures the object path was shortened by ½ wavelength. Images constructed from these holograms display only the changes which have occurred during the time elapsing between exposures. In such images, obtained from holograms recorded before the end of the latency period, the fiber appears weakly illuminated against a dark background, the distribution of brightness being fairly uniform throughout the volume of the fiber but distinctly different from that in images obtained from differential or non-differential control holograms made without stimulating the fiber. The weak image present during latency sets in within a msec. or two of stimulation and persists without pronounced change until the very end of the latency period, when the intensity increases markedly. The onset of tension is accompanied by a further abrupt intensification and by the appearance of interference fringes which course axially through the now-prominent pattern of cross-striations.

M-AM-Po14 DIFFUSION IN AN ELLIPTICAL CYLINDER: A REASSESSMENT OF THE DIFFUSION COEFFICIENT FOR OXYGEN IN MUSCLE. Michael Mahler, Dept. of Physiology, UCLA, Los Angeles, Ca 90024

The perimeter of a transverse section of a frog sartorius muscle lying on a flat surface is well approximated by a hemi-ellipse whose major axis (of length 2m, the muscle width) is about 5 times as long as the semi-minor axis (of length ℓ, the muscle thickness). In a previous study of O_2 diffusion in this muscle (M. Mahler, J. Gen. Physiol. 71:533, 1978), the tissue was treated as a plane sheet. For a hemi-elliptical cylinder, the diffusion equation predicts that after a step change (ΔP) in PO_2 at the upper surface, the time course of P_{O_2} at the midpoint of the closed, lower surface is:

$$\Delta P[1 + \sum_{m=1}^{\infty} \sum_{n=0}^{\infty} C_{2n,m}\, ce_{2n}(\tfrac{\pi}{2}, q_{2n,m})\, Ce_{2n}(0, q_{2n,m})\, e^{-q_{2n,m}(\sinh^2\xi_o)4Dt/\ell^2}]$$

where $\xi=\xi_o$ specifies the boundary ellipse in elliptical coordinates; ce_{2n} and Ce_{2n} are the standard and modified Mathieu functions of order 2n; $\{q_{2n,m}\}$ are the zeros of $Ce_{2n}(\xi_o,q)=0$; D is the diffusion coefficient for O_2; and $\{C_{2n,m}\}$ are constants. This is an S-shaped curve which relatively quickly becomes monoexponential, and adequately fits the actual time course previously measured. D can thus be calculated from the rate constant (k) of the monoexponential phase. Tissue geometry affects the predicted value of k as follows:

ξ_o	1.0	0.5	0.4	0.3	0.2	0.1	0(sheet)
$2m/\ell$	2.62	4.32	5.22	6.86	10.1	20.0	∞
$k/(D/\ell^2)$	4.57	3.56	3.22	3.02	2.87	2.67	$\pi^2/4=2.47$

D in this muscle thus appears to be about 30% smaller than the values previously published. Recalculated values for 22.8°, 10°, and 0°C, respectively, are 1.09, 0.80, and 0.63 x 10^{-5} cm^2/sec. USPHS Grant HL 11351.

M-AM-Po15 A BIOCHEMICALLY- AND STRUCTURALLY-BASED MODEL OF STRIATED MUSCLE CONTRACTION. M.B. Propp and T.L. Johnson (Intr. by B.H. Bressler), Massachusetts Institute of Technology, Cambridge, MA 02139.

A model of muscle contraction incorporating structural and biochemical data and assuming the cross-bridge theory has been developed. From structural studies, the modes of cross-bridge attachment to actin and the position-dependent rate constant for attachment have been derived. From in vitro studies of actomyosin ATPase, the reaction mechanism and its associated rate constants have been derived. The values of the in vitro rate constants have been used to determine a positional dependence for the in vivo rate constants. The physiological properties which any model of muscle contraction should predict and which have been obtained by experiment to date have been summarized for an idealized muscle fibre -- the dependences of force, stiffness, and ATPase rate on temperature and ATP concentration, for an isometric contraction: of force, stiffness, and ATPase rate on steady-state velocity and of the force-velocity relation on temperature and ATP concentration, for an isovelocity contraction: and of the rate constants for the four phases of a tension transient on temperature, ATP concentration, and step amplitude.

It was necessary to extend and to unify the theories of Markov processes and nonequilibrium thermodynamics in order to develop a model which exhibited the equivalence of time-reversal invariance and equilibrium, reciprocity of the linearized system if and only if the linearization is about equilibrium, and the inequality of the second law. The model has suggested methods for simulating the behaviour of muscle without solving a partial differential equation. Incorporating the values found for the structural parameters and rate constants into the model, the physiological properties of muscle (described above) have been predicted and compared to those derived from experiment. Supported by NSF/ENG-77-28444

M-AM-Po16 ^{31}P NMR AND MULTI-EQUILIBRIA ANALYSIS OF INTRACELLULAR FREE Mg^{2+} IN PERFUSED AND ISCHEMIC ARRESTED GUINEA PIG HEARTS, S.T. Wu, G.M. Pieper, J.M. Salhany*, and R.S. Eliot, Cardiovascular Center UNMC and VA Medical Center, Omaha, Nebraska 68132

The concentration of intracellular free Mg^{2+} in perfused guinea pig hearts has been estimated based on the Mg^{2+} dependent separation between the α and β phosphorus resonances from ^{31}P NMR spectra of intracellular ATP (Gupta, R.K. and Moore, R.D. (1980) J. Biol. Chem. 255, 3987-3993) combined with a computer assisted analysis of the multi-equilibria involved (Nanninga, L.B. (1961) Biochem. Biophy. Acta 54, 338-344). Both control and ischemic arrested hearts were studied. The value of free Mg^{2+} so determined was 2.5±0.7mM. This value is in good agreement with Nanninga's calculation but disagrees with the analyses by Gupta and Moore which were both determined using frog skeletal muscle. The four-fold discrepency results from discounting the influences of the protonated and the potassium-bound forms of ATP in the Gupta-Moore analysis. When the Gupta-Moore results are analyzed by our methods there is good agreement. We have found that free Mg^{2+} does not change significantly during ischemic arrest despite the severe acidosis which occurs. The higher value of free Mg^{2+} found in this study would suggest that a regulatory role for Mg^{2+} in metabolism is unlikely.

*J.M. Salhany is an Established Investigator of the American Heart Association

M-AM-Po17 CHARGE MEASUREMENTS OF MUSCLE PROTEINS Katy Jennison, Gerald F Elliott (Open University, UK), Carl Moos (SUNY, Stony Brook)

Muscle proteins from rabbit psoas were separated, purified, and concentrated by centrifugation to gels of 100-200 mg/ml (similar to concentrations in intact muscle). The Donnan potentials were then measured with a KCl-filled microelectrode and the net fixed charge in the gel was calculated. Gels measured included actin with and without troponin-tropomyosin, myosin, myosin rod, myosin and C-protein, and actomyosin complex. At 100mM KCl, pH7, the net negative charge per actin monomer (including its proportionate troponin-tropomyosin, as in the thin filament) was ~15 electrons; per myosin molecule the charge was ~70 e and per myosin rod ~75 e, suggesting that the head carries very little net charge. These charges are ionic strength-dependent, indicating a large amount of ion-binding. These figures compare well with calculations based on amino acid composition and with titration data. Measurements on A- and I-bands of intact glycerinated relaxed muscle also accord, but in rigor a considerably higher A-band charge (roughly double) is found (Bartels and Elliott, Abstracts of the European Muscle Meeting, Salzburg 1980). In our gel measurements the myosin charge is enhanced by a number of additions (e.g. C-protein) but an increase of this magnitude has only been observed in our (few) measurements in actomyosin.

This work supported by grants from Muscular Dystrophy Association and NSF (PCM-7726785) to CM, and by NIH grant GM26392 to Maynard Dewey (SUNY, Stony Brook).

M-AM-Po18 MYOFILAMENT-BOUND Mg and Ca: ELECTRON PROBE ANALYSIS OF SKINNED MUSCLE FIBERS. T. KITAZAWA, H. SHUMAN and A.P. SOMLYO. Pennsylvania Muscle Institute, University of Penna.

We wished to determine the divalent cation (Me^{2+}) bound to F-actin in situ. It can be estimated that thin filaments (actin + tropomyosin + troponin) should contain approximately 16 mmole of bound Me^{2+}/Kg dry wt. (1 mole/mole G-actin). Skinned fibers isolated from frog sartorius muscles were washed with TrisCl or LiCl solutions containing no added Ca, Mg, or ATP, extracted with 0.5 percent Triton X-100 for 30 min, and incubated for an additional 30 min in solutions in which contaminant Ca^{2+} and Mg^{2+} were buffered with EGTA or EDTA. The fibers were frozen in supercooled Freon 22 and ultrathin (100 to 150nm) cryosections were cut at -110°C. Electron probe analysis with astigmated spots to cover, respectively, the I- or A-bands was used to measure the bound elements. The results are summarized below:

		Bound Mg [m mole/Kg dry wt. ± S.D.]		Bound Ca		
$[Ca^{2+}]$	$[Mg^{2+}]$	I-band	A-band	I-band	A-band	
$<10^{-10}$M	$\leq 10^{-6}$M	10.7±4.3	3.3±3.0	1.2±1.7	0.6±1.3	n=49

Regions of the I-band not including the Z-line were also analyzed with focussed probes and found to contain 14.7±3.0 mmol/Kg dry wt. of Mg (n=4). The Ca concentrations measured are near the minimal detectable levels for the probe parameters used and the values are subject to further refinement of the background fitting technique. However, the measured Ca content is very much lower than the concentration that would be expected if this were the Me^{2+} bound to F-actin, while the Mg concentration measured is close to the theoretically expected value. We conclude, in agreement with several biochemical studies, that Mg is the unexchangeable divalent cation on F-actin in frog striated muscle. Supported by HL15835 to the Pennsylvania Muscle Institute and by MDA to T.K.

M-AM-Po19 THE EFFECT OF OSMOTIC VARIATIONS ON RESTING SARCOMERE LENGTH OF ISOLATED CARDIAC CELLS. K.P. Roos, A.J. Brady and S.T. Tan,* Dept. of Physiology, University of California, Los Angeles, Los Angeles, California 90024

Isolated cardiac muscle cells were prepared by the enzymatic digestion of adult rat myocardium (Brady et al., Nature 282:728, 1979). These cells demonstrate the characteristics of an intact membrane in that they tolerate external free Ca^{++} in the mM range and electrical excitation elicits phasic contraction. Their characteristic A-I band striation pattern was directly imaged and recorded using phase contrast microscopy and a computer coupled solid state detector. The digitized striation pattern profiles of isolated cells were analyzed with an individual striation spatial resolution of .05 μm. Individual and averaged sarcomere lengths were calculated from the striation pattern profiles of untethered isolated cells. Average resting sarcomere lengths from 13 cells in isotonic media (300 mOsm/kg H_2O) ranged from 1.77 μm to 1.91 μm with a mean of 1.83 ± .04 μm. To measure the effect of tonicity upon sarcomere length, striation patterns were recorded from 64 additional cells from 8 independent heart preparations bathed in Tyrode's solutions of various osmolarities. Increasing osmolarity (hypertonic) with sucrose up to 2 fold elicits a decrease in sarcomere length corresponding to the cube root of volume change expected in a perfect and uniform cellular osmometer. Decreasing osmolarity (hypotonic) by dilution did not linearly extend sarcomere length beyond control lengths. The sarcomere length increased with decreasing tonicity to a maximum level of about 1.93 μm at 220 mOsm/kg H_2O where it remained despite further hypotonic stress. These observations indicate a non-linear longitudinal elasticity in isolated rat cells subjected to hyper- or hypotonic stresses.

M-AM-Po20 OSMOTIC CONTRIBUTIONS TO THE STABILITY OF THE A-BAND LIQUID-CRYSTAL. Ernest W. April, Department of Anatomy, Columbia University, New York, N.Y. 10032

The osmotic contribution to the stability of the A-band lattice in striated muscle is demonstrated. Measurements of low-angle X-ray diffraction patterns produced by the myosin filament lattice of crayfish (Orconectes) long tonic fibers has enabled quantitation of physiological and experimental osmotic forces. In addition, since there is a force balance in the liquid-crystalline A-band lattice, these determinations enable precise estimates of the electrostatic repulsive forces and effective charge density along the myosin filaments. Diffraction patterns were recorded either on film or in one-sixth the time with a position sensitive detector interfaced to a computer. Initially, intact muscle fibers were calibrated as osmometers with standard solutions of NaCl, K Propionate and sucrose, the osmotic pressures of which were determined by freezing point depression. Osmotic pressures of solutions containing various concentrations of polyvinylpyrrolidone (M.W. 10000, 40000, 360000) and Dextran (360000) were determined by comparable shrinkages produced in intact muscle fiber osmometers. Due to the impermeability of the A-band to the large molecules, the A-band regions of skinned fibers exposed to the the same solutions undergo osmoticly induced volume changes. Since a pressure of 7.34×10^6 dynes/cm^2 returns the lattice of the skinned fiber to dimensions approximating intact fibers, it must be assumed that the electrostatic repulsive force under normal physiological conditions is approximately equivalent. Further, the relationship between unit-cell volume and electrostatic force approximates a log function between the minimal interaxial separation (27 nm) and maximal spacing (63 nm) at the experimental sarcomere length of 9.6 um, confirming the role of electrostatic forces.

[Supported in part by grants from NIH (AM15876) and the Muscular Dystrophy Association.]

M-AM-Po21 DEXTRAN T500 DECREASES SKINNED FIBER WIDTH, TENSION, AND ATPase. Brian Krasner and David Maughan, Dept. Physiology, Harvard Medical School, Boston, MA 02115 and Dept. Physiology & Biophysics, Univ. Vermont School of Medicine, Burlington, VT 05405

Dextran T500 ($\bar{M}_n$=180,800 D) is a long chain polymer that, in solution, does not penetrate the filament lattice of skinned muscle fibers, thereby reducing fiber width through osmotic compression. We tested the hypothesis that lattice compression produces a coupled reduction of ATPase and active force. Chemically-skinned single fiber segments (3-5 mm long, sarcomere spacing ca. 2.5 um) from rabbit soleus muscles were attached to a force transducer and immersed in solutions from which ADP as an end product of ATP hydrolysis was determined by high pressure liquid chromatography. Fiber widths were measured from light micrographs in a parallel set of experiments. We measured widths, force, and ATPase of fibers in relaxing (pCa > 8) and contracting (pCa = 5.2) solutions at 22°C. Dextran T500 was varied from 0 to 26% w/v. Increasing Dextran concentration from 0 to 5% shrank the fibers by ca. 24% (to approximately their in situ width); active force increased by 6% while the associated ATPase rate decreased by 7%. Increasing Dextran concentration further, from 5 to 22%, produced an additional 20-25% reduction in fiber width with a roughly linear, parallel reduction in active force and ATPase rate to ca. 0 and 12% of maximum, respectively. These results suggest a strong coupling of active force generation and ATPase activity in shrunken fibers, with a change in cross-bridge attachment angle accounting for a divergence of force and ATPase in swollen fibers.

Supported by PCM-78-10477 (BK) and Am. Heart Assoc. 78-634, 79-165, and NIH/HL 21312 (DM).

M-AM-Po22 MYOFIBRIL SHORTENING VELOCITY AND pCa: ANALYSIS BY MEANS OF A PATTERN RECOGNITION PROGRAM. Franklin Fuchs, Paul Demchak*, C.C. Li*, and H.T. Tai*, Departments of Physiology and Electrical Engineering, University of Pittsburgh, Pittsburgh, PA 15261

To obtain a direct measurement of sarcomere shortening velocity at zero load (Vmax) we have expanded on the approach of Honig and Takauji (Eur. J. Cardiol. 4, suppl: 5, 1976) in which shortening in myofibril suspensions was initiated by rapid injection of MgATP and terminated by rapid addition of EGTA. Experiments were done with myofibrils prepared from glycerinated rabbit psoas bundles having an initial sarcomere length of 2.6 - 2.9 μm. The reaction was carried out at 5°C in order to extend the reaction time (3-5 sec) and thereby reduce mixing artifacts. A series of Polaroid phase contrast micrographs was made before and after shortening. These were digitized and then analyzed by means of an interactive pattern recognition program which provided a mean sarcomere length based on measurement of 200 - 400 sarcomeres in each experiment. The Ca^{2+} dependence of Vmax was determined on the basis of the change in mean sarcomere length at different pCa values. Vmax ranged from 0.060 $\pm$ 0.004 μm/sec at pCa 7.0 to 0.100 $\pm$ 0.004 μm/sec at pCa 5.0. Thus Vmax appears to be a Ca^{2+}-dependent parameter, although the Vmax-pCa relationship is not nearly as steep as the force-pCa relationship.

This work was supported by a grant from the Western Pennsylvania Heart Association.

M-AM-Po23 THE EFFECT OF CALCIUM ON THE MAXIMUM VELOCITY OF SHORTENING (V_{max}) IN MAMMALIAN FAST AND SLOW SKELETAL MUSCLE FIBERS. RICHARD L. MOSS, Department of Physiology, University of Wisconsin, Madison, WI 53706.

The present study was done in order to investigate the relationship between maximum shortening velocity (V_{max}) and the free Ca^{2+} concentration in mammalian skinned muscle fibers. Psoas and soleus muscles were obtained from young male rabbits (approx. 2.5 kg), and bundles of about 20 fibers were dissected and stored for 2 to 10 days as previously described (Moss and Julian, 1980). Single fibers were then stripped free in relaxing solution and mounted between a motor and force transducer. Each fiber was viewed and photographed through a microscope during activations in solutions (100 mM KCl; 4 mM EGTA; 10 mM imidazole, pH 7.00; 4 mM ATP; 1 mM $MgCl_2$) containing various amounts of free Ca^{2+}. V_{max} was measured using either the load-stepping or slack-test procedures (Moss and Julian, 1980) at temperatures of 10,13 or 15°C. The estimations of V_{max} by the load-stepping technique were done only if the shortening records under load were linear. At 10°C and in maximally activating solutions (pCa 5.49), a mean V_{max} of 1.05±11 ML/s was measured with the slack test in the psoas fibers, while at pCa's which resulted in isometric tensions that were less than 0.8 of the maximally developed tension, V_{max} was 0.52±11 ML/s. Similar proportional decreases in V_{max} were observed in the psoas fibers at 13 and 15°C and in the soleus fibers at 15°C. The relative magnitude of the effect of Ca^{2+} on V_{max} was similar regardless of the technique used to measure V_{max}. Thus, a distinct effect of $[Ca^{2+}]$ on V_{max} has been shown to occur in mammalian skeletal muscle. The occurrence of this effect in both fast and slow muscle types may indicate that the underlying mechanism in the two cases is similar. (Supported by NIH grant HL25861 and a grant from the MDA).

M-AM-Po24 SEGMENT LENGTH ANALYSIS OF LOAD-INDUCED LENGTH TRANSIENTS IN MAMMALIAN CARDIAC MUSCLE. P.R. Housmans, L.H.S. Chuck, V.A. Claes and D.L. Brutsaert. (Intr. by N.M. De Clerck). Department of Physiology, University of Antwerp, Antwerp, Belgium.

A new method has been developed to measure length, velocity and force simultaneously on a central segment of isolated cardiac muscle. This approach bypasses the problems of damaged ends and immediately adjacent weaker segments of isolated cardiac muscle preparations in the analysis of rapid length transients in response to abrupt increases in load. Thin (cross-sectional area <.25 mm^2) right ventricular cat papillary muscles and trabeculae of a uniform cylindrical shape were removed from hearts which, prior to cardiectomy, were injected through the left ventricle with a homogeneous suspension of 15μ carbonated microspheres (3M, NRF015). Either these microspheres lodged in the capillaries of the core of the muscle, or microelectrode tips (tip diameter <1μ) inserted through the core of the muscle were used as markers for a central muscle segment. Strong transillumination (DC-powered halogen lamp, max. 150 W) of the preparation projected a shadow of the markers onto a 1024-element photodiode array (Reticon, CCPD-1024, RC-702A), which gave a segment length signal that was updated every 1.5 ms. Using feedback circuitry, isometric, preloaded and afterloaded isotonic contractions of undamaged central muscle segments were obtained. An abrupt increase in load during shortening provoked a three-phasic muscle lengthening (Housmans and Brutsaert, Nature, 262, 56-58, 1976): an elastic phase 1, a viscous slow phase 2, and a rapid phase 3 lengthening. The concomitant segment lengthening however consisted only of phases 2 and 3. Phase 1 lengthening therefore represents extension of damaged ends and of weaker muscle segments, whereas the load-induced phase 2 and 3 lengthening are a property of the intact contractile apparatus.

M-AM-Po25 PASSIVE CONTRIBUTIONS TO LOAD CLAMP DETERMINED SEGMENT SHORTENING VELOCITIES IN ISOLATED FERRET PAPILLARY MUSCLE. D.A. Whalen,* D.A. Martyn,* L.L. Huntsman, Center for Bioengineering, University of Washington, Seattle, WA 98195.

Load clamps from segment length (SL) isometric conditions to near zero loads were carried out during diastole and during contractions in papillary preparations using a servo system capable of completing tension steps within 5 milliseconds. The measurement system used permits assessment of length changes in the healthy central segment (SL) of the papillary muscle, thus bypassing artifacts secondary to ends damaged from coupling clamps (Huntsman et al., Am. J. Physiol 237(2):H131-H138, 1979). Force, SL, and SL velocity were measured. Diastolic tension steps resulted in velocity-time records with early (1-3 msec.) peaks of 8-10 SL/sec. and time constants of decay of 20-25 milliseconds. Velocity-time records obtained from load clamps in contracting muscle showed biphasic responses, with the first phase lasting 30-40 milliseconds and having a form similar to that obtained in the diastolic muscle, with peak velocities of 10-12 SL/sec. It would appear that, when observing healthy segment length changes, there is a viscoelastic response to a tension step in diastolic muscle which has its counterpart in the early phase of the velocity-time record obtained from load clamps in actively contracting muscle. This results in high velocity transients which mask the true contraction velocity for up to 30-40 milliseconds after completion of the tension steps. (Supported by NIH GM07604, NIH HL07403, and NIH HL20613.)

M-AM-Po26 TENSION RESPONSES TO RAMP AND STEP CHANGES OF LENGTH IN AMPHIBIAN SKELETAL MUSCLE. Bernard H. Bressler, Department of Anatomy, University of British Columbia, Vancouver, Canada.

Isolated sartorii of the toad (Bufo bufo) and the ventral head of the semitendinosus muscle of the frog (Rana pipiens) were given controlled velocity releases of varying speed from the plateau of an isometric tetanus with the muscle maintained at 0°C. The tension responses to ramp shortening complete in greater than 3.5 msec revealed at least two distinct phases on the tension records. There was a fast initial drop in tension followed by a definite inflexion and a change of slope of the tension record. As the speed of the imposed length change was increased, the inflexion point appeared at a lower tension. The first phase of the tension record is believed to represent the unloading of an undamped elastic element within the muscle, most likely the cross-bridge compliance. The remainder of the tension record is dominated by the processes which govern the early recovery of tension. With step changes of length complete in 0.9 msec the T_1 and T_2 tension transients originally described by Huxley and Simmons (J. Physiol. 143: 60, 1971) in single frog fibers were clearly seen in the whole muscle preparation. Evidence is presented which indicates that the tension-extension curve obtained with ramp shortening is most likely a combination of the T_1 and T_2 curves described by Huxley and Simmons. Finally, the appearance of the inflexions on the tension records obtained with relatively slow ramp changes of length does not support the suggestion that the tension transients seen with step changes of length are due solely to buckling of the ends of the fibers. (Supported by the Medical Research Council of Canada).

M-AM-Po27 CHANGES IN COMPLEX AXIAL STIFFNESS WITH REDUCTION OF FIBER WIDTH IN RELAXED SKELETAL MUSCLE. Michael R. Berman and David W. Maughan, Department of Physiology and Biophysics, University of Vermont, Burlington, Vermont 05405.

Chemically skinned single fiber segments (0.5-2 mm long; 2.2μm average sarcomere length) from frog semitendinosus and rabbit soleus muscles were mounted between a displacement generator and a force transducer and immersed in a series of relaxing solutions (pCa>8, pMg 3, pMgATP 2.5, ionic strength 0.15 M, T = 22°C) to which had been added different amounts of the non-penetrating long chain polymer Dextran T500 ($\bar{M}_n$ = 180,800 D). The osmotic compressive pressure exerted by the Dextran T500 served to reduce fiber width by a known amount. We applied small amplitude (20μm) length stretches (10 msec rise time; 0.9 or 2 sec duration) to the reduced width fibers and recorded the resulting force responses. We measured no discernible force response to stretch until fiber width had been reduced to 0.90-0.92 of its initial (ca. in-situ) width. In-situ width was measured in relaxing solution containing 5% w/v Dextran T500. Over the range of fiber widths investigated (0.7-1.0 of in-situ width) the amplitude of the initial force response to stretch, the decay time of force during the hold portion of the stretch and the force level maintained after decay all increased with further reduction in fiber width. Additionally, the time course of the force response to stretch in reduced width fibers was similar to that observed in fibers of in-situ width which had been put in rigor by deleting ATP, Mg and creatine phosphate from the bathing solution. These results suggest the possibility that even in relaxed fibers there may be some form of interaction between crossbridges and thin filaments solely as a consequence of the reduced interfilament separation attendant on reduced fiber width. Supported by American Heart Association grant 78-634 and NIH/HL grant 21312.

M-AM-Po28 EFFECT OF OSMOTIC COMPRESSION ON CALCIUM ACTIVATION AND FORCE PRODUCTION OF SKINNED RABBIT MUSCLE FIBERS. R.E. Godt and J.L. Morgan, Department of Physiology; Medical College of Georgia; Augusta GA 30912.

Single fibers from rabbit soleus muscle were mechanically skinned in low Ca^{2+} ($<10^{-8}$M) "relaxing" solution (see below) at room temperature. After stretch to a striation spacing of 2.6μm, fibers were activated in a series of solutions containing (in mM): 3 MgATP, 1 Mg^{2+}, 15 phosphocreatine, 5 EGTA, 20 PIPES, 17-28 KCl (so that ionic strength was 0.15M), 0.5 mg/ml creatine kinase, pH 7, 10°C, with varying $CaCl_2$. The long-chain polymer, Dextran T-500 (Mn= 180,000), at a concentration of 10% (0.1gm/ml), was added to compress the fibers osmotically. Fiber width in 10% Dextran relaxing solution was 71 (±3 SE)% of that in Dextran-free solution. Maximal calcium-activated force (pCa 4) in Dextran-containing solution was 82(±3 SE)% of that in Dextran-free solution. A similar inhibition of force by osmotic compression has been reported previously for skinned fibers from frog skeletal muscle compressed with polyvinylpyrrolidone (PVP, $\bar{M}n$=40,000) or Dextran T-500 (Godt & Maughan, Biophys.J. 19, 1977, p103ff; Maughan & Godt, Circ. 62, 1980, III-167) and from dog ventricle compressed with PVP (Fabiato & Fabiato, J. Gen. Physiol. 72, 1978, p667ff). On the other hand, activation by calcium (i.e. the relation between relative force and pCa) appeared to be essentially unaffected by compression, as has been observed in skinned fibers from dog ventricle in PVP-containing solutions (Fabiato & Fabiato, op. cit.). Thus the effect of osmotic compression does not appear to be unique to muscle type, species, or osmotic agent.

(Supported by U.S.P.H.S. grant AM-25851)

M-AM-Po29 THE EFFECT OF PRE-STRETCH ON THE ATP DEPENDENT CALCIUM TRANSPORT BY SARCOPLASMIC RETICULUM OF MECHANICALLY "SKINNED" MUSCLE FIBERS. D. Applegate* and E. Homsher (SPON:W.F.H.M. Mommaerts). Dept. of Physio., U.C.L.A., Los Angeles, Ca. 90024

Pre-stretching muscle fibers to sarcomere lengths greater than 3.6μ is commonly used as a technique to abolish thick and thin filament interaction. This technique has been widely used in the field of excitation-contraction coupling to eliminate electrical or optical movement artifacts. Pre-stretching whole muscles was also used in the energetics field to estimate activation heat, (e.g. Homsher (1972), Smith(1972)). An underlying assumption in such experiments using pre-stretched muscles or muscle fibers is that the sarcoplasmic reticulum is unaffected by the stretch. However, relaxation is known to be length dependent (Wilkie (1961), relaxation time increasing with stretch. The Ca^{2+} transport by the SR of mechanically "skinned" fibers, dissected from Rana catasbiana semitendinosus muscles, was measured in fibers stretched to sarcomere length 3.8μ and compared to that measured in fibers at sarcomere length 2.3μ (rest length), to test whether the increased relaxation time in stretched muscles is due to a stretch dependent inhibition of the ATP dependent Ca^{2+} transport by the SR. All experiments were carried out at pCa 6 with oxalate present. The methods were as described in Fed. Proc.(1980), Vol. 39 #3, Abst. 151. The results showed no significant difference in Ca^{2+} uptake/μg/min between stretched and rest length fibers. The ratio of uptake rate/μg fiber protein (stretched:rest) was 0.99 ± 0.10 (S.E.M.), n=10. The results indicate that the increased relaxation time for stretched muscles can not be accounted for by an inhibition of Ca^{2+} uptake by SR. However, one cannot conclude that pre-stretching the fiber does not affect the SR release of Ca^{2+}. There is evidence for a length dependent inhibition of Ca^{2+} release (e.g. Taylor et al. (1975), Frank and Winegrad (1976). Supported by USPHS HL 11351 and MDA grant C791127.

M-AM-Po30 DETECTION OF AN INTERMEDIATE BETWEEN FREE CALCIUM AND FORCE IN SINGLE MUSCLE FIBERS Ellis B. Ridgway and Albert M. Gordon. Medical College of Virginia, Richmond, VA 23298 and University of Washington, Seattle, WA 98195.

Using aequorin-injected, length controlled single muscle fibers from the barnacle, Balanus nubilus, voltage clamp stimulation gives rise to a transient increase in light (the calcium transient) preceeding the isometric twitch force response. When the muscle fiber is released (allowed to shorten) by a few percent during the calcium transient, extra light is seen implying extra free calcium. By releasing at different times during the contraction, the time course of the extra calcium can be measured. Taking into account the non-linearity of the aequorin reaction with calcium, the amount of extra calcium has a time course which is intermediate between the calcium transient and the twitch force response. The amount of extra calcium rises after the calcium transient and before force, and falls after the calcium transient and before force relaxation. The amount of extra light is not correlated with the instantaneous force at the time of the release, but is correlated strongly with the amount of force redeveloped subsequent to the release. The amount of extra light increases with increased peak force whether achieved by increased stimulation or summation of force due to a second stimulus. Increasing the temperature decreases the amount of extra light observed. The results support the conclusion that this length/force change is sampling the filament bound activating calcium and thus that (1) the calcium binding to the contractile filaments is length and/or force dependent and (2) there is a state of bound calcium with a time course that is intermediate between the calcium transient and force. (Supported by NIH Grants NS08384 and NS10919.)

M-AM-Po31 HEAT AND TENSION-TIME INTEGRAL IN RESTED AND PACED TWITCHES OF RAT PAPILLARY MUSCLE. Norman R. Alpert, Robert P. Goulette*, and Louis A. Mulieri. Dept. Physiol. & Biophys., Univ. of Vermont, Burlington, VT 05405

We studied rested (5 min interval), single twitches and paced (5 sec interval), single twitches of left ventricular papillary muscles (2.2±.5mg, 0.45±.09 mm^2 area, mean ± SE) from 191±29 g rats. We used deposited film, bismuth antimony thermopiles (Mulieri et al., Am. J. Physiol. 233 C146-C156, 1977) with high thermal resolution and long-term stability to allow initial and recovery heat measurements in single twitches without averaging. The tension-time integral of the rested twitch (R) was 13% higher ($p<.005$) than the paced twitch (P) while the peak twitch tension was 4% higher ($p<0.025$). The extra tension-time integral of R was accompanied by an inordinate amount of extra total heat liberation per tension-time integral (R/P = 1.35, $p<.05$). While the initial heat per tension-time integral was not significantly different in R vs P, the recovery heat per tension time integral was different (R/P = 2.17, $p<.005$). This discrepancy is not simply related to the increased tension-time integral since prolongation of the twitch by elevation of Ca^{2+} to 11 mM in the presence of caffeine (5 mM) or tetanization does not cause a comparable discrepancy. Supported by PHS #RO1 17592.

M-AM-Po32 LOWERED MECHANICAL THRESHOLD IN MALIGNANT HYPERTHERMIA SUSCEPTIBLE (MHS) PORCINE SKELETAL MUSCLE DEMONSTRATED BY K-CONTRACTURES. Esther M. Gallant, G.A. Gronert and S.R. Taylor, Departments of Pharmacology and Anesthesiology, Mayo Foundation, Rochester, MN 55901. (Intr. by J. Wiggins).

Initiation of MH is related to defects occurring in skeletal muscle of MHS humans and swine. We previously reported that 2% halothane, an MH triggering agent, causes a small depolarization (ΔVm) of intact MHS porcine muscle cells (Muscle & Nerve 2:491, 1979), and hypothesized that the initiation of MH might occur by the interaction of this depolarization with a lowered mechanical threshold in MHS cells. Consequently, we determined the relationship between $[K^+]_o$ and contracture force, and found that MHS muscle contracts in response to lower levels of K^+ than normal muscle. The relationship between $[K^+]_o$ and Vm was measured on thin strips of intact surface cells. These measurements were made in solutions with the Cl^- substitute NO^-_3 because $[Cl^-]_i$ might increase as $[K^+]_o$ increases. The steady-state Vm was not hyperpolarized 10 min after the 114mM NaCl normally present was replaced by an equal amount of $NaNO_3$ ($[Cl^-]_o$ now 9.4mM; Vm = -85.7mV in NaCl and -83.8mV in $NaNO_3$). When $[K^+]_o$ was varied from 2 to 200 mM with NO^-_3 as the predominant anion, an equal ΔVm was observed at each concentration in normal and MHS muscle cells. Low levels of halothane (0.5%) did not change the relationship between Vm and $[K^+]_o$ for MHS muscle cells. The line fitted to the data by least squares analysis had a slope (48mV/decade change at 38°C) which is not that predicted by the Nernst equation for a membrane permeable only to K^+. Nevertheless, the mechanical threshold of MHS porcine skeletal muscle evidently is lower than normal and may play a role in MH initiation upon exposure to halothane. Supported by the Minnesota Heart Assn. and the Muscular Dystrophy Assn. of America.

M-AM-Po33 LOW SUBSTRATE CONCENTRATION INDUCES SKINNED SOLEUS MUSCLE FIBER TENSION WITH SMALL ATPase. Brian Krasner, Department of Physiology, Harvard Medical School, Boston, Mass. 02115.

The actomyosin complex goes through several intermediate states during ATP hydrolysis. Several of these states may be important in the development of isometric tension in intact and skinned muscle fibers. Changing (MgATP) in the micromolar range may change the relative concentrations of these states thereby changing the relationship between isometric tension developed and rate of ADP released. I therefore decided to study changes in isometric tension and rate of ADP release (ATPase) that occur when skinned soleus fibers (low substrate activated) are exposed to bathing solutions containing 0-20 μM (MgATP). The ionic composition of the bathing solutions was EDTAt 15 mM, pH 8, ionic strength 0.30, (K^+) 200 mM, no added calcium. All solutions contained 0.5 mM total ATP; magnesium was added to vary (MgATP): no tension develops in a solution with no added Mg, but there is an ATPase of 0.3 μmoles/g/sec. As (MgATP) increases to 1 μM, tension increases to a maximum of 0.7 kg/cm^2, but there is no detectable increase in ATPase (i.e. change in ATPase less than 0.1 μmoles/g/sec). Increases in (MgATP) to 20 μM inhibit tension development and reduce ATPase to 0.2 μmoles/g/sec. For comparison, a standard calcium activating solution (pH 7, ionic strength 0.18, 4 mM EGTA, 0.5 mM (MgATP), 5 mM ATP, pCa 5.2) induces a tension of about 1.4 kg/cm^2 with ATPase of about 1 μmole/g/sec. Thus, the ATPase "cost" of low substrate tension is much less than the "cost" of calcium activated tension. These data suggest that low substrate tension in comparison with standard calcium activated tension involves a longer lasting actomyosin complex. (NSF grant #PCM-78-10477; NIH grant #5 F32 AM05832-02).

M-AM-Po34 RATES OF Ca^{++} ACTIVATION IN CHEMICALLY SKINNED VASCULAR AND VISCERAL SMOOTH MUSCLES. John W. Peterson, III Massachusetts General Hospital, Neurosurgical Service, Boston MA and II Physiologisches Institut der Universitat Heidelberg, West Germany

Samples of pig carotid artery and guinea-pig taenia coli were prepared in a relaxing physiological saline (pH 7.4, 37°C). Chemical skinning was achieved by a modified glycerination method. Tissue samples were incubated 5 min in cool glycerinating solution: 50% glycerol/50% relaxing solution (20 mM imidazole, 5 mM EGTA, 5 mM MgATP, pH 6.85)/2 mM DTE; then placed immediately in a freezer at -30°C. This procedure produces a contractile preparation which is extremely permeable but is not strongly extracted; as evidenced by various enzymic activities. As opposed to usual 10-15% of maximum force obtained with glycerinated tissues, these tissues develop 50-90% of full physiological force. Preparations were ready within 2 hours and stored up to six months with no noticeable degradation of function.

Maximal rates of Ca^{++}-activated tension development were measured under conditions where Ca^{++} diffusion was not rate-limiting (Ca jumps) by pre-incubating in very low EGTA concentrations, then "jumping" into very high Ca-EGTA solutions. The responses of the two tissues differ strongly. The skinned artery contracts at an essentially constant time-course irrespective of the free-Ca^{++} concentration. Taenia coli, on the other hand, shows a strong dependence on free $[Ca^{++}]$.

A similar difference was seen in the response to ATP-γ-S, which caused a relatively rapid maximal contraction in the skinned artery in the absence of Ca^{++}. In the taenia coli, it appears instead that phosphorylation goes slowly and incompletely in the absence of Ca^{++}. Ca^{++} present during the ATP-γ-S incubation however leads to a maximal contraction which is maintained in the absence of Ca^{++}.

M-AM-Po35 PHOTOLYSIS OF CAGED-ATP IN THE ORGANIZED MUSCLE FILAMENT LATTICE. M.J. Hibberd*, Y.E. Goldman, J.A. McCray and D.R. Trentham, Department of Physiology and Department of Biochemistry and Biophysics, University of Pennsylvania, Philadelphia, PA, 19104 and Department of Physics and Atmospheric Science, Drexel University, Philadelphia, PA,19104.

Caged-ATP (Kaplan et al., Biochemistry, 17, 1929-35, 1978) is being used to study the kinetics of crossbridge detachment by ATP in muscle fibers. Single fibers or small bundles of glycerinated rabbit psoas muscle fibers were cycled between relaxation and rigor with the following series of solutions: (1) Relaxing Solution: (mM) MgATP, 5; Mg^{2+}, 1; Ca^{2+}, <1nM; Reduced Glutathione, 2-10; EGTA, 30; Creatine Phosphate (CP), 11; Creatine Phosphokinase (CPK), 1mg/ml; TES buffer, 100;pH 7.1 at 25°C; Ionic Strength, 200. (2) Rigor: as (1) but without MgATP, CP or CPK. (3) Backup Rigor: as (2) but with CP and CPK. (4) Caged-ATP: as (3) but with 1mM Caged-ATP. Muscle tension was monitored with a high bandwidth transducer. After rigor tension had stabilized in solution (4), the Caged-ATP was photolysed using 347 nm radiation from a frequency doubled ruby laser or a 200W Hg arc lamp. ATP liberation was monitored with a luciferin-luciferase assay. Full relaxation of rigor tension was obtained within 1 second upon release of 100-200 μM ATP. Light pulses in the absence of Caged-ATP or in the presence of Caged-ADP (which released ADP) did not cause cause relaxation. Photodamage was minimal and several rigor-photolysis-relaxation cycles could be obtained from each preparation. The results indicate that the Caged-ATP photolysis method is applicable to investigation of the kinetics of contraction.

Supported by MDA and NIH Grants HL15835 and AM00745

M-AM-Po36 TRANSVERSE IMPEDANCE OF SINGLE FROG SKELETAL MUSCLE FIBERS. B.A. Mobley and G. Eidt*, Department of Physiology and Biophysics, University of Oklahoma College of Medicine, Oklahoma City, OK 73190 and Mucina Manufacturing Company, Detroit, MI 48240.

The transverse electrical impedance of single frog skeletal muscle fibers was measured at 31 frequencies that ranged from 1 to 100,000 Hz. Each fiber was bathed entirely in Ringer's solution, but it was positioned so that a central length of 5 mm. was in a hollow plastic disk and was electrically isolated from the ends of the fiber. The diameter of the segment of the fiber in the disk was measured, and then the segment was pressed from opposite sides by two insulating wedges. A grounded shield was embedded in each wedge. Electrical current was passed transversely through the segment between two platinum-platinum black electrodes which were located in the pools of Ringer's solution within the disk. The results were corrected for stray parallel capacitance, series resistance of the Ringer's solution between the fiber and the electrodes, parallel shunt and membrane resistance of the fiber and the phase shift of the measuring apparatus. A nonlinear least squares routine was used to fit a lumped equivalent circuit to the data from six fibers. The equivalent circuit of the fibers contained three parallel branches; each branch was composed of a resistor and capacitor in series. The model also included a seventh adjustable parameter that was designed to account for the degree of compression of the fibers by the insulating wedges. The branches of the equivalent circuit were assumed to represent the electrical properties of: 1. The myoplasm in series with the membrane capacitance that was exposed directly to the pools of Ringer's solution, 2. The capacitance and series resistance of the transverse tubules that were exposed directly to the pools of Ringer's solution, 3. The membrane capacitance in series with the shunt resistance between the fibers and the insulating wedges. (Supported by NSF Grant PCM 79-19087 and Established Investigatorship 75-205 from American Heart Association.)

M-AM-Po37 PHARMACOLOGICAL COMPARISON OF E.C. COUPLING AND THE SKELETAL MUSCLE Ca^{++} CHANNEL. E. McCleskey and W. Almers, Univ. of Washington, Seattle, WA 98195.

Local anesthetics have previously been shown to block the Ca^{++} channel in the muscle cell membrane and to inhibit e.c. coupling, as measured with strength-duration curves. Is this Ca^{++} channel involved in e.c. coupling, and is it pharmacologically similar to the Ca^{++} release sites expected to exist in the sarcoplasmic reticulum? Fibers from a frog sartorius muscle were voltage clamped with two microelectrodes and pulses of different amplitude and duration were applied. Pulses yielding just-detectable contractions were recorded and plotted as strength-duration curves. The cell membrane Ca^{++} channel was blocked with Mn^{++}, Ni^{++}, D-600, and nifedipine. 10 mM Mn^{++} and 10 mM Ni^{++} cause a slight depression of e.c. coupling which can be mimicked by varying membrane surface charge with 20 mM Mg^{++}. 250 µM D-600 and 150 µM nifedipine both enhance e.c. coupling slightly. It is concluded that the Ca^{++} channel is not involved in the early steps of e.c. coupling. Blockade of the Ca^{++} release site of the SR was attempted by pressure-injecting Ca^{++} channel blockers into the myoplasm. The concentration of injected material was estimated by injecting fluorescein along with the drug, measuring the fluorescence of the muscle after injection, and comparing the signal to references. D-600, nifedipine, and Ni^{++} were injected to concentrations above 250 µM, 25 µM, and 5 mM respectively. These concentrations would cause significant or complete block of Ca^{++} channels in the cell membrane. Yet, no effect on e.c. coupling was seen. Finally, muscles were soaked in 250 µM D-600 and 150 µM nifedipine for 24 hours and no effect was seen beyond the enhancement mentioned above. We suggest that the SR Ca^{++} release site is pharmacologically different from the cell membrane Ca^{++} channel. (Supported by PHS CM07270-06 and PHS AM17803-07.)

M-AM-Po38 BIPHASIC TWITCH AND TETANIC RESPONSES OF EMBRYONIC CHICK SKELETAL MUSCLE. Peter J. Reiser* and Bradford T. Stokes* (Intr. by Philip B. Hollander) Department of Physiology, Ohio State University, Columbus, Ohio 43210.

The isometric contractile properties of twitch and tetanic responses of 46 chick posterior latissimus dorsi (PLD) muscles have been studied during the final week of embryonic development (days 14-20) at a bath temperature of 24.2±0.2°C (mean±S.E.). Particularly in the younger muscles (days 14-16), the twitch response consists of a rapid phase of force generation followed by a tonic component (TC) during which force development and relaxation are much slower. The day-to-day changes in normalized peak tension (Pot), time to peak tension (t_{Pot}) and maximal rate of force development (max. dP/dt)/Pot of the rapid phase have been examined. All these parameters change significantly ($P<0.005$) between days 14 and 20. Pot, t_{Pot} and (max. dP/dt)/Pot change 334%, 66%, and 354%, respectively. The relative magnitude of the tonic component to that of the rapid phase was approx. 1.0 at day 14 and gradually decreased to less than 0.1 at day 20. The time to half-relaxation of the TC decreased from 14.8±0.3 (n=7) at day 14 to 9.1±1.1 sec (n=4) at day 16. From day 17 to 20, the TC typically consisted of a phase of slow relaxation without any additional force development such that relaxation of the twitch response was biphasic. The tetanic response to different frequencies of stimulation was also examined. The response of the younger muscles consisted of an abrupt increase in tension above the peak tetanic tension at the termination of a 4 sec stimulus train. The magnitude of this additional tension increased with increasing stimulus frequency between 40 and 100 Hz. The relaxation kinetics of the tetanic response during the final week of embryonic development paralleled those of the twitch response; by day 20 the TC had disappeared. Further experiments are in progress to test the ionic bases of these phenomena. Supported by the Muscular Dystrophy Association and the National Science Fdn.

M-AM-Po39 INTRACELLULAR pH AND MYOCARDIAL FUNCTION IN NORMAL AND ISCHEMIC HEARTS: A ^{31}P NMR STUDY. William E. Jacobus and Myron L. Weisfeldt. Department of Medicine/Physiological Chemistry, Johns Hopkins University School of Medicine, Baltimore, MD 21205

Correlations between changes in intracellular pH (pHi) and isovolumic ventricular developed pressure (LVDP) have been assessed by ^{31}P NMR in the isolated, perfused rabbit heart during conditions of respiratory acidosis and global ischemia. Intracellular pH was estimated from the chemical shift (δ_O) of the Pi resonance according to the equation $pH=pK-\log(\delta_O - \delta_B)/(\delta_A-\delta_O)$. The NMR constants relative to the creatine phosphate peak are $pK=6.90$, $\delta_A=3.290$ and $\delta_B=5.805$. Excellent agreement was noted between the ideal titration curve and NMR data for Pi in both dilute solution and a concentrated heart homogenate. Mono-and divalent cations at physiological concentrations did not influence the Pi titration curve. Hearts were perfused at 37° with phosphate free Krebs' Bicarbonate buffer since it was noted that buffer Pi contributed significantly to Pi peak area and chemical shift. With Pi free buffer, heart pHi was 7.18±.01 (M±SEM, n=16). LVDP was stable for more than 1 hour in hearts perfused with Pi free buffer. Hearts were subjected to respiratory acidosis ($95\%O_2+5\%CO_2$ mixed with $65\%O_2+35\%CO_2$), and mild hypoxic acidosis ($65\%O_2+30\%N_2+5\%CO_2$ mixed with $65\%O_2+35\%CO_2$). With either form of respiratory acidosis,a pHi change of only-0.22 resulted in a 50% depression of LVDP,suggesting a tight coupling between pHi and LVDP. In hearts subjected to either transient total ischemia (40s) or steady state partial ischemia,a 50% reduction in LVDP was associated with only a-0.09 pHi acidification. These results suggest that the fall in contractility observed at the onset of ischemia cannot be fully accounted for in terms of intracellular acidosis. Other factors must play an important role in the initial ischemic depression of myocardial function. (Supported by HL 22080 and HL 17665, W.E.J. is an E.I. of A.H.A.).

M-AM-Po40 EFFECTS OF Ni^{++} AND MUSCARINE ON PRIMARY PACEMAKER CELLS IN RABBIT SINO-ATRIAL NODE. Erwin F. Shibata and W. Giles (Intr. by S. Hamilton), Department of Physiology and Biophysics, U.T.M.B., Galveston, Texas 77550

We have studied the effects of $NiCl_2$ (0.5 to 1.5 mM) and muscarine-Cl (10^{-8} to 10^{-5} M) on the spontaneous pacemaker activity in the rabbit sino-atrial node. Standard microelectrode techniques were used to locate 'primary' or leading pacemaker cells. These pacemaker cells are (i) insensitive to tetrodotoxin (10^{-6} g/ml) and (ii) fire 10-40 msec before the crista terminalis is activated. Effective doses of muscarine or $NiCl_2$ (with total divalent cation concentration held constant by removal of $MgCl_2$) produced a negative chronotropic effect accompanied by the following changes in intracellular electrical activity: (i) decrease in slope of pacemaker potential, (ii) decrease in action potential height, and (iii) small (2-6 mV) hyperpolarization of the maximum diastolic potential. In addition, we have observed that $NiCl_2$ (0.75 mM) and muscarine (10^{-8} M) act synergistically to produce these effects (i-iii above). Since $NiCl_2$ is a potent blocker of the slow inward current, i_{si}, these results suggest that a reduction of i_{si} may underlie cholinergic actions in mammalian primary pacemaker tissue. Moreover, they indicate that the magnitude and time course of i_{si} is an important determinant of the slope of the diastolic depolarization in primary pacemaker cells. (Supported ty USPHS Grant HL-25409 and American Heart Association Grant 77-691.)

M-AM-Po41 ELECTRICAL CONSTANTS OF SINGLE FROG ATRIAL CELLS. J.R. Hume and W. Giles, Department of Physiology & Biophysics, University of Texas Medical Branch, Galveston, Texas 77550

An enzymatic dispersion procedure has been used to obtain single atrial myocytes from Rana catesbeiana. These cells are normally quiescent and microelectrode impalements yield stable resting membrane potentials near -88 mV (Giles and Hume, J. Physiol., in press). Experiments utilizing two microelectrodes, one for injecting current and simultaneously measuring potential via a bridge circuit and an independent voltage measuring electrode, have been carried out in order to determine the electrical constants of isolated single cells. In cells which maintain a normal resting potential, very small differences in the steady-state voltage response to injected currents could usually be detected by signal averaging several (7-20) responses. Using a model consisting of a linear cable with sealed ends, and using an average cell diameter of 5 μm, the mean values (± S.E.) for the passive electrical constants were calculated:

$R_i = 118.1 \pm 24.5\ \Omega$ cm, $R_m = 7.9 \pm 1.2 \times 10^3\ \Omega\ cm^2$, $C_m = 2.2 \pm 0.3\ \mu F\ cm^{-2}$
$r_i = 6.0 \pm 1.2 \times 10^8\ \Omega\ cm^{-1}$, $r_m = 5.0 \pm 0.8 \times 10^6\ \Omega$ cm, $\lambda = 921.3 \pm 29.5\ \mu m$.

In cells in which a significant depolarization of the membrane potential was produced by the second microelectrode impalement, values of λ are considerably shorter as a result of a lower R_m. Our results show that for isolated atrial cells which have a normal resting membrane potential (approx. -80 mV), λ (mean, 921 μm) considerably exceeds the length of an individual cell (mean, 204 μm). (Supported by a NSF Fellowship (J.R.H.); and grants from the American Heart Association (77-691) and N.I.H. (HL-25409).

M-AM-Po42 MEMBRANE SIALIC ACID AND ELECTROPHYSIOLOGY OF CARDIAC PURKINJE FIBERS. R.D. Nathan and M.L. Bhattacharyya. Department of Physiology, Texas Tech University Health Sciences Center, Lubbock, TX 79430.

Spontaneous or driven canine Purkinje fibers were treated with neuraminidase (0.1-1.5 U/ml), an enzyme which catalyzes specifically the hyrolysis of sialic acids bound to glycoproteins, glycolipids, and oligosaccharides. Release of up to 60% of these anionic residues from the sarcolemma, as verified by a fluorometric assay for free sialic acid, resulted in altered action potential configuration, fluctuations in the membrane potential, and arrhythmic beating. Within minutes after the addition of neuraminidase, driven fibers depolarized and exhibited action potentials with reduced durations, amplitudes and upstroke velocities, together with slight elevations in the initial phase of the plateau (Fig.). These effects were dependent upon the concentration of the enzyme (trace 1 is control, trace 2 is 0.25 U/ml, and trace 3 is 0.75 U/ml; driven at 60/min) and potentiated by bubbling the Tyrode's solution with oxygen. In spontaneous fibers, such changes were sometimes accompanied by arrhythmic beating due to significant beat-to-beat variations in the "take-off" potential. Removal of sialic acid also induced fluctuations in the membrane potential which were enhanced substantially by 2-min periods of rapid stimulation (150-180 beats/min). Our results suggest that the presence of sialic acid residues may be important for the maintenance of normal electrical activity in canine Purkinje fibers. Supported by grants HL 20708 and 07289.

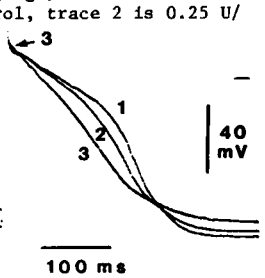

M-AM-Po43 THE EFFECT OF OLIGOMYCIN ON INDUCED PACEMAKER ACTIVITY IN FROG ATRIAL FIBERS.

K.-S. Tan and C.E. Challice, Physics Department, University of Calgary, Calgary, Alberta, T2N 1N4, Canada.

Rhythmic pacemaker activity can be induced in frog atrial trabeculae by applying a sustained depolarizing current. 0.05 μg/ml oligomycin renders this arrhythmic by gradually decreasing the amplitude of the action potential and gradually increasing the firing duration. Also, the slope of diastolic depolarization is gradually decreased, leading eventually to complete abolition of activity after 65±2 sec. The depolarizing current necessary for the induction of pacemaker activity, in the presence of oligomycin, is increased. By removing the inhibitor and returning to normal physiological conditions, induced pacemaker activity is re-established within 50 sec, with the rhythmic pattern and frequency remaining substantially unaltered. On the other hand, addition of adrenaline during inhibition increases the rate of diastolic depolarization, leading to a re-establishment of induced pacemaker activity, but this rate remains less than that for the normal Ringer condition by 38.3±3.2%, and also the rhythmic frequency is less by 26.7±2.7%.

Control of diastolic depolarization which leads to induced pacemaker activity is affected by the outward current which is activated following the depolarization of the action potential. During inhibition, the total outward current is increased and this is believed to be a prime factor in the decrease in diastolic depolarization. The addition of oligomycin is thought to lead to K^+ accumulation in the extracellular space, thereby shifting the reversal potential of the outward current toward a more positive value such that an increase in the depolarizing current is necessary in order to induce pacemaker activity.

M-AM-Po44 ACTIONS OF LIDOCAINE, QUINIDINE AND TETRODOTOXIN ON MEMBRANE CURRENTS UNDERLYING THE CARDIAC ACTION POTENTIAL PLATEAU. T.J.Colatsky, Department of Physiology, Cornell Medical College, New York, NY 10021.

The effects of lidocaine and quinidine on rabbit cardiac Purkinje fibers were compared at 37°C using action potential and voltage clamp measurements. At therapeutic concentration (5μg/ml), lidocaine shortened the action potential, while quinidine lengthened it. Slow response activity was not greatly altered by either drug. When membrane potential was held constant between -40 and -50 mV by applying the two-microelectrode voltage clamp, holding current consistently became more outward with lidocaine (+3±2 nA, mean±S.D.), but either did not change or became more inward with quinidine (-2±4 nA). Both drugs reduced the outward tails elicited on repolarization to -40 mV and which are associated with delayed rectification (i_x). The depression of i_x by quinidine (70±12%) was greater than that produced by lidocaine (17±8%) and is consistent with the observed prolongation of the action potential. To evaluate possible inhibition of steady-state sodium channels by lidocaine, experiments were performed using tetrodotoxin (TTX). TTX (0.1-5 μM) shortened the action potential, reducing its duration to 50% of control at ~1 μM. Voltage clamp experiments revealed a small TTX-sensitive component of steady-state current in the plateau range of potentials. In the presence of 10 μM TTX, lidocaine appeared to have little additional effect on steady membrane currents. These data suggest that (1) lidocaine and quinidine differ substantially in their modification of membrane channels, (2) a TTX-sensitive "window" current exists in the rabbit Purkinje fiber and helps maintain the plateau, and (3) the decrease in action potential duration seen with lidocaine may result primarily from block of these steady-state sodium channels. (Supported by USPHS grant HL 24279 and an E.I. from the A.H.A.)

M-AM-Po45 MORPHOMETRIC ANALYSIS OF DOG PURKINJE STRANDS; B.R. Eisenberg and I.S. Cohen, Departments of Physiology, Rush University, Chicago, IL 60612, and SUNY, Stony Brook, NY 11794.

Previous voltage clamp experiments suggest that the dog Purkinje strand is a favorable preparation for electrical analysis: it has a simple response to hyperpolarizing voltage steps and a small depletion current. These studies suggested that the myocytes in Purkinje strands from dogs are loosely packed. Therefore, we are measuring the structure of these strands. Relative volumes are estimated from light and electron micrographs by point count ratios and relative surface areas by intersection count ratios. Strands have a thin interrupted epithelial layer and a thick outer connective tissue sheath. The core of the strand usually contains myocytes and looser connective tissue. The volume of myocyte per unit volume of strand is very variable and ranges from 10 to 50% (mean 30%). The myocytes are usually well separated but some preparations have a tighter syncytial organization, looking like ventricular trabeculae.

We are concerned with small extracellular volumes in which ions could accumulate. Narrow (< 0.1 μm wide) spaces occupy only 0.6% of the myocyte volume (range 0.4 to 0.9%). Clefts and other small spaces (0.1 to 1 μm occupy only 2% of the volume (range 0.4 to 4.3%). One third of the membrane of the myocytes face a narrow (< 0.1 μm) space; one third face a cleft (0.1 to 1 μm); and one third face an extracellular space (> 1 μm). We conclude that the dog Purkinje strand is one of the best natural preparations available for voltage clamp studies, although even the canine strand contains a substantial amount of narrow extracellular space. The great variability in structure suggests that the morphology of each preparation used in physiological experiments must be measured.

M-AM-Po46 MECHANISM OF NOREPINEPHRINE HYPERPOLARIZATION OF CANINE CORONARY SINUS CELLS. Penelope A. Boyden, David C. Gadsby, and Paul F. Cranefield. The Rockefeller University, New York.

In the quiescent coronary sinus, norepinephrine (NE) induces a dose-dependent hyperpolarization which does not reflect enhanced Na+/K+ exchange (Boyden et al, 1980). We investigated the change in membrane conductance underlying this response by measuring steady membrane potentials at the end of 800 msec hyperpolarizing current pulses (amplitude, 5-200nA). Currents were injected via a second microelectrode near the midpoint of small preparations (about 1mm long and 0.2 mm wide). Conductance changes in response to both NE and carbachol (Cch) were compared in each preparation. Over the range of external K+ concentrations, $[K]_o$, examined (4 to 32 mM), the hyperpolarization caused by both NE (10^{-7} to 10^{-5}M) and by Cch (10^{-8} to 10^{-6}M) was associated with an increase in membrane slope conductance. Plots of steady membrane potentials against applied current obtained under control conditions, and in the presence of 10^{-5}M NE and of 10^{-6}M Cch, yielded current-voltage curves which all crossed at potentials negative to the control resting potentials. When a maintained current pulse was used to increase the membrane potential beyond the reversal potential, superfusion with either drug caused a depolarization of the membrane potential instead of the expected hyperpolarization. The reversal potentials of the currents induced with both NE and Cch varied linearly with log $[K]_o$: the least squares regression lines fit to these data had slopes of 61 mV for both NE and Cch (coefficient of determination 0.97-0.99), closely similar to that predicted by the Nernst Equation for a pure K+ electrode. We conclude that both NE and Cch increase the membrane potential of coronary sinus cells by increasing membrane conductance to K+ ions. Supported by USPHS HL-14899.

M-AM-Po47 POST-DRIVE MEMBRANE CURRENTS IN CANINE CARDIAC PURKINJE FIBERS. R. Falk and I. Cohen, Dept. of Physiology & Biophysics, SUNY at Stony Brook, Long Island, New York 11794

Canine Purkinje fibers of small radius were cut to lengths of less than 1.5mm and voltage clamped using two microelectrodes. Brief depolarizing voltage clamp pulses (10-50ms) were delivered at rapid frequencies (every 100-200ms) for variable duration trains (15sec-4min). At the end of the train the membrane potential was clamped at the holding potential, V_H, and a slowly decaying outward current ($\tau \approx 60$-80sec) was recorded. It has been proposed that Na^+ loading during rapid stimulation elevates the activity of an electrogenic Na^+-K^+ pump thereby giving rise to a decaying outward current at the end of the train, as pump activity returns to control values (Vassalle, 1966). The magnitude of the post-drive current we recorded depends on both the duration of the train and the frequency with which the brief clamp pulses are delivered during the train. The current magnitude saturates for trains of 2-4min duration. Phasic Na^+ loading through the fast inward channel induces a major portion of this slowly decaying outward current if pulse potentials, V_p, (during the train) are more negative than -15mV. This is indicated by the following results: (1) changing the pulsing protocol from 50ms duration pulses delivered every 100ms to 10ms duration pulses delivered every 100ms has only a small effect on the current's magnitude; (2) altering V_H during the train from -80mV to -55mV eliminates most of this current; (3) this current is negligible in the presence of 2.3×10^{-5}M TTX; (4) single depolarizing clamp pulses held for 1 min or more elicit smaller magnitude outward currents of much more rapid time course than those seen following comparable clamp trains. However, steady state Na^+ loading may substantially contribute to pump activation for V_p more positive than -15mV. At the more positive V_p the two different clamp protocols elicit current of similar time course.

M-AM-Po48 ELECTRICAL PROPERTIES OF AMPHIUMA HYPOGASTRIC ARTERY. J. Francis Heidlage & Nels C. Anderson Jr. Physiology Dept., Duke Univ. Medical Center, Durham, N.C. 27710.

Our laboratory has been studying stomach cells of *Amphiuma* as a model of smooth muscle structure and function. We are extending these studies to include vascular smooth muscle. Standard intracellular microelectrode techniques have been used on the intact artery, which has a mean diameter of 250 μm. Experiments are conducted in HEPES-buffered Ringer solution (pH 7.4) at room temperature. Cells are impaled with 17-35 MΩ microelectrodes. The observed resting potential is -57 ± 3 mv (mean ± SEM, n = 93). Increasing the external potassium concentration depolarizes the cells; the mean slope of the E_m *vs.* log $[K]_o$ curve is about 30 mV per tenfold change. Raising the external potassium concentration from 2 to 10 mM usually induces a transient hyperpolarization of 3 - 5 mV which may be due to activation of electrogenic sodium transport. Depolarizing and hyperpolarizing intracellular current pulses of 320 msec. duration are applied via a bridge circuit. The input resistance, calculated as the slope of the current-voltage relation at small displacements about the resting potential, is about 40 MΩ for cells with RMP near the mean; cells with low (≅ -25 mV) or high (≅ -85 mV) RMP exhibit considerably lower input resistance (20 - 25 MΩ). The low input resistance in hyperpolarized cells is consistent with a selective increase in the potassium conductance. Replacement of external Ca^{++} with Ba^{++} (0.5 or 1 mM) depolarizes the tissue and increases the membrane resistance. No spontaneous action potentials have been observed in normal Ringer. In general, this tissue appears to exhibit membrane electrical phenomena similar to those of tonic mammalian vasculature. Supported by USPHS grant NIAMDD 1-F32-05926.

M-AM-Po49 FOUR IONIC CURRENTS IN SINGLE, FRESHLY ISOLATED SMOOTH MUSCLE CELLS STUDIED WITH VOLTAGE CLAMP AND MICROPERFUSION. Joshua J. Singer and John V. Walsh, Jr., Dept. of Physiology, University of Massachusetts Medical School, Worcester, MA. 01605.

Membrane currents were studied with a two microelectrode voltage clamp in single smooth muscle cells enzymatically dissociated from stomach muscularis of Bufo marinus. Since we have shown that Ca^{++} ions carry the inward current of the action potential and that TEA slows its repolarization (AJP-Cell, 239: C162, 1980), $[Ca^{++}]_o$ was elevated and TEA was present to maximize the net inward current. From a holding level near -80 mV, a large positive command step caused three currents: (1) an initial inward current, followed by (2) an outward current which reached a large peak after several hundred milliseconds and then decayed over a period of seconds to (3) a smaller steady-state outward current. When a less negative holding potential (near -20 mV) was employed or when cells were studied in solutions with low $[Ca^{++}]_o$ (.16mM) and high $[Mn^{++}]_o$, the net inward current was eliminated revealing a fourth current, an early transient outward current; the large peak in the outward current was also absent, suggesting that it was due to a Ca^{++}-activated g_K. To corroborate this we altered the ionic environment in the vicinity of the cell, while it was clamped, by pressure ejection of solutions from a micropipette (tip diameter: 2-6μ), approximately 50μ away from the cell. Microperfusion in this way with a solution having a high Mn^{++} concentration (when the cell was originally in a solution high in Ca^{++}) decreased the inward current substantially and greatly diminished or eliminated the peak in the outward current, both reversibly. In another series of experiments without TEA, the peak outward current was an order of magnitude greater, in agreement with our earlier findings that $g_{K(Ca)}$ in these cells is TEA-sensitive. The net inward current also decayed faster.
Supported by NSF PCM-7904938 and NIH 14523

M-AM-Po50 INTRAMEMBRANOUS PARTICLE AGGREGATION IN CHEMICALLY-SKINNED MUSCLE FIBERS IS NOT DUE TO LIPID PHASE TRANSITION. A. B. Eastwood and K. R. Bock* Laboratory of Muscle Morphology, Departments of Anatomy and Neurology, Columbia University.

Mammalian skeletal muscle fibers can be chemically skinned by exposure to a solution containing 140mM potassium propionate, 5mM EGTA, 2.5mM $MgCl_2$, 2.5mM ATP, and 5mM imidazole, pH 7.0, at 277 K for several hours; they are then permeable to Ca, ATP, and EGTA (Wood, et al., Science, 187:1075-1076). The plasma membrane of chemically skinned fibers is disrupted so that glycogen particles escape thru holes visible in thin sections (Eastwood, et al., Tissue & Cell, 11:553-566). Intramembranous particles (IMPs) of the plasma membrane are aggregated on freeze-fracture (FF) replicas of chemically skinned fibers. To determine whether IMP aggregation is a result of a lipid phase transition due to lowered temperature during skinning, we examined FF replicas of rabbit psoas fibers treated in several ways: 1. After normal chemical skinning, fibers were kept at 297 K for up to 1 hour before fixation; 2. Fibers were skinned at 297 K or 304 K for 1 to 3 hours before fixation. These and control (freshly fixed) fibers were fixed with glutaraldehyde, cryoprotected with 30% glycerol, and frozen in solidifying Freon 22 (113 K). IMPs were aggregated in plasma membrane fracture faces of all chemically skinned fibers, regardless of temperature pre-treatment. We conclude that IMP aggregation in plasma membranes of chemically skinned fibers is not due to a lipid phase transition but reflects an alteration of membrane structure caused by chemical skinning.

Supported by NIH (NS11766) and MDA (H. H. Merritt Center and a scholarship to K. R. B.).

M-AM-Po51 RHYTHMIC CONTRACTION OF ARTERIAL SMOOTH MUSCLE. P.G. Stein and S.P. Driska, Physiology Dept., Medical College of Virginia, Va. Commonwealth Univ., Richmond, VA 23298

Smooth muscle from large arteries is generally thought to only contract tonically but we have found that many muscle strips from the pig carotid artery (74%, N=172) could be induced to contract rhythmically. Muscle strips were stretched to about 65% of the optimum length for force development and allowed to equilibrate at 37°C. Isometric stimulation with 10 μM histamine produced an average tonic active force (TAF) of 1.2×10^5 N/m^2 - about equal to that elicited by 124 mM K^+ at this muscle length. After 14±6 (SD) minutes exposure to histamine, this active force developed oscillations between a maximum of 121% and a minimum of 38% of TAF. The period of the oscillation was constant for a given strip but varied among strips from 1.4 to 8.1 minutes and the oscillations have continued for up to 6 hours. Muscles allowed to shorten isotonically showed no change in frequency of oscillation. Muscles frozen at the peak of contraction had more extensive phosphorylation of the myosin light chain than did those frozen between contractions (59% vs. 36%, respectively). Oscillations could be stopped in the relaxed state by removing the histamine or Ca^{2+} from the bath, or by adding H_1-receptor blockers or 1.6mM Mn^{2+}. The rhythmic contractions could be converted to sustained contractures by addition of 10^{-6}M ouabain, other vasoconstrictors, or more histamine. Propranolol, bretylium, phentolamine and treatment with 6-hydroxydopamine did not block the oscillations, suggesting that adrenergic nerve terminals are not involved in this response. Tetraethylammonium chloride (4mM) induced qualitatively different contractions which were irregular in both frequency and amplitude. These oscillatory contractions should be useful in the study of excitation-contraction coupling in vascular smooth muscle. Supported by NIH grant 1R23HL24881-01 and a Faculty Grant-In-Aid from Virginia Commonwealth University.

M-AM-Po52 CONTRACTILE RESPONSES OF INTRAFUSAL MUSCLE FIBERS. R.S. Wilkinson and C.C. Hunt, Dept. of Physiology, Washington University School of Medicine, St. Louis, Mo. 63110.

Isolated cat muscle spindles were decapsulated in the equatorial region and mounted in a chamber on an inverted microscope. Intrafusal muscle fibers were viewed with Nomarski optics; movement and sarcomere length changes were recorded with a Locam cine camera. Fibers were impaled with 3M KCL-filled micropipettes (80-200 MΩ); current was passed through a bridge circuit. Resting membrane potentials (average of 103 fibers = 48 mV) did not differ significantly between nuclear bag and nuclear chain fiber types. Depolarizing current produced graded contractile responses in both bag and chain fibers with no sign of contractile inactivation. In chain fibers the focus was typically at the point of impalement. In bag fibers the focus was usually some distance away, toward the pole on the side of the impalement; occasionally contractile foci towards both poles were observed. Contractile responses were more rapid in chain than in bag fibers. In both type fibers oscillatory movement of sarcomeres was observed during depolarizing pulses. In some fibers, particularly those with low resting potentials, hyperpolarizing pulses caused relaxation, indicating the tonic nature of contractile activation in these fibers.
(Supported by grants from U.S. Public Health Service (NS 0707) and MDAA.)

M-AM-Po53 MORPHOLOGY AND FUNCTION OF ISOLATED CARDIAC MYOCYTES. B.A. Wittenberg, and T.F. Robinson (Intro. by J. Wittenberg). Albert Einstein College of Medicine, Bronx, N.Y. 10461

We have developed a reproducible preparation of isolated adult rat heart myocytes in which an estimated 20-25% of the myocytes originally present in the ventricles are recovered as rectangular cells (10×10^6 cells per heart). Up to 5.5×10^6 cells per heart remain striated, rectangular and quiescent for 1 hr in solutions of 1 mM free calcium ion activity and contract only in response to electrical stimuli. Resting sarcomere lengths are normal in the living state, and after fixation and preparation of individual cells for electron microscopy, sarcomere shrinkage does not exceed 5%.

Individual cells have been identified by light microscopy and selectively processed for electron microscopy. Both the cell coat and plasmalemma are intact and continuous in all rectangular cells. The functional integrity of the plasmalemma is demonstrated by the normal response to electrical stimulation and by the maintenance of normal permeability barriers toward extracellular calcium ion, succinate, and ADP. The sarcomeres contract uniformly along the entire length of the cell. Dying myocytes "beat" spontaneously and asynchronously, and eventually become irreversibly rounded.

The steady state oxygen pressure required to maintain the cellular respiration at maximal values is unexpectedly low, 2 torr, with half maximal respiration at 0.15 torr at 20°C. This suggests that the intracellular impediment to oxygen diffusion of the myoglobin-containing heart myocytes is minimal.

This work was supported in part by NIH HL19299 (BAW); NIH HL24336, NY Heart GIA, NIH RCDA HL 00568 (TFR).

M-AM-Po54 ELECTRICAL ACTIVITY OF CULTURED CARDIOMYOCYTES OF THE ADULT RAT(1). S.L. Jacobson and G.A.R. Mealing, Department of Biology, Carleton University, Ottawa, Ontario, Canada K1S 5B6.

We have been studying the electrophysiology of primary cultures of cardiomyocytes of the adult rat prepared by the method of Jacobson (2). Ventricular cells in culture for 10 to 25 days have a mean resting potential of -55 ± 5 (S.E.) mv. and are sometimes spontaneously contractile. Spontaneous cells can be shut off by hyperpolarizing current injection. Action potentials can be evoked by depolarizing current pulses from shut-off, from normally quiescent, and from spontaneous cells. Electrical and mechanical activity is usually synchronous. Action potentials have durations from 80 to 200 msec. with overshoots of up to 20 mv. Maximum upstroke rate ($\dot{V}_{max}$) of the action potential of unhyperpolarized cells is 1-12 $V\text{-sec}^{-1}$ and these action potentials can be abolished reversibly by D600 at 3.3×10^{-6} g/ml, but are unaffected by tetrodotoxin (TTX) at 3.3×10^{-5} g/ml. Hyperpolarization to ~100 mv. increases $\dot{V}_{max}$ to as much as 60 $V\text{-sec}^{-1}$ and the high frequency component of this type of action potential is TTX sensitive at 3.3×10^{-5} g/ml. By contrast, ventricular cells from the neonatal rat, cultured by the same method do not show $\dot{V}_{max}$ in excess of 12 $V\text{-sec}^{-1}$ regardless of hyperpolarization. Further experiments are in progress.

1) Supported by grants (to SLJ) from the Ontario Heart Foundation and the Muscular Dystrophy Association of Canada.

2) Jacobson (1977) Cell Structure and Function 2: 1-9.

M-AM-Po55 PREVENTION OF FIBROBLAST PROLIFERATION IN RAT CARDIAC MONOLAYER CULTURES. Richard B. Robinson. Dept. of Pharmacology, Columbia Univ., New York, NY 10032.

Although primary cardiac cultures can be initially enriched in muscle cells by pre-plating to remove fibroblasts, heterogeneity is a problem in long term (>1 week) cultures due to the rapid proliferation of residual fibroblasts. Since fibroblasts are reported to lack the necessary enzyme to use D-amino acids, I have attempted to overcome fibroblast overgrowth by maintaining cardiac cultures (prepared by trypsinization of minced newborn rat ventricles) in Minimal Essential Medium containing either D-valine (DMEM) or L-valine (LMEM) and 10% horse serum (HS). In some experiments the HS was dialyzed (DHS) to remove endogenous L-amino acids, and then supplemented with insulin. Insulin had no effect on fibroblast proliferation, but was important to maintain normal muscle cell (M) morphology in DHS. The substitution of D- for L-valine did not affect initial fibroblast survival, since the % M after 1 day in culture (as determined by morphological criteria in phase-contrast) was identical in all media (LMEM+HS=91.0±6.9% M; DMEM+DHS=92.1±7.9% M). In LMEM+HS the % M decreased exponentially with time, reaching half the day 1 value ($t_{\frac{1}{2}}$) after 10±4 days. Substitution of DMEM for LMEM, in normal HS, increased $t_{\frac{1}{2}}$ to 16 days. A comparable increase in $t_{\frac{1}{2}}$ occurred if DHS was substituted for HS, both in LMEM, suggesting that dialysis somewhat affected the serum's ability to support cell proliferation. However, when cells were grown in DMEM+DHS, fibroblast proliferation was completely abolished, as indicated by the % M remaining constant with time. Muscle cells grown in DMEM+DHS continued to beat spontaneously. Preliminary data suggest they exhibit similar action potential parameters to control cells. It is concluded that D-amino acid substitution may provide a convenient method of controlling fibroblast proliferation in primary cardiac cultures. Supported by NIH HL-12738 and the New York Heart Association.

M-AM-Po56 THE EFFECTS OF CESIUM IONS ON SPONTANEOUS ACTIVITY AND ON THE UNDERLYING PACEMAKER CURRENTS IN CHICK EMBRYONIC HEART CELL AGGREGATES. Alvin Shrier and John R. Clay, Dept. of Physiology, McGill University, Montreal, PQ, Canada H3G 1Y6; Lab. of Biophysics, NINCDS, MBL, Woods Hole, MA 02543; and Dept. of Anatomy, Emory University, Atlanta, GA 30322.

We have investigated the effects of externally applied cesium ions on re-aggregates of electrically coupled cells dissociated with trypsin from 7 day old chick embryonic hearts. These preparations beat spontaneously and rhythmically in tissue culture medium containing low levels of potassium ions (K_o=1.3mM) with a beat rate (BR) of 1.2±.1 beats/sec (n=16; ±s.d.). Application of 0.5mM Cs^+ suppressed beating; 1.5mM Cs^+ restored BR to control level; 3mM Cs^+ further increased BR to a level greater than control (1.8±.2 b/s). Intracellular recordings revealed that quiescent preparations in .5mM Cs^+ rested at potentials in the -90 to -100mV range. Moreover, the maximum diastolic potential of spontaneous AP's was reduced from -98 (control) to -75mV (2.5mM Cs^+), and the AP duration was increased from 160 (control) to 400ms (2.5mM Cs^+). Both the maximum overshoot potential and threshold were approximately unchanged by Cs^+. Voltage clamp analysis revealed that 2mM Cs^+ blocked both a potassium ion pacemaker current, I_{K_2}, which we have characterized elsewhere (Shrier and Clay, 1980, Nature, 283, 670-71; Clay and Shrier, 1981, J. Physiol., In press), and a second time dependent current, I_x, (Clay and Shrier, 1981, ibid.), which appears to be involved in the repolarization process. The reversal potential of the Cs^+ (2mM) sensitive background current was -79mV, which differs markedly from E_K (-125mV). This result and the suppression of beating in .5mM Cs^+ indicate that Cs^+ blocks inward background current channels; the blockade of I_{K_2} indicates that Cs^+ also blocks K channels. Consequently, Cs^+ is not a selective blocker of any single type of ionic channel in the embryonic heart.

Supported by grants from the NIH and the MRC, Canada.

M-AM-Po57 DOUBLE OVERLAP OF THIN FILAMENTS IN ISOLATED RAT HEART MYOCYTES. T.F Robinson and B.A. Wittenberg. Albert Einstein College of Medicine, Bronx, N.Y. 10461

We have used electron micrographs of serial transverse sections of selected ventricular myocytes to analyze the configurations of myofilament overlap at rest and in contraction. Cells were prepared enzymatically[1] and individual myocytes that were striated and quiescent in solutions with a free calcium ion activity of 1 mM were selected. Each cell was photographed at rest, after fixation, and after embedment in a thin epoxy slab. No shortening was observed upon fixation; overall shrinkage was measured from the photomicrographs and did not exceed 5%.[2] The numbers of thin and thick filaments were counted within myofibrillar regions that contained approximately 350-400 thin filaments. In a resting cell with an average sarcomere length of 1.95 μm the ratio of thin to thick filaments is 2:1, except for small regions at the center of the A band. In a contracted cell with average sarcomere length of 1.73 μm the myofibrils had a highly packed lattice. Section-by-section analysis revealed that thin filaments did flex in double overlap in the ventricular cells, as reported for atrial and papillary muscles,[3] but the 4:1 ratio occurred across the entire areas of counting. In view of these findings, it is unlikely that some of the thin filaments bend back during contraction. 1. Wittenberg BA: In Oxygen: Biochem. & Clin. Aspects (WS Caughey, ed.) Acad. Press, NY, p. 35 (1979). 2. Robinson TF, Aronson RS, Cohen-Gould L, Sorenson AL, Wittenberg, BA & Sonnenblick EH: In 38th Ann. Proc. Electron Micr. Soc. Amer. (GW Bailey, ed.) San Fran., p. 574 (1980). 3. Robinson TF & Winegrad S: J. Physiol. (Lond.) 286, 607 (1979).

This work was supported in part by NIH 24336, NY Heart GIA, NIH RCDA HL 00568 (TFR); NIH HL 19299 (BAW).

M-AM-Po58 MICROWAVE EFFECT ON ACTIVE AND PASSIVE ^{24}Na EFFLUX FROM HUMAN RBC's

P. D. Fisher+, M. J. Poznansky+, W. A. G. Voss*
+ Dept. of Physiology and * Biomedical Engineering, University of Alberta, Edmonton, Alberta, Canada.

The effects of low level 2450 MHz microwaves at an absorption rate of ∿ 30mW/ml of suspension on total and on ouabain insensitive ^{24}Na flux from human red blood cells were examined. RBC's washed and loaded with ^{24}Na using parachloromercuribenzene sulfonate were exposed in a waveguide system under temperature-controlled conditions for 1 or 2 hours. The difference in the amount of extravesicular ^{24}Na at the beginning and at the end of the test periods were used as an index of flux rate. Experiments were run, in parallel, using exposed and sham-irradiated (control) samples at a variety of temperatures between 7°C and 35°C.

The results indicate that microwaves have a significant effect on ^{24}Na efflux from RBC's only in the temperature range 22-25°C. The effect on ^{24}Na efflux appears to be two fold. The microwaves caused, approximately, a 25% increase in the total efflux. The increase was due to, typically, a 40% increase in the ouabain insensitive component which was countered by a 10% decrease in the ouabain sensitive portion. The implications of such findings at the membrane level will be discussed.

M-AM-Po59 K^+-DEPENDENT Na + Cl UPTAKE BY SQUID GIANT AXON. John M. Russell, Dept. of Physiology and Biophysics, University of Texas Medical Branch, Galveston, Texas 77550.

In the presence of the normal extracellular potassium concentration (10 mM), the squid giant axon exhibits an ATP-dependent co-uptake of Cl and Na that can be blocked by furosemide but not by ouabain or TTX. (J. Gen. Physiol. 73: 801, 1979). I now report that the removal of extracellular K^+ (replaced by Na^+) inhibits both Cl^- and Na^+ influx into internally dialyzed axons treated with 10^{-5} M ouabain and 10^{-6} M TTX. Cl^- influx measured with ^{36}Cl fell by 13.9 ± 2.4 pmoles/cm^2-sec while ^{22}Na influx decreased 11 ± 0.6 pmoles/cm^2-sec. Previous work has shown that the ATP-dependent portions of the Cl^- and Na^+ fluxes were 16 and 12 pmoles/cm^2-sec, respectively. Thus, removal of external potassium was as effective an inhibitor of Cl-Na uptake as ATP-depletion.

K^+ influx was studied using ^{42}K to determine whether it had properties in common with Cl-Na uptake. These experiments showed ^{42}K influx to be inhibited by raising $[Cl]_i$, decreasing $[Cl]_o$ or $[Na]_o$ and by the agent furosemide. All these are properties shared with Cl/Na uptake. These data suggest a coupled Na-K-Cl uptake mechanism exists in the squid axolemma. Supported by NIH grant NS-11946.

M-AM-Po60 AMILORIDE-SENSITIVE Na FLUX IN NEUROBLASTOMA-GLIOMA HYBRID CELLS: AN ELECTROGENIC PATHWAY. Martha Eaton O'Donnell and Mitchel Villereal (Introduced by J. MacIntyre) Dept. of Pharmacol. and Physiol. Sciences, Univ. of Chicago.

Previous reports indicate that mitogenesis of neurons can be induced by increasing cell Na via Na channel activation with veratridine and that the earliest electrophysiological event following serum-stimulation of quiescent neuroblastoma cells is an increase in Na permeability. In light of recent observations that serum stimulation of quiescent fibroblasts activates an amiloride-sensitive Na permeability pathway, we sought to determine whether neuroblastoma x glioma NG108-15 hybrid cells have an amiloride-sensitive component of Na influx and whether such a pathway is electrogenic. ^{22}Na uptake was measured in NG108-15 cells in Hepes-buffered Eagle's minimal essential medium (EMEM) containing 10% calf serum and 5 mM ouabain. The Na uptake under these conditions is significantly inhibited (approx. 40%) by the presence of 1 mM amiloride. The membrane potential of the NG108-15 cells was estimated from the steady state distribution of the lipophilic cation ^{3}H-TPP according to the method of Lichtshtein et al. (Proc. Natl. Acad. Sci. USA 76:650-654, 1976). The value of the membrane potential measured in control cells, -71.3 mV, is in reasonable agreement with reported values for NG108-15 cells. For cells equilibrated with ^{3}H-TPP, the addition of 1 mM amiloride leads to an immediate (within 2 minutes) increase in ^{3}H-TPP concentration which levels off at a value corresponding to a membrane hyperpolarization on the order of 20 mV. Thus, the amiloride-sensitive Na influx pathway in NG108-15 cells appears to be electrogenic. This work was supported by DA 02575, USPHS. M. O'Donnell is supported by 5 T32 MH-14274, Neurobehavioral Sciences Research Training Program.

M-AM-Po61 Ca^{2+} TRANSPORT AGAINST A MEMBRANE POTENTIAL IN CYTOCHROME OXIDASE VESICLES RECONSTITUTED WITH MITOCHONDRIAL MEMBRANE PROTEINS. R.N. Rosier*and T.E. Gunter (Intr. by K.K. Gunter) Dept. of Rad. Biol. and Biophys., Univ. of Rochester, Rochester, NY 14642.

Energy-dependent Ca^{2+} accummulation into cytochrome oxidase vesicles (COV) has recently been shown. Generation of an internally positive membrane potential through externally added ascorbate and phenazine methosulfate (PMS) and internally trapped cytochrome c prevented Ca^{2+} influx (1). Both Ca^{2+} uptake and generation of an internally positive membrane potential could be observed, in contradistinction, when COV's energized as described above, were reconstituted with complex V, a mitochondrial protein complex containing the uncoupler binding site. Control experiments, based both on diS-C_3-(5) fluorescence and on oxidative phosphorylation in COV's, reconstituted with hydrophobic protein, and external oligomycin sensitivity conferring protein, and the mitochondrial ATPase F_1, verified that the energization conditions used, produced internally positive membrane potentials. The observed electron-transport dependent Ca^{2+} uptake under these conditions of energization produced Ca^{2+} concentration gradients, which were always greater than those of the corresponding nonenergized controls (an average of 3 times greater) and rates of uptake which were always faster (an average of 1.6 ± 0.7 nmoles/mg min faster) than those of nonenergized controls. The transport was inhibited by removal of substrate, PMS, or O_2 or by addition of CN^- or uncouplers. Partially purified mitochondrial hydrophobic protein fractions, other than complex V, were found to be less effective than complex V or completely ineffective in reconstituting Ca^{2+} uptake into internally positive vesicles. The internally positive, complex V-COV system was also found to transport Mn^{2+} and Rb^+ but not Na^+.

Supported by NIH (AM-20359) and DOE (DE-AC02-76EV03490). (1) R.N. Rosier and T.E. Gunter. FEBS Lett. 109 99 (1980).

M-AM-Po62 TIME COURSE OF ACTIVE NA TRANSPORT AND OXIDATIVE METABOLISM FOLLOWING TRANSEPITHELIAL POTENTIAL PERTURBATION IN TOAD URINARY BLADDER. Stanley J. Rosenthal, John G. King, & Alvin Essig. Boston University School of Medicine, Dept. of Physiology, Boston, MA 02118.

The use of an Ussing chamber with well defined mixing characteristics coupled to a mass spectrometer permits the concurrent evaluation of transepithelial current and oxidative metabolism with improved temporal resolution. The time-course of the amiloride-sensitive current I^a and the rate of suprabasal CO_2 production $J^{sb}_{CO_2}$ were observed in 10 toad urinary bladders at short-circuit and after clamping $\Delta\psi$ at 100mV, serosa positive. Following perturbation of $\Delta\psi$ (0→100mV), I^a declined sharply within 1/2 min, remained near constant ~15 min, and then increased slightly. $J^{sb}_{CO_2}$ declined more gradually, remained near constant at ~4-7 min, and then declined further. Detailed analysis revealed an early quasi-steady state with near constancy of $J^{sb}_{CO_2}$ starting at 2.9±1.1 (SD) min and lasting 4.7±1.8 (SD) min, followed by relaxation to a later steady state at about 15 min. During the early quasi-steady state, I^a was also nearly constant. Considering that in steady states $I^a/F=J^a_{Na}$, the rate of transepithelial active Na transport, during the early quasi-steady state mean values ±SE of J^a_{Na}, $J^{sb}_{CO_2}$ and $(J^a_{Na}/J^{sb}_{CO_2})$ were respectively 29.9±1.7%, 59.4±3.2%, and 56.4±5.7% of values at short-circuit. Corresponding values during the late steady state were 41.4±6.0%, 38.3±6.1%, and 111.3±8.6%. Thus the flow ratio $J^a_{Na}/J^{sb}_{CO_2}$ was depressed significantly during the early quasi-steady state, but returned later to the original value. The results of measurements of I^a and $J^{sb}_{O_2}$ in 3 hemibladders were qualitatively similar. The findings are consistent with earlier studies, indicating incomplete coupling between transport and metabolism.

M-AM-Po63 INFLUENCE OF BASOLATERAL $[K]_i$ ON THE ELECTRICAL PARAMETERS OF THE CELLS OF ISOLATED EPITHELIA OF FROG SKIN. R. S. Fisher and S. I. Helman. Department of Physiology and Biophysics, University of Illinois, Urbana, IL 61801.

The basolateral potassium concentration dependence of apical and basolateral membranes of the cells of frog skin was investigated in isolated epithelia. After removal of the corium, the epithelia were short-circuited and impaled with microelectrodes from either apical or basolateral solutions. $[K]_i$ was increased in steps for about 20 to 40 seconds from 2.4 to 8, 14.4, 24, 50, and 100 mM. With 10^{-4} M amiloride in the apical solution, I_{sc} was near zero and remained unchanged by increases of $[K]_i$. In the absence of amiloride, measurements were made of the intracellular voltage, V^{sc}_0, and the Thévenin electrical parameters of the basolateral membranes (E_i and R_i) and the apical membranes (E_o and R_o). As expected, increases of $[K]_i$ depolarized the V^{sc}_0. (ΔE_i = 50.3 mV/decade at $[K]_i$ > 8 mM.) With increasing $[K]_i$, both E_i and R_i fell from control values of 105.3 ± 3.8 mV and 1096 ± 140 Ω cm^2 to 36.9 ± 2.6% and 32.5 ± 2.8% of control, respectively, at 100 mM $[K]_i$. The R_o remained essentially constant for $[K]_i$ up to 50 mM. The mean E_o of the apical barrier was not significantly different from zero for skins bathed with 100 or 10 mM Na in the apical solution. This idea is supported by the finding that the changes of I_{sc} (% of control) were the same as the changes of V^{sc}_0 (% of control), a circumstance to be expected if the E_o is zero and the R_o is constant being independent of the influence of $[K]_i$ on the I_{sc}. These data support our previous conclusion that at physiologically negative intracellular voltages, the mean E_o of the apical barrier is not significantly different from 0 mV, being attributed most likely to the electrical rectification of the Na flux at the apical membranes of the cells. (Supported by HEW PHS AM 16663.)

M-AM-Po64 THE RELATIONSHIP BETWEEN ACIDIFICATION AND SODIUM ENTRY IN ISOLATED FROG SKIN. D.J. Benos, Department of Physiology and LHRRB, Harvard Medical School, Boston, Massachusetts 02115.

Acidification of the external medium by isolated frog skin epithelium (Rana catesbeiana, Rana temporaria, and Caudiverbera caudiverbera) and its relationship to Na uptake was studied. Acidification was measured by the pH-stat technique under short-circuit or open circuit conditions. The results of this study demonstrate that a) acidification by the isolated frog skin is not directly coupled to Na or anion transport; b) acidification can be inhibited by the diuretic drug amiloride, but only at high external Na concentrations (this inhibition amounts to a maximum of 60% at 10^{-4}M external amiloride); c) acidification rate is controlled by the metabolic production of CO_2, and probably results from CO_2 diffusion from the cells into the external medium; and d) the positive correlation between net Na absorption and net acidification observed in whole animal studies cannot be replicated in the isolated skin preparation, even when the frogs were first chronically stressed (for at least two weeks) by salt depletion, a physiological state comparable to that employed in the in vivo experiments. This work was supported by NIH Grant AM-25886.

M-AM-Po65 CHANGES IN THE $(K^+ + H^+)$-ATPase DISTRIBUTION ASSOCIATED WITH SECRETORY STATES OF THE OXYNTIC MUCOSA. J. M. Wolosin and J. G. Forte. (Intr. by D. Warnock) Dept. of Physiology-Anatomy, Univ. of California, Berkeley, CA 94720.

Biochemical evidence is presented for changes in the environment of the $(K^+ + H^+)$-ATPase enzyme, located at the apical pole of the mammalian oxyntic cell, following in vivo gastric stimulation. HCl secretion in rabbits was stimulated by histamine and repressed in control animals by metiamide administration. Differences between groups are referred to as the change induced by tissue stimulation. The gastric fundic mucosae from both groups were homogenized, fractionated by differential centrifugation and the distribution of various activities measured. Stimulation resulted in a redistribution of K^+-ATPase between the various membrane pellets. In the microsomal pellet the activity was reduced to less than half with a concomitant increase in the heavier membrane fractions normally associated with nuclei and mitochondria. Density gradient fractionation of the mitochondrial pellet produced a membrane preparation of high specific K^+-ATPase activity in the stimulated case. Structural studies revealed these membranes to be far bigger and apparently denser than the K^+ATPase-rich microsomal vesicles associated with the non-stimulated state. When fractions were analyzed by SDS-PAGE the redistribution of enzymatic activity was closely matched by shifts in a 100,000 M.W. polypeptide. The specific nature of the process described is indicated by the lack of change in the distribution of other enzymatic activities ($(Na^+ + K^+)$-ATPase, pepsinogen) to stimulation. Preliminary data aimed at identifying the processes responsible for the observed changes is presented. It is proposed that the large membrane vesicular fraction of the stimulated tissue derives from the elaborate apical plasma membrane associated with the secretory state; the smaller microsomal vesicles of the control animals derive from the abundant tubulovesicles present in resting oxyntic cells (Supported by USPHS).

M-AM-Po66 TISSUE $|K^+|$ DURING STIMULATION OF H^+ SECRETION IN FROG GASTRIC MUCOSA. Leopoldo Villegas (Introd. by L. Sananes) Centro de Biofísica y Bioquímica, Instituto Venezolano de Investigaciones Científicas, IVIC, Apdo. 1827, Caracas 1010A, Venezuela.

In non-stimulated frog gastric mucosa the $|K^+|$ was significantly reduced when the transmucosal electrical potential difference (p.d.) was abolished by replacing the Cl^- by $SO_4^=$ in the solution or by passing current from an external circuit (Fed. Proc. 19, 1710, 1980). In this state oxyntic cells cytoplasm contains a large number of vesicotubules representing from 6 to 40% of the cytoplasmic volume which disappear following stimulation of H^+ secretion (Berglindh et al. Scand. J. Gastroenterol. Suppl. 55, 7, 1979). After 1 h stimulation using 10^{-4}M histamine in Cl^- solution the $|K^+|$ was reduced ($P < 0.005$) from 281.8 ± 4.3 to 260.4 ± 4.4 μEq/g d.w. and the total water was reduced ($P < 0.01$) from 4.84 ± 0.09 to 4.48 ± 0.10 g/g d.w. In mucosae incubated in $SO_4^=$ solution, the $|K^+|$ was reduced ($P < 0.05$) from 318.1 ± 2.9 to 306.2 ± 4.3 μE/g d.w. and the total water was reduced ($P < 0.005$) from 5.65 ± 0.10 to 5.19 ± 0.11 g/g d.w. The effect of change of the p.d. on the $|K^+|$ reported in the resting mucosa was not observed in the histamine stimulated mucosa. The correlation coefficient between $|K^+|$ and transmucosal potential difference was $r=0.14$ for $n=40$ in the mucosae incubated in Cl^- solution and $r=0.06$ for $n=50$ in the mucosae incubated in $SO_4^=$ solution. The reduction of $|K^+|$ following stimulation and the independence of $|K^+|$ from p.d. in stimulated mucosae suggest that the fraction of $|K^+|$ which depends on the potential difference must be related to the content of the vesicotubules that open to the lumen of the gastric gland during stimulation.

M-AM-Po67 ACTIVE AND PASSIVE PROPERTIES OF THE APICAL AND BASOLATERAL MEMBRANES OF THE RABBIT URINARY BLADDER. S.A. Lewis, N.K. Wills and J.L.C. de Moura Dept. Physiology, Yale Medical School, New Haven, CT.

The rabbit urinary bladder transports Na^+ from urine to blood. This Na^+ transport system can be stimulated after placing the rabbit on low Na^+ diets for 2 weeks (by increasing plasma aldosterone levels; see Lewis and Diamond, 1976, J.Memb.Biol.). This study was designed to investigate the influence of such a dietary regime on three systems (i) the apical membrane passive permeability, (ii) the basolateral membrane permeability and (iii) the basic properties of the Na^+-K^+ pump. These three systems were assessed using conventional and ion specific microelectrodes in conjunction with antibiotics (for studying the pump properties) and current-voltage (I-V) relationships for studying apical membrane selectivity. Low Na^+ diet caused the I_{sc} (short circuit current) to double (from 2.2 to 4.3μAmps/cm^2). Basolateral membrane potential did not significantly change (-52mV for control to -55mV for diet, neither did Intracellular K^+ activity (89mM-control and 92mM-diet) nor the intracellular Na^+ activity (5.8mM control and 5.6mM diet.). Using conventional and ion specific microelectrodes and also I-V relationships, it was found that the amiloride sensitive apical membrane pathway had a Na^+ to K^+ selectivity of 2.6 in control bladders and >9 in diet bladders. Antibiotics nystatin and gramicidin D were used to access the k_m (half maximal activity of Na^+ or K^+ to activate the pump), V_{max} (maximal current generated by the pump) and Hill coefficient (η) of the pump for the two conditions. The k_m was 14 and 2.3mM for Na^+ and K^+ respectively. The η was 2.8 and 1.8 for Na^+ and K^+ respectively. These parameters were independent of diet as was the V_{max} of ≃ 20μAmps/cm^2. (Supported by N.I.H. grant AM-20851 and AM-06033.)

M-AM-Po68 THE VOLTAGE-CURRENT RELATIONSHIP OF EPITHELIAL POTASSIUM ACTIVE TRANSPORT IN THE LARVAL MIDGUT OF THE HORNWORM, MANDUCA SEXTA. R. L. Duncan and J. T. Blankemeyer, Dept. of Physiological Sciences, College of Veterinary Medicine, Oklahoma State University, Stillwater, OK 74078.

The epithelia of many species have been modeled as an electrical circuit with electrical terms applied to the characteristics of the active transport system or pump. Civan (1970) demonstrated, using Voltage-Current (V/I) plots on the toad bladder, that by increasing the hyperpolarization of the tissue, the tissue resistance will shift substantially at the point where the hyperpolarization exceeds the driving force or EMF of the pump. The midgut of Lepidopteran larvae actively transports K from hemolymph to lumen with a PD of 100 mV and an I_{SC} of 600 μA/cm^2. K active transport is rapidly inhibited by N_2 and changes with the hemolymph K concentration. The V-I plot of the midgut was measured by clamping the voltage of the tissue at 20 mV intervals from -100 mV to 300 mV, lumen positive, with a pulse time of 800 msec. The applied voltage and current were measured at the end of the pulse. The V-I plot was linear near the PD but there was a definite breakpoint at 240 mV (PD∿100 mV). Epithelial resistance at voltages lower than the breakpoint was 73-Ω-cm^2 while the resistance above the breakpoint was 45-Ω-cm^2. The breakpoint voltage decreased whereas the epithelial resistance increased with decreasing K concentration. Nitrogen caused the breakpoint to disappear after the PD reached 0.

M-AM-Po69 ADH-INDUCED INCREASE IN TRANSEPITHELIAL CAPACITANCE IN TOAD BLADDER. David L. Stetson, Simon A. Lewis and James B. Wade. Department of Physiology, Yale University School of Medicine, New Haven, Connecticut, 06510.

Antidiuretic hormone (ADH) is known to increase both transepithelial sodium transport and water flow across the toad urinary bladder. Recent morphological studies indicate that the mechanism mediating the change in water permeability may involve fusion of cytoplasmic membranes (containing intramembrane particle aggregates) with the luminal membrane. Because capacitance is directly proportional to membrane area, we have measured epithelial capacitance to assess the possible role of membrane area changes in the action of ADH. Using transient analysis to monitor epithelial capacitance, ADH addition (20 mU/ml) caused a 28 ± 4% (n = 8) increase in capacitance within 30 min. Removal of ADH caused a return of capacitance to control levels within 30 min. An increase in capacitance with ADH stimulation was also observed in the absence of a transepithelial osmotic gradient and the change was not blocked by mucosal amiloride (.05 mM) indicating that the capacitance change is not due to cell swelling or increases in cell sodium. Pre-incubation with methohexital (0.3 mM in the serosal chamber), an agent known to inhibit the hydroosmotic response without affecting the increase in sodium transport, was found to block the capacitance increase due to ADH. These observations indicate that changes in membrane area are associated with ADH-induced changes in water permeability. The finding that the increase in sodium transport is not related to capacitance changes leads to the speculation that pre-existing apical sodium channels may be activated by ADH. This work was supported by N.I.H. grants AM-20851 to S.A.L. and AM-17433 to J.B.W.

M-AM-Po70 SELENIUM SECRETION INTO MILK AND BINDING TO MILK PROTEINS. J. C. Allen, and W.J. Miller, University of Georgia, Athens.

The mechanism of selenium secretion by the mammary gland and characteristics of Se bound to milk were investigated. Sodium selenite ($Na_2^{75}SeO_3$) was injected into the jugular vein of lactating goats fed corn-soy diets. Blood and milk samples were collected hourly for 8 hours and daily for 1 week. Whole blood, plasma, whole milk and the casein, whey and cream fractions of milk were counted for ^{75}Se. The isotope was primarily associated with the casein portion of milk. The association of selenium with the whey fraction was greater for the early time periods than later, and varied between animals. The activity based on protein content was greater in casein than in whey. The peak concentration of ^{75}Se in whole milk occurred in the 3 hour sample. This corresponds with the time required for secretion of isotopic precursors of protein. Thus the mechanism for secretion of selenium and protein may be the same. The goats were killed on day 7 following ^{75}Se dosing. Kidney had the highest ratio activity and liver was slightly higher than mammary tissue. Subcellular organelles of liver, kidney and mammary tissue were obtained by homogenization and differential centrifugation. All organelle fractions contained significant ^{75}Se. The selenium in the radioactive milk was in a tightly bound form. It could not be removed from the protein fraction by dialysis against water or saline. Dialysis against EDTA removed a small amount of ^{75}Se from the milk. Adding reduced glutathione to milk before acid precipitation caused a substantial reduction of ^{75}Se in the casien fraction and an increase in the specific activity of whey. (Sponsored by N. Delamere)

M-AM-Po71 SODIUM AND POTASSIUM DISTRIBUTION IN MAMMARY TISSUE FROM PREGNANT AND LACTATING MICE. Margaret C. Neville, Sally E. Berga and Susan J. Peper. Department of Physiology, University of Colorado Medical School, Denver, Colorado, 80262.

The ratio of $[K^+]$ to $[Na^+]$ in milk from many species is about three and is thought to represent the ratio of intracellular $[K^+]$ to $[Na^+]$ in the mammary alveolar cell (Peaker, M. Symp. Zool. Soc. Lond. 41:113-134, 1977). We have investigated this problem in milk and mammary tissue from pregnant and lactating mice using flame photometry to obtain Na^+ and K^+ levels. Extracellular space was determined from the rapidly effluxing sodium or sucrose space and cell water, by drying or from the 3-O-methyl-glucose space.

Tissue	Extracellular Space	Water Content	$[Na^+]$		$[K^+]$	
	ml/g tissue	g/g tissue	Tissue µmol/g	Cell mM	Tissue µmol/g	Cell mM
Milk	--	--	--	26.5 ± 1.8	--	41.8 ± 1.7
Lactating	0.45 + .02	0.71 + 0.01	64.6 + 3.9	35.2 ± 15.	27.4 ± 2.8	95 ± 11
Pregnant	0.19 ± .01	0.30 ± 0.01	26.5 ± 1.1	22.7 ± 14.	17.5 ± 0.5	162 ± 6

The ratio of $[K^+]$ to $[Na^+]$ in the milk is about two whereas that in the cell water is about three. These data suggest that paracellular processes may play a role in milk secretion. The results also show that there is a substantial increase in tissue extracellular space, tissue water and cell sodium and a decrease in cell potassium during the transition from pregnancy to lactation. The change in water content reflects the very high fat content of the gland from late pregnant animals. The other changes may result from changes in monovalent cation permeability or in the activity of Na/K ATPase at the time of lactogenesis. (Supported by NIH grant AM 15807.)

M-AM-Po72 CHARACTERIZATION OF LIGHT ACTIVATED LIV-MET TRANSPORT IN *HALOBACTERIUM HALOBIUM* ENVELOPE VESICLES. Russell E. MacDonald, Richard V. Greene and Stephen Millar, Section of Biochemistry, Molecular and Cell Biology, Cornell University, Ithaca, N.Y. 14853

Previous work showed that illuminated *Halobacterium halobium* R1 cell envelope vesicles accumulate 19 out of the 20 commonly occurring amino acids. The amino acids are translocated by symport with Na+. Competition studies indicate that leucine, isoleucine, valine and methionine share a common carrier. The uptake of these amino acids can be driven by a membrane potential (interior negative) and/or a Na+ concentration gradient (outside > inside). A detailed analysis of this group of amino acids is presented. **Cross competion** experiments suggest that more than one carrier is involved in the translocation of these amino acids. In an all NaCl system, the addition of excess amino acids from this group inhibits the rate of L-[^{3}H] leucine efflux from vesicles in the absence of light. However, in the light, the addition of excess amino acids from this group enhances L-[^{3}H] leucine efflux. Addition of an amino acid not in this group (threonine) has little effect on the efflux rate. Triphenylboron (TPB^-), a membrane permeant anion, stimulates the rate of L-[^{3}H] leucine in all cases. A working model which accounts for the above phenomena is presented.

This work was supported by Grant GM 23225A from the National Institute of Health and Grant PCM 7609718 fron the National Science Foundation.

M-AM-Po73 ALTERED STATES OF REACTIVITY OF THE (Na,K)-ATPase TOWARD ATP IN THE PRESENCE OF OLIGOMYCIN. A.S. Hobbs and R.W. Albers, NINCDS, NIH, Bethesda, MD 20205, J.P. Froehlich, NIA, NIH, Baltimore, MD 21224.

Inhibition of the (Na,K)-ATPase by oligomycin, which results in increased levels of phosphorylation, is believed to be due to stabilization of the enzyme in the E_1 conformation. In order to further test this hypothesis, the effect of oligomycin on the $E_1 \rightleftharpoons E_2$ interconversions and phosphorylation reaction was examined using the acid quench-flow technique. Consistent with its proposed mechanism of action, oligomycin slowed the K^+-stimulated rate of the E_1 to E_2 conformational transition, an effect potentiated by preincubation with Na^+. When the oligomycin-treated enzyme was briefly exposed to K^+ to generate E_2 and later mixed with ATP + Na^+ to convert E_2 to E_1, two phases of phosphorylation were observed. Further studies showed that the enzyme affinity for oligomycin is greatly reduced in the E_2 state and that the slow phase of E-P accumulation following exposure to K^+ is due to rebinding of the inhibitor to E_1. Preincubation with Mg^{2+} and oligomycin also produced a biphasic pattern of phosphorylation on addition of ATP, Na^+ and K^+. The ratio of rapid to slow components was 1:1 at oligomycin concentrations producing maximal inhibition. Addition of Na^+ to the preincubation medium, however, converted the biphasic kinetics to a pattern in which all of the enzyme phosphorylated rapidly. These results suggest that in the presence of oligomycin states containing bound Mg^{2+} or Mg^{2+} + Na^+ are kinetically distinguishable, the latter behaving as if they existed predominantly in an oligomycin-stabilized E_1 conformation. States containing bound Mg^{2+} behaved like only 50% of the enzyme was inhibited initially, possibly resulting from the comparatively lower affinity of the E_1 state for oligomycin in the absence of Na^+, and limited solubility of the inhibitor in water.

M-AM-Po74 THE COUPLING RATIO OF THE Na-K PUMP IN THE LOBSTER CARDIAC GANGLION. David R. Livengood, Armed Forces Radiobiology Research Inst., Bethesda, MD 20014

An electrogenic Na-K pump has been previously demonstrated in the large neurons of the lobster cardiac ganglion. The pump coupling ratio was determined by two different electrophysiological techniques. A grapical analysis plotting exp(VF/Rt) vs. K_o after the pump was blocked by ouabain was used to determine values for K_i, PNA/pk and the pump coupling ratio γ (Gorman and Marmor, J. Phys. 1974, 242:35-48). These measurements were made 5 to 8 h after the cells were penetrated with microelectrodes. Therefore, these measurements constitute non-sodium loaded steady state values. The value obtained for the pump coupling ratio under these conditions was 1.44 $\pm$ 0.06 (N=9) or close to 3 sodiums for 2 potassium. The second technique used to measure the coupling ratio was to iontophoretically inject Na ions into the neuron. Neurons were penetrated with 3 microelectrodes, 2 of which were filled with 2M Na-citrate, the third electrode contained either 2M K-citrate or 3M KCl. By passing current between the Na salt containing electrodes, reproducible amounts of Na could be injected into the cell soma. The injection system was calibrated by injecting ^{24}Na-citrate into counting vials from representative microelectrodes (calculated transport No. = 0.92). By knowing the Na load injected into the cells, and by measuring the time-current area produced by the Na activation of the Na-K pump, one can calculate the coupling ratio. The calculated ratio was 1.50 $\pm$ 0.04 (N=19) which is not significantly different from the value obtained by the previous method. This value then represents a sodium loaded experimental situation. However, when Na is removed from the bathing solution the coupling ratio shifts to 2 Na to 1 potassium (2.1 $\pm$ 0.1, N=3). These results suggest that the pump normally operates with a 3:2 ratio both at rest and under Na load. In the absence of external Na, however, the pump can operate in a nonpotassium saturated condition.

M-AM-Po75 SODIUM PUMP ACTIVITY IN CARDIAC SARCOLEMMAL VESICLES: INHIBITION BY PALMITYLCARNITINE. Barry J.R. Pitts and Cynthia H. Okhuysen. Section of Cardiovascular Sciences, Dept. of Medicine and the Dept. of Biochemistry. Baylor College of Medicine, Houston, TX 77030.

Sarcolemmal vesicles have been isolated from dog heart which exhibit sodium pump activity. This is observed as an ATP-stimulated uptake of ^{22}Na into inside-out vesicles. This is only partially inhibited by high concentrations of ouabain even after a long period of incubation. Digitoxigenin diffuses more readily into the vesicles and completely inhibits(Ki≈10 μm). The vesicles exhibit a high level of Na, K-ATPase activity (~100μmol/mg/h) which is similarly inhibited by ouabain and digitoxigenin. It is estimated that ~20% of the vesicles are inside-out. For sodium pump activity, varying ATP indicated a Km of 0.37 mM. Varying external NaCl and internal KCl gave maximal activity at ~40 mM Na and ~100 mM K. Kinetics for Na were sigmoidal (n=1.7 on a Hill plot). 3 Na were taken up per ATP hydrolyzed in agreement with previous results of red cells. The vesicles also exhibit ATP-dependent digitoxigenin-inhibited ^{22}Na:Na-exchange.

Palmitylcarnitine (PCN), a metabolite which increases several fold in myocardial ischemia following cessation of β-oxidation of fatty acids, inhibits ATP-dependent ^{22}Na uptake by 80% at a ratio of 1.8 μmol PCN/mg vesicle protein and 50% inhibition was obtained 0.7 μmol PCN/mg. Inhibition depends on the ratio not on the free concentration of PCN. Addition of 1.8 μmol PCN/mg after maximum ATP-dependent ^{22}Na uptake had been achieved resulted in rapid release of ^{22}Na indicating that PCN makes the vesicles leaky. If PC also makes the sarcolemma leaky in myocardial ischemia this could explain how enzymes such as CPK are released into the circulation. (Supported in part by HL 22813, HL 25292 and by a grant-in-aid from AHA. Texas Affiliate).

M-AM-Po76 PARTIAL PURIFICATION AND PRELIMINARY CHARACTERIZATION OF SQUID BRAIN Na^+,K^+-ATPase. Gerda E. Breitwieser. Department of Physiology and Biophysics, Washington University School of Medicine, St. Louis, MO.

Crude homogenates of squid brain contained Na^+,K^+-ATPase at a specific activity of 0.4-0.5 U(umol P_i/min)/mg (approx. 50% ouabain-sensitive). A membrane fraction was produced by two different methods: (1) cytoplasmic organelles were pelleted at 8000 xg followed by a high speed pelleting of total membrane at 25,000 xg (microsomes); (2) retaining the total membrane fraction on a 1.195M sucrose cushion followed by fractionation of the membranes on a 40, 35, 30, 20% (w/v) discontinuous sucrose gradient, resulting in three distinct membrane fractions: F1 (band at 20-30% interface), F2 (30-35% interface), and F3 (35-40% interface). Method (1) resulted in the production of microsomes with specific activity of 0.7 U/mg (approx. 60% ouabain-sensitive). Method (2) resulted in membrane fractions having specific activities: F1, 2.4 U/mg (89% ouabain-sensitive); F2, 2.6 U/mg (77% ouabain-sensitive); F3, 1.9 U/mg (83% ouabain-sensitive). Method (2) was used in all subsequent work. Detergent inactivation of ouabain-insensitive ATP hydrolysis activity was attempted. Both SDS (0.5 mg/ml) and Brij-58 (5.0 mg/ml) were effective, resulting in a membrane fraction with 100% ouabain-sensitive activity. The molecular weight of the large subunit was determined by SDS-PAGE to be approx. 100,000 daltons (larger than the dog kidney enzyme run in the same system). The purified squid Na^+,K^+-ATPase has a broad pH optimum centered at pH 7.0, a K_m for ATP of 0.42 ± 0.06 mM, and a K_i for ouabain of 0.32 ± 0.04 uM. The effect of Mg^{++} on hydrolysis activity was examined at 3 mM ATP. The effects of Na^+ and K^+ on total activity were examined over a wide range of concentrations, and a model for their interactions developed. (Supported by NIH grant NS 11223 to P. De Weer).

M-AM-Po77 MECHANISM OF Na^+ FOR Ca^{2+} EXCHANGE IN CARDIAC SARCOLEMMAL VESICLES STUDIED BY STOPPED-FLOW SPECTROPHOTOMETRY. Masaaki Kadoma and Jeffrey Froehlich, NIA, NIH, Baltimore, MD 21224; John Sutko and John Reeves, Depts. of Physiology, Internal Medicine and Pharmacology, University of Texas Health Science Center, Dallas, TX 75235.

Cardiac sarcolemmal (SL) membrane vesicles exhibit Na^+ for Ca^{2+} exchange activity, in which the transmembrane movement of Ca^{2+} in one direction is coupled to the movement of Na^+ in the opposite direction. Using stopped-flow spectrophotometry and the Ca^{2+} sensitive dye Arsenazo III, we examined the initial time course of Na^+-stimulated Ca^{2+} efflux in SL_{2+} vesicles in the presence and absence of valinomycin. SL vesicles were loaded with Ca^{2+} in the presence of 160 mM KCl, suspended in 160 mM KCl containing 30 µM Arsenazo III and then mixed with a medium containing 30 µM Arsenazo III and variable amounts of NaCl (0-160 mM) plus sufficient KCl to bring the monovalent cation concentration to 160 mM. The initial velocity of the Na^+-stimulated Ca^{2+} efflux increased sigmoidally with [NaCl] reaching half-saturation at 30 mM NaCl. The Hill coefficient for the v vs [Na^+] plot was 2.53, consistent with a stoichiometry of 3 Na^+ per Ca^{2+} for the exchange process. At NaCl concentrations above 10 mM two phases of Ca^{2+} efflux were resolved. Valinomycin-treated vesicles showed only a single phase of Na^+-stimulated Ca^{2+} efflux with a rate equal to that of the initial phase measured in the absence of the ionophore. The results suggest that after a brief initial period of rapid Ca^{2+} efflux in the absence of valinomycin, the rate of Na^+ for Ca^{2+} exchange is reduced due to the accumulation of positive charge within the vesicle resulting from the electrogenic nature of the exchange process. Valinomycin provides a pathway for dissipation of the charge allowing the exchange process to proceed at a maximal rate throughout the entire time course.

M-AM-Po78 PERMEABILITY OF RED CELL LIPIDS TO WATER. James A. Dix and A.K. Solomon. Biophysical Laboratory, Harvard Medical School, Boston, MA 02115.

The diffusional permeability coefficient, P_d, of human red cells to water, is 5.5 cm s^{-1} by THO diffusion (Barton and Brown, J. Gen. Physiol. 47, 839, 1964) which agrees satisfactorily with P_d = 4.4 cm s^{-1} given by Conlon and Outhred (Biophys. Biochim. Acta 511, 408, 1978) based on proton NMR T_1 and T_2. When water permeation has been maximally inhibited by parachloromercuribenzene sulfonate (pCMBS), P_d drops by about 50%. Macey et al (Biomembranes 3, 341, 1973) have suggested that the remaining 50% of the water permeates by diffusion through red cell lipids. After correction for the fractional lipid area of the membrane, the putative lipid P_d would have to be 4.8 cm s^{-1} (see Conlon and Outhred), much larger than that in phosphatidylcholine lipid bilayers containing cholesterol, where P_d ranges from 0.4 to 2.2 cm s^{-1}. Thus, it seems unlikely that red cell lipids can account for the water permeation remaining after pCMBS treatment. We have investigated the lipid permeation path by perturbing red cell membranes with the lipophilic anesthetic, halothane, which partitions into extracted red cell lipids and increases water permeability in red cell liposomes by 30% (20 mM halothane). However, 20 mM halothane has no effect on water permeability, either in intact cells or in cells maximally inhibited with pCMBS. The fluorescence of a membrane bound probe, N-phenyl-1-naphthylamine (NPN), is quenched by halothane. Data from quenching and fluorescence lifetime experiments indicate that halothane quenches NPN by a diffusional mechanism in both extracted red cell lipids and intact ghosts, and suggest that halothane is equally partitioned into extracted red cell lipids and into intact red cell lipids. These experiments indicate either that there is no water pathway through intact red cell lipids, or that lipid structure in the intact cell differs significantly from liposome structure. Supported in part by NSF PCM 7822577.

M-AM-Po79 DEPENDENCE OF WATER AND NONELECTROLYTE PERMEABILITY OF RED CELLS ON HYDROSTATIC PRESSURE. D.M. Karan* and R.I. Macey, Dept. of Physiology-Anatomy, Univ. of California, Berkeley 94720.

Using a newly developed stopped flow photometer (Karan and Macey, Rev. Sci. Instrum. 51, 1042, 1980), the pressure dependence of water and non-electrolyte permeabilities of human red cells were measured over a range of 1 to 680 atmospheres. Activation volumes ($\Delta V^{\dagger}$) were estimated from the slopes of log (permeability) vs pressure plots, using at least 30 permeability-pressure points per plot. In our initial experiments, we detect no change in the osmotic permeability to water over this pressure range (i.e., $\Delta V^{\dagger} \sim 0$). However, when water channels are closed by application of saturating dosages of PCMBS, the activation volume for water transport through the remaining pathway (presumably lipid) equals 18 ml/mole. Further, the activation volume of solutes presumed to penetrate the membrane via the lipid path appear to be discretely distributed. Implications of activation volumes in units comparable to the molar volume of water will be discussed. Research supported by ONR Contract #N00014-77-6-0482, NR201-188 and N.I.H. Grant No. GM18819.

M-AM-Po80 CALCIUM CONTENT AND TRANSPORT PROCESSES OF RAT ERYTHROCYTES INFECTED WITH RODENT MALARIA PARASITES (P. CHABAUDI). K. Tanabe, R. B. Mikkelsen and D.F.H. Wallach. Dept. of Therapeutic Radiology, Tufts-New England Medical Center, Boston, MA 02111

Regulation of intracellular calcium levels of intraerythrocytic malaria parasites and their host cells is important for parasite growth. We examined total calcium content and Ca^{2+} transport of P. chabaudi infected rat erythrocytes by atomic absorption spectrophotometry and $^{45}Ca^{2+}$ influx/efflux measurements. Erythrocytes were purified to less than 0.1% white cell contamination and separated on metrizamide gradients into cell fractions enriched in early (ring, early trophozoite), late (late trophozoite, schizont) and gametocyte stages of parasite development. At all stages of parasite development, infected cells showed higher levels of Ca than non-infected (66 picomoles/10^7 cells) with the latter stages, schizont- and gametocyte-rich fractions having 5 to 40 times greater Ca contents. Both enhanced $^{45}Ca^{2+}$ influx and reduced $^{45}Ca^{2+}$ efflux rates for parasitized cells relative to non-infected cells contribute to these increased intracellular Ca levels. At extracellular $[Ca^{2+}]$=1 mM, the $^{45}Ca^{2+}$ influx rate for schizont-enriched cells was 5 times the rate for non-infected cells. If cells are equilibrated for 30 min. at 37°C with 1 mM $^{45}Ca^{2+}$ and efflux initiated by dilution into saline ± 0.1 mM EGTA, the $^{45}Ca^{2+}$ of non-infected cells is reduced by 70% after 20 min., whereas the $^{45}Ca^{2+}$ levels of schizont infected erythrocytes are depleted by only 20%. Ca^{2+} efflux from infected erythrocytes is only slightly enhanced (<20%) by 5 µM antimycin A, 0.1 to 1.0 mM chloroquine or 1 mM NaCN. The rate of Ca^{2+} efflux is increased more than 50% by 1 µM carbonyl cyanide m-chlorophenyl hydrazone, a proton ionophore, and by 10 µM dicyclohexylcarbodiimide, an inhibitor of bacterial and mitochondrial H^+-ATPases. These results suggest that a non-mitochondrial proton gradient may regulate $[Ca^{2+}]$ in Plasmodium infected erythrocytes. Supported by N.I.H. AI 16087

M-AM-Po81 THE SELECTIVITY OF THE EXTERNAL ANION EXCHANGE TRANSPORT SITE OF RED BLOOD CELLS M. A. Milanick and R. B. Gunn, University of Chicago, Chicago, IL 60637.

The external anion transport site of human red blood cells is not selective for halides despite the reported nine fold difference in K-se (K^{Cl}se = 65mM; K^{Br}se = 7.5mM), the concentration of anion which causes half-maximal self-exchange flux. In both major classes of models for this obligatory one-for-one exchange, the ping-pong and the sequential models, the external concnetration of ion X required for half-maximal velocity, K^X-out, is a function of the concentration and maximal transport rate (and thus species) of internal ion. Thus K-se measurements (where the ion concentrations on both sides of the membrane are varied together) may not reflect the K-out values of the individual ions under similar internal ionic conditions. Additionally, the interference of different anions at the modifier sites may contribute to differences in K-se. To make comparable measurements of K^X-out we have determined ^{125}I efflux at 18°C from red cells with iodide as the only internal halide, into K-halide/K-gluconate media; K(total) = 150mM. K^X-out ≃ 1 mM for Cl, Br, and I indicating that all three halides have the same apparent affinity (within a factor of 2) for the external transport site and perhaps the same nonselectivity might be expected for the internal transport site. Further support for the apparent lack of halide selectivity comes from inhibition studies at 0°C. We measured ^{36}Cl efflux at constant internal chloride and several outside chloride and iodide concentrations and found that K^{Cl}-out = $K^{I}_{I\text{-out}}$ = 3mM. Thus the six fold difference between K^{Cl}-se and K^{I}_{I} measured by Cl self-exchange at anion equilibrium (Dalmark,J.G.P. 67: 223, 1976) also does not reflect differences in the outside affinities since with fixed internal conditions K^{Cl}-out = $K^{I}_{I\text{-out}}$. Supported in part by NIH grants HL-20365 and GM-28893.

M-AM-Po82 THEORETICAL ANALYSES OF THE ROLE OF DIFFUSION BOUNDARY LAYERS IN O_2 UPTAKE BY ERYTHROCYTES. V.H. Huxley and H. Kutchai., Sloan-Kettering Institute, New York, NY 10021 and Dept. of Physiology,University of Virginia, Charlottesville, VA 22908.

O_2 uptake by suspensions of red blood cells (RBC) was experimentally shown in the stopped-flow apparatus to be significantly limited by extracellular diffusion boundary layers (DBL) in normal buffer and buffer containing bovine serum albumin (BSA) to decrease extracellular oxygen solubility and diffusivity (Huxley and Kutchai). Theories of mass transfer to the surface of particles in flow have been used to estimate the effect of DBLs on the rate of RBC O_2 uptake and compared with our experimental results. Models of O_2 uptake by RBCs in laminar flow (Harriott,Friedlander) predicted a larger DBL effect than was experimentaly observed. The more complex theory of mass transfer to particles in turbulent flow (Levich) predicted an O_2 permeability of the DBL which closely matched the experimental values. These hydrodynamic analyses show that the dependence of O_2 uptake rate on RBC size (Holland and Forster) can be explained in terms of DBL effects. Our studies are consistent with the interpretation that RBCs in rapid mixing devices are incompletely mixed with the suspending medium and that in the immediate vicinity of the RBC oxygen mass transfer is limited by molecular diffusion.

(Supported by NIH grants HL17967 and RCDA HL00014)

M-AM-Po83 PHLORETIN BINDS TO BAND 3, THE ANION TRANSPORT PROTEIN OF THE RED BLOOD CELL MEMBRANE. Stuart A. Forman, A. S. Verkman, James A. Dix and A. K. Solomon, Biophysical Laboratory, Harvard Medical School, Boston, MA 02115.

Phloretin, an inhibitor of anion exchange and glucose and urea transport in the human red cell, binds to high affinity protein sites (1.5 μM at pH 6) and low affinity lipid sites (54 μM at pH 6) on the red cell membrane (Jennings and Solomon, J. Gen. Phys. 67, 381, 1976). Equilibrium binding and kinetic studies indicate that one protein binding site is band 3, the major integral protein of the red cell membrane. Equilibrium phloretin binding is competitive with the binding of an anion transport inhibitor, 4,4'-dibenzoamido-2,2'-disulfonic stilbene (DBDS), which binds specifically to band 3 (Dix et al, Nature 282, 520, 1979). The apparent binding constant of phloretin to red cell ghost band 3 in 28.5 mM citrate buffer, pH 7.4, 23°C, determined from equilibrium binding competition, is 1.8 ± 0.3 μM, in agreement with the high affinity site above. Stopped-flow kinetic studies show that phloretin decreases the rate of DBDS binding to band 3 in a purely competitive manner, with an apparent phloretin inhibition constant of 1.6 ± 0.4 μM. Both the apparent phloretin binding and inhibition constants are similar to the K_I of phloretin for the inhibition of anion exchange, 2-5 μM. The total number of DBDS binding sites on the red cell membrane, 1.2×10^6 (≈ one binding site per band 3 monomer), is approximately half the total number of phloretin protein binding sites, 2.5×10^6. These studies suggest that phloretin inhibition of anion exchange in red cells results from a specific interaction between phloretin and a transport inhibition site on band 3. Supported in part by NIH 2 ROL HL14820.

M-AM-Po84 THERMODYNAMICS OF STILBENE BINDING SITES ON HUMAN RED CELL BAND 3. A. S. Verkman, James A. Dix and A. K. Solomon, Biophysical Laboratory, Harvard Medical School, Boston, Mass. 02115

Binding of 4,4'-dibenzoamido-2,2'-disulfonic stilbene (DBDS) to band 3 (B3) in 28.5 mM citrate (isoionic strength) has been measured both by centrifugation and by an improved fluorescence enhancement method. The stoichiometry is 3.2 ± 0.1 nmol/mg (1.2×10^6 sites/cell) and the apparent dissociation constants are K_1^s = 65 ± 4 nM and K_2^s = 820 ± 100 nM based on the minimal reaction scheme: B3 $\overset{DBDS}{\rightleftharpoons}$ B3-DBDS $\overset{slow}{\rightleftharpoons}$ DBDS-B3 $\overset{DBDS}{\rightleftharpoons}$ $(DBDS)_2$-B3 (Nature 282, 520, 1979). DBDS binding affinity to both sites increases with increasing citrate showing that there is no simple competition between citrate and DBDS. In citrate, both K_1^s and K_2^s depend upon ionic strength (μ); the dissociation constants depend linearly upon $\mu^{-1/2}$ with the same slope, indicating that the electrostatic properties of the two sites are similar. In 112 mM Cl^- (in isoionic buffer), K_1^s = 455 ± 14 nM and K_2^s = 1.4 ± 0.1 μM; the number of sites remains unchanged. Thermodynamic parameters have been measured in 28.5 mM citrate under conditions which minimize their model dependence. The apparent activation entropies and enthalpies of the two bimolecular associations are nearly the same: for the first, ΔH = 1.4 ± 0.4 kcal/mol and ΔS = 26 ± 5 eu; for the second, ΔH = 1.5 ± 1.5 kcal/mol, ΔS = 30 ± 5 eu. These data, in conjunction with the ionic strength dependence, show the two sites to be virtually identical; the difference between K_1^s and K_2^s results from the conformational change. The seeming identity of the two bimolecular reaction sites, the first before the conformational change and the second, after, shows that the system is symmetrical and suggests that the two sites may be interchangeable. Supported in part by NIH 2 R01 GM 15692.

M-AM-Po85 "RATE CONSTANT INHIBITION" - A POSSIBLE MECHANISM FOR STILBENE INHIBITION OF ANION EXCHANGE. James A. Dix, A. S. Verkman and A. K. Solomon, Biophysical Laboratory, Harvard Medical School, Boston, MA 02115 (Intro. by E. A. Dawidowicz).

A minimal reaction mechanism for 4,4'-dibenzoamido-2,2'-disulfonic stilbene (DBDS) interaction with human red cell band 3 (B3) has previously been suggested (Dix et al, Nature 282, 520, 1979): B3 $\overset{DBDS}{\rightleftharpoons}$ B3-DBDS $\overset{slow}{\rightleftharpoons}$ DBDS-B3 $\overset{DBDS}{\rightleftharpoons}$ $(DBDS)_2$-B3. Detailed kinetic analysis of stopped-flow experiments based on this mechanism indicates that Cl^- inhibition of DBDS binding is entirely non-competitive, but this is not a firm conclusion since rate constants obtained from temperature-jump experiments without Cl^- differ from stopped-flow rate constants. Hence, the minimal mechanism is not a complete description. However, evidence for the non-competitive inhibition does not rest on this mechanism alone; our previous observation that Cl^- accelerates the slow conformational change in the second step means that Cl^- inhibition must have a significant non-competitive component. Previous classical studies using Michaelis-Menten kinetics, however, have shown that stilbenes are competitive inhibitors of anion exchange (see Knauf, Curr. Top. Mem. Trans. 12, 249, 1979). Classically, net forward reaction velocity is given by the product of the rate constant, k, and the enzyme-substrate concentration, [ES]. Inhibition is effected by reduction of [ES] as a result of competition for the enzyme reaction site. In Rate Constant Inhibition, [ES] remains unaffected by the inhibitor which acts instead by reducing the rate constant, k, by an allosteric mechanism. The assumption that each DBDS molecule bound to a band 3 monomer turns off the transport function of that monomer leads to a complete formal analogy between rate constant inhibition and competitive inhibition, thus allowing the minimal reaction scheme to satisfy the constraints imposed by classical studies of stilbene inhibition. Supported in part by NIH 2 R01 GM 15692.

M-AM-Po86 NIFLUMIC ACID SENSES THE CONFORMATION OF THE TRANSPORT SITE OF THE HUMAN RED CELL ANION EXCHANGE SYSTEM. Philip A. Knauf, Nancy Mann* and Foon-Yee Law*. Dept. of Rad. Biol. & Biophys., Univ. of Rochester Med. Ctr., Rochester, NY 14642 and the Hosp. for Sick Children, Toronto, Ontario, Canada M5G 1X8.

The anti-inflammatory drug niflumic acid (NA) was found by Cousin and Motais (J. Membr. Biol. 46:125-153) to act as a very potent non-competitive inhibitor of red cell anion exchange. Since NA binding is inhibited by disulfonic stilbenes, which are competitive inhibitors of transport, it probably binds to the anion transport protein, band 3, perhaps near the transport site. To test for effects of the transport site conformation on NA binding, we imposed chloride gradients across the membrane to change the number of inside-facing and outside-facing transport sites, and then measured the inhibitory effect of NA on chloride exchange at 0°C. With 150 mM Cl^- in the medium, chloride exchange was 50% inhibited by 0.63±0.01(SEM, n=4) μM NA. When external Cl^- was reduced to 10 mM, exchange was 50% inhibited by only 0.31±0.02 μM NA. When nystatin was used to lower internal Cl^- to 10 mM in parallel with external Cl^-, the increase in inhibitory potency was prevented. The increase does not seem to be related to the increase in membrane potential, since when 10 μM valinomycin was used to reverse the membrane potential, the effect of the chloride gradient on NA inhibitory potency was not reversed. Considered in light of our earlier demonstration that chloride gradients (with $Cl_i > Cl_o$) can be used to increase the proportion of outside-facing transport sites, the data suggest that despite the fact that NA interacts with both the loaded and unloaded forms of the transport site, NA binds to band 3 only when the transport site is in the outside-facing form. NA can therefore be used to monitor the fraction of transport sites which are in the outside-facing form. Supported by NIH and MRC(Canada).

M-AM-Po87 ADIPOCYTE HEXOSE TRANSPORT AS EXAMINED BY FLUORESCENT GLUCOSE ANALOGS

Mario Di Paola*, Frederick Maxfield#, and Randall Murphy*, *Department of Chemistry, New York University, New York, NY 10003 , and #Department of Pharmacology, School of Medicine, New York University, New York, NY 10016

Fluorescent hexose analogs have been prepared from glucosamine and dansyl chloride, fluorescein isothiocyanate, or rhodamine isothiocyanate. These derivatives are found to bind reversibly to rat adipocytes. The rate of binding is stimulated by insulin (10 - 100 nM) ; binding is inhibited by phloretin (100 μM). A blue shift is observed in the emission of dansyl-glucosamine upon the addition of adipocytes, deconvolution of which yields two bands corresponding to 505 and 460 nm. The intensity of the 505 nm band increases linearly with increasing dansyl-glucosamine concentration, while the intensity of the 460 nm band saturates in the micromolar concentration region. The appearance of the 460 nm component is inhibited by phloretin. We therefore hypothesize that the 460 nm band corresponds to dansyl-glucosamine which is specifically associated with the adipocyte hexose transporter. By measuring the intensity of the 460 nm emission, we can determine the amount of cells associated with dansyl-glucosamine without having to separate the cells from the unbound material. Thus, using a stopped-flow fluorometer we are able to examine the rapid kinetics of insulin stimulated hexose transport. We have also utilized fluorescence microscopy to directly observe the dansyl-glucosamine in isolated rat adipocytes.

M-AM-Po88 EFFECTS OF RESERPINE ON EPINEPHRINE TRANSPORT INTO CHROMAFFIN GHOSTS AND ACID-LOADED LIPOSOMES. Michael Zallakian, Jane Knoth, George Metropoulos,* and David Njus, Department of Biological Sciences, Wayne State University, Detroit, Michigan 48202.

Acid-loaded liposomes take up epinephrine presumably because epinephrine crosses the liposome membrane as a weak base in its uncharged form. This uptake, dependent on the transmembrane pH gradient, is not inhibited by reserpine. Liposomes rapidly collected on Millipore filters contain the same amount of 3H-epinephrine whether reserpine is present or not. Reserpine does, however, allow epinephrine to equilibrate across the membrane more quickly. Reserpine accelerates epinephrine leakage occurring during elution of epinephrine-containing liposomes down a Sephadex G-50 column. Reserpine-treated vesicles retain less 3H-epinephrine than untreated samples. Epinephrine uptake into acid-loaded liposomes apparently occurs via an electroneutral reserpine-insensitive pathway. Chromaffin granules, the catecholamine storage vesicles of the adrenal medulla, take up catecholamines through an electrogenic exchange for protons ($2H^+$/catecholamine cation) driven by an H^+-translocating ATPase. The uptake of epinephrine into chromaffin granule ghosts is inhibited by reserpine whether it is driven by the pH gradient or by the membrane potential. In contrast to liposomes, ghosts do not take up epinephrine by a reserpine-insensitive electroneutral pathway but by a reserpine-sensitive electrogenic pathway. Reserpine concentrations which inhibit epinephrine uptake do not accelerate the efflux of 3H-epinephrine from ghosts or promote the exchange of external 14C-epinephrine for internal 3H-epinephrine. Reserpine apparently does not facilitate epinephrine equilibration across the ghost membrane but binds competitively and reversibly to a catecholamine-translocating protein. The different effects of reserpine on epinephrine uptake imply that acid-loaded liposomes are not a good model for chromaffin granule ghosts. Supported by NSF (Grant BNS-7904752) and the Michigan Heart Association.

M-AM-Po89 pH DEPENDENCE OF CATECHOLAMINE TRANSPORT IN CHROMAFFIN GHOSTS IMPLIES CATIONIC FORM IS TRANSLOCATED. Jane Knoth, Jill Isaacs,* and David Njus, Department of Biological Sciences, Wayne State University, Detroit, Michigan 48202.

Catecholamines are accumulated into adrenal medullary chromaffin granules by an electrogenic exchange for protons. The stoichiometry previously determined is 2 H^+ per catecholamine cation or 1 H^+ per neutral or zwitterionic catecholamine. As yet, there has been no conclusive evidence as to whether the cationic or neutral form of the amine is translocated. Because the pK of the amine is high (serotonin = 9.8; dopamine = 10.6), the cationic form is the predominant species (99-100%) when the pH is below 7.8. The neutral form represents ∿0.1% of the catecholamine at pH 7 and ∿1% at pH 8. Because the neutral species increases in concentration by a factor of 10 with a 1 unit increase in pH while the concentration of the cationic species is independent of pH, it should be possible to tell which species is translocated from the pH dependence of the apparent K_m for transport. Because the log fraction for the neutral species increases linearly with pH, the K_m values should decrease by the same factor if it is the neutral species that is translocated. When the concentration dependences of serotonin and dopamine uptake are tested at various pH's and displayed on Lineweaver-Burk plots, the K_m values are pH-independent and V_{max} increases with pH. These results indicate, therefore, that the cationic species is translocated.

Supported by NSF Grant BNS-7904752.

M-AM-Po90 EXPERIMENTAL CHARACTERIZATION OF ELECTROOSMOTIC TRANSPORT OF NON-ELECTROLYTES. A. Zelman[1], D. Gisser[2], R. Chu[1] and G. Odell[3]. [1]Center for Biomedical Engineering, [2]Department of Electrical and Systems Engineering and [3]Department of Mathematics, Rensselaer Polytechnic Institute, Troy, NY 12181.

The purpose of this research is to develop an experimental basis for the transport process called "selective filtration of non-electrolytes by electroosmosis". Membranes are specially chosen to sorb non-electrolytes and repel electrolytes. Electroosmosis is used to transport urea, glycerol and glucose. Complete description of this phenomena requires the measurement of ten transport coefficients. To reduce ambiguities to a minimum, an experimental apparatus was constructed to simultaneously measure during each experiment the transport of water, non-electrolyte, electrolyte and electric current. Sufficient data was collected to accurately evaluate all the transport coefficients from a single non-steady state experiment.

An automatic data acquisition system was assembled to minimize human error. Both sides of the membrane contain identical hardware as a double check on all measurements. Concentration and concentration differences are monitored: electrolyte by conductivity and non-electrolyte by spectrophotometry. Volume transport is measured gravimetrically by electronic balances. Data is sampled every few minutes and sorted on punched tape. The four transport equations are numerically integrated, solved simultaneously and the transport coefficients determined along with a complete error analysis.

M-AM-Po91 LITHIUM FLUXES ACROSS SQUID AXON MEMBRANE. Barbara E. Ehrlich and John M. Russell Department of Physiology and Biophysics, Albert Einstein College of Medicine, Bronx, NY, University of Texas Medical Branch, Galveston, TX, and Marine Biological Laboratory, Woods Hole, MA.

Since the discovery that lithium (Li^+) salts are the most effective treatment for manic-depressive illness, questions have been raised about cell handling of Li^+. These questions include (a) although this ion is not normally present in the body, do endogenous transport mechanisms carry Li^+ (b) if so which ones, and (c) are the same pathways used in all cells? Many transport studies have used the erythrocyte (RBC) as a model system because it was not technically possible to measure the small Li^+ movements expected across nerve membranes. By using a very sensitive method for Li^+ analysis, flameless atomic absorption spectroscopy, it was possible to measure endogenous Li^+ levels in squid hemolymph and axoplasm, to monitor Li^+ movements across the axon membrane, and to compare Li^+ flux pathways in nerve and RBC. Li^+ influx was measured using the internal dialysis technique. To measure efflux, axons were preloaded by stimulating the cells in 425 mM Li^+ sea water and Li^+ washout was followed. When Na^+ was present in the external solution, Li^+ influx increased linearly. At low Li^+ levels the removal of external Na^+ increased influx three-fold. The converse was true for efflux. Efflux into Na^+-free sea water was barely detectable. However, the addition of external Na^+ markedly increased the Li^+ efflux. The Na^+-dependence measured in these experiments show that both Li^+ influx and efflux can occur via the Na^+-Li^+ countertransport mechanism. In addition, Li^+ movements through the Na^+ channel, via the Na^+-K^+ pump, and via a leak were measured. These results suggest that the Li^+ transport pathways previously identified in RBC also function in squid axon.

Supported by a Grass Foundation Fellowship and Grant NS11946.

M-AM-Po92 WEAK ACID PERMEABILITY IN BARNACLE MUSCLE FIBERS, SEPARATELY DETERMINED FOR THE NEUTRAL AND IONIZED SPECIES. David W. Keifer and Albert Roos, Department of Physiology and Biophysics, Washington University Medical School, St. Louis, Mo. 63110.

The time course of the intracellular pH (pH_i),measured on exposure of barnacle muscle fibers to high levels of weak acids,was used to determine separately the membrane permeability to the neutral, P_{HA}, and the ionized, P_{A^-}, species of the weak acid. On exposure to the weak acid, the pH_i rapidly fell to a plateau value, as the more permeable neutral species equilibrated across the membrane and dissociated. In the plateau phase the pH_i slowly declined as the anion of the weak acid was driven from the cell down its electrochemical gradient. The transmembrane pH_i regulatory mechanism was inhibited by a low outside pH of 6.8, so that the pH_i changes observed were solely due to movement of the weak acid. From the initial and plateau rates of fall of pH_i, the intracellular buffering power, and the driving forces on the fluxes, the two permeabilities, P_{HA} and P_{A^-}, were determined. For the weak acid 5,5-dimethyloxazolidine-2,4-dione (DMO), $P_{HA} = 1.9 \times 10^{-4}$ cm/sec and $P_{A^-} = 1.5 \times 10^{-7}$ cm/sec. Permeabilities have also been determined for butyrate, isobutyrate, propionate, salicylate, formate, acetate, and others. These weak acids had values for P_{HA} of the order of 10^{-3} cm/sec, with the exception of salicylate where P_{HA} was of the order of 10^{-1} cm/sec. P_{A^-} was always at least two orders of magnitude smaller than P_{HA}, and often too small to be measured. On removal of salicylate and formate pH_i increased only slightly, possibly due to metabolic events during the long exposure to the weak acids. (Supported by NIH National Research Service Award 1-F32-GM07239-01 to D. Keifer and NIH Grant HL-00082 to A. Roos. Present address of D. Keifer: Botany Department, University of California, Davis, Calif. 95616)

M-AM-Po93 KINETICS OF SERUM-DEPENDENT AND SERUM-INDEPENDENT Na FLUXES IN HUMAN FIBROBLASTS Mitchel L. Villereal. Dept. of Pharmacol. and Physiol. Sciences, U. of Chicago.

Previous studies indicated that amiloride completely inhibits the serum-dependent component of Na influx while inhibiting less than 10% of the serum-independent component(Villereal, J. Cell. Physiol.,submitted). We sought to characterize kinetically these two components of Na influx to test the hypothesis that they represent two distinct Na transport systems. For cells assayed in serum-free medium a plot of initial Na influx versus $[Na]_o$ ($[Na]_i \sim 10$ mM) gives a simple saturation curve with a $K_{1/2} = 70$ mM and a $V_{max} = 14.5$ µmol/g prot/min. A similar plot of initial Na influx versus $[Na]_o$ in the presence of 10% FBS gives a nonsaturating curvilinear response which appears to be biphasic. A plot of the serum-dependent Na influx versus $[Na]_o$ (obtained by subtracting the curve in the absence of FBS from the curve in the presence of 10% FBS) gives a simple saturation curve with a $K_{1/2} = 338$ mM and a $V_{max} = 42.2$ µmol/g prot/min. The effect of intracellular Na on Na influx was tested by preloading cells with Na in a digitoxin-containing medium prior to measuring ^{22}Na influx. A plot of Na influx versus $[Na]_o$ ($[Na]_i \sim [Na]_o$) in the absence of serum gives a curve which appears to saturate around 80 mM Na (flux = 100 µmol/g prot/min) and then declines with increasing [Na] (flux = 40 µmol/g prot/min at 150 mM). In contrast to Na influx in control serum-deprived cells, Na influx in Na-loaded cells is amiloride-sensitive.. Since the peak Na influx of 100 µmol/g prot/min is greatly in excess of the V_{max} for control serum-deprived cells, internal Na must somehow stimulate Na influx. The fact that Na influx in Na-loaded cells is amiloride-sensitive suggests that a high $[Na]_i$ activates the amiloride-sensitive Na pathway which is normally only minimally operative in the absence of serum. A possible explanation is that elevating the $[Na]_i$ results in a rise in the $[Ca]_i$, a maneuver that we have shown activates the amiloride-sensitive pathway(ref. above). (Supported by GM 28359 PHS)

M-AM-Po94 B.V.Bronk, Departments of Physics, Astronomy, and Microbiology, Clemson University Clemson,S.C.29631 Physical Definition of Life. To determine ultimate sources of biological variability, a physical definition of life was attempted (1). This needs to include all organisms from protists to people, but must exclude many physical systems which though possessing highly organized dynamics, are clearly non-living. Many well-known difficulties with such a definition were avoided by: (1)abandoning the individual organism and considering instead a minimal living system in contact with a specified test environment;(2) taking an operational viewpoint.i.e. incorporating into our postulates, thought experiments testing for a living system (L.S.). These experiments needn't be practically realizable, but should be approachable to arbitrary accuracy by laboratoryexperiments. The defining rules follow:(1) No physical laws are violated; (2) An L.S. maintains certain life properties with zero probability of cessation when placed in a suitable initial state into a suitably maintained test environment;(3) The test environment consists of a medium containing elementary units and is suitably maintained if all parameters fall within specified respective ranges; (4) Life properties include: (a) higher information density than the test environment; (b) higher energy density than the test environment; (c) total living mass tends to increase when test environment is suitably maintained; (d) L.S. may be specified by a finite number of parameters including minimum distance between viable units; (e) No environment exists into which an L.S. may be immersed and be immediately in thermal equilibrium. ---In addition to making specific predictions, the above rules provide criterea which any theoretical model of a living system should satisfy to be complete as well as an experimental framework for classifying any system as living or non-living

(1) Bronk,B.V. pp 37-70 in Applied Stochastic Processes, ed. G. Adomian, Academic (1980).

M-AM-Po95 A THEORETICAL MODEL FOR MITOCHONDRIAL OSCILLATIONS. Teresa Ree Chay, Department of Biological Sciences, University of Pittsburgh, Pennsylvania, PA 15260.

Studies on the oscillatory phenomena which occur in mitochondria are of great importance for an elucidation of the functional behavior of metabolism and for a better understanding of the biological rhythms. We present a model for the mitochondrial oscillations based on the chemi-osmotic model of Mitchell. Our model incorporates stoichiometries of H^+ translocation obtained by Alexandre et al and makes the use of the rate parameters which obey irreversible thermodynamic requirements. Our model exhibits oscillations, under certain external conditions, in the components involved in the electron transfer system and also in the energy transducing system. The period of oscillations agrees approximately with that observed in the experiment.

This work was supported by NSF Grants PCM76-81543 and PCM79-22483.

M-AM-Po96 MODELS of DENSITY DEPENDENT OSCILLATIONS in YEAST

John Aldridge - Dept. Genetics, Children's Hospital, Boston, Mass. 02115

Glycolytic oscillations in yeast are density dependent in well stirred, whole cell suspensions. At both high and low cell densities, no oscillations are observed, whereas at an intermediate density all cells appear to oscillate in mutual synchrony. The chemical mediator of synchrony is unknown; however additions of the nonphosphorylated glycolytic intermediates, acetaldehyde and pyruvate, will phase shift the synchronized cell suspension and perturb the intercellular ATP/ADP ratio. One can model this system therefore as a series of nonlinear oscillators hooked in parallel through simple linear permeation of an oscillator variable through the intercellular pool. Addition of this extra linear relationship has been shown to cause bifurcation to a periodic solution as a function of cell density, which mimicks that observed experimentally. Permeation through a well stirred intercellular pool may also produce more complicated bifurcations, such as hard excitation, which may help explain amplitude resetting, a phenomenon observed in both yeast suspensions and Drosophila eclosion rhythms.

M-AM-Po97 NYSTATIN AND VALINOMYCIN PHASE SHIFT THE CIRCADIAN CLOCK OF NEUROSPORA.

Noriyuki Koyama and Jerry F. Feldman, Thimann Laboratories, University of California, Santa Cruz, Santa Cruz, CA. 95064.

Nystatin and valinomycin, two chemicals which alter permeability properties of membranes, induced phase shifts of the circadian clock of Neurospora crassa when administered as 3-hour pulses to cultures grown in liquid medium. The magnitude and sign (advance or delay) of the phase shifts were dependent on both the phase of the cycle at which the pulse was administered and on the concentration of the drug. Both drugs produced large phase delays during the late subjective night (circadian time 2200) with a sharp transition ("breakpoint") to maximum phase advances at dawn (circadian time 0000). The phase response curves (PRCs) - a plot of phase shift vs. phase of the cycle at which pulse was administered - are similar to the PRC for visible light, except that the "breakpoint" for light occurs about 6 hours earlier and light gives much larger phase advances than the chemicals. They PRCs for nystatin and valinomycin are also quite different from the PRC for cycloheximide, an inhibitor of cytoplasmic protein synthesis. These results suggest that either membrane depolarization or altered transport of K+ can cause phase shifts of the circadian clock of Neurospora. (Supported by Grant GM-22144 from the National Institute of General Medical Sciences.)

M-AM-Po98 THE EFFECT OF COUGH ON HEART RATE: RESPONSE MIMICS AN OVERDAMPED OSCILLATOR.

Jeanne Y. Wei. Harvard Medical School and Beth Israel Hospital, Boston, Massachusetts.

Although the effect of cough on arterial, venous and intrathoracic pressures have been studied, the changes in heart rate following cough have not been well characterized. To investigate the chronotropic response to cough, sixteen subjects, 22 to 56 years of age without cardiac or pulmonary disease, were studied in the supine position. Following a rest period, on command, each subject rapidly coughed three times consecutively. The coughs were evenly spaced over a three-second period. Continuous electrocardiographic recordings were analyzed from forty seconds before (control) to forty seconds after the coughs. The instantaneous heart rate were determined from successive R-R intervals. About two seconds or three beats after the last of the 3 voluntary coughs, the mean instantaneous heart rate rose from 71 $\pm$ 3 beats/min (range 55 to 88) to 92 $\pm$ 3 beats/min (range 71 to 107), resulting in a maximal rate change of 36 $\pm$ 2% ($p < .001$). The period during which the increase in heart rate remained significant ($p < .05$) was about 15 seconds. The response can be well described by a gamma function, i.e.

$$y = At^{\alpha}e^{-\beta t}$$

where $A = 24.0$, $\alpha = 0.38$, $\beta = .19$, $p < .001$.

Thus, the heart rate response as a function of time following cough inscribes an asymmetric curve with a shorter ascending phase and a tapered longer descending phase. This response is similar to that of an overdamped oscillator.

M-AM-Po99 A STATISTICAL THERMODYNAMIC MODEL FOR THE ESTIMATION OF RATES OF REPHASAL OF BIOLOGICAL RHYTHMS. C.M. Winget, N.W. Hetherington, J.R. Beljan, and L.S. Rosenblatt, NASA-Ames Research Center, Moffett Field, CA; Wright State University, Dayton, OH; Geneticon, Walnut Creek, CA.

Following transmeridian jet flights (or photoperiod alterations) biological rhythms depart from their pre-shift (initial) steady state, enter a transient state and then reach a new (final) steady state (recovery). Many investigators have ignored the transient state since the time series is then non-stationary. We assume that within each cycle the data are stationary and follow successive cycles. We transform the harmonic fit to the data to a vector and measure the difference vector (resynchrony vector) between the measured data vectors and the final steady-state vector. If we further assume that the physiological rhythm (e.g., body temperature) is complex and is controlled by a large number of underlying processes, and that at any instant in time each process is either operative or inoperative we have an analogy to dipole moments. Using the methods of statistical thermodynamics as extended by absolute rate theory we have determined the trajectory of the difference vector: $A_{(ts)} = A \pm \exp(\alpha + \beta t)$ where $A_{(ts)}$ is the dot product component of the resynchrony vector, A is the asymptote representing complete resynchrony, α is a measure of the extent of desynchrony and β is the rate constant. In practice, we estimate t_{95}, the time required for 95% recovery. In an extension of this work we have shown that the rates of rephasal of pairs of rhythms (a second-order resynchrony process) follows the same trajectory as that given above. Examples of the use of the model will be presented.

M-AM-Po100 A CONTINUOUS AXIOM A SYSTEM. O. E. Rössler, Div. Theor. Chem., University of Tübingen, 7400 Tübingen, W. Germany

Chaotic oscillations occur in nonlinear 3-variable systems almost as easily as periodic oscillations do in nonlinear 2-variable systems. As a consequence, many of the 2-variable model equations used in nerve dynamics, hormonal regulation and biochemical networks may produce chaos after being replaced by more realistic, at least 3-variable ones. There was one mathematical drawback, however: all the continuous chaotic systems known either possessed a non-differentiable cross-section ('Lorenz type') or contained within the chaotic convolute a periodic attractor - that is, were not of "axiom A" type in the sense of Smale[1]. The following 4-variable system is proposed as a first continuous example in this abstractly simplest (everywhere differentiable and everywhere hyperbolic) class:

$$\dot{x} = 100(2z^2-1-x)g(X-.3)g(R+.8)+x(-YR+Xh(R))$$

$$\dot{y} = 100(2zw-y)\ \ g(X-.3)g(R+.8)+y(-YR+Xh(R))$$

$$\dot{z} = 200(2x^2-1-z)g(Y-.6)g(.8-R)+z(\ XR+Yh(R))$$

$$\dot{w} = 200(2xy-w)\ \ g(Y-.6)g(.8-R)+w(\ XR+Yh(R)),$$

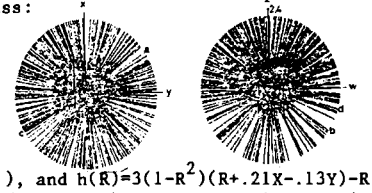

where $X=x^2+y^2$, $Y3+z^2+w^2$, $R=\sqrt{X^2+Y^2}-2$, $g(s)=.5(1-s/\sqrt{s^2+.001}\ )$, and $h(R)=3(1-R^2)(R+.21X-.13Y)-R$. As the numerical simulation shows, the system functions like two single-handed clocks which take turns resetting the other toward twice the time told by the first. (The letters a, b, c, d in the Figure indicate a sequence of four such resetting events.) The result appears to be the formation of a solenoid attractor[1]. Simpler examples may be found soon.

[1]Smale, S., Differentiable dynamical systems, Bull. Amer. Math. Soc. 73, 747-817, 1967.